New synthetic pathways to mono- and bis-dithiolene compounds of molybdenum and tungsten related to the active sites of the molybdopterin containing oxidases

Dissertaition

zur Erlangung des Doktorgrades

der Mathematisch-Naturwissenschaftlichen Fakultäten

der Georg-August-Universität zu Göttingen

vorgelegt von

Qingwei Zhang

aus Dalian, Liaoning

(V. R. China)

Göttingen 2007

D7

Referent: Jun.-Prof. Dr. C. Schulzke
Korreferent: Prof. Dr. J. Magull

Tag der mündlichen Prüfung:

Dedicated to my parents
for their love and affection

Acknowledgement

Abbreviations

acac	acetylacetonate
ADH	aldehyde dehydrogenease
AH	acetylene hydratase
AOR	aldehyde ferredoxin oxidoreductase
bdt	benzene-1,2-dithiol
cat.	catalyst
calcd.	calculated
CAR	carboxylic acid reductase
chd	*trans*-1,2-cyclohexanediol
dec.	decomposition
Dg	Desulfovibrio gigas
DME	ethyleneglycol dimethylether
DMF	dimethyl formamide
DMS	dimethyl sulfide
DMSO	dimethyl sulfoxide
EI	electron impact ionization
equiv	equivalent(s)
Et	ethyl
Fd	ferredoxin
FDH	formate dehydrogenase
FMDH	N-formylmethanofuran dehydrogenase
FOR	fromaldehyde ferredoxin oxidoreductrase
g	gram(s)
GAPOR	glyceraldehydes-3-phosphate ferredoxin oxidoreductase
h	hour(s)
IR	infrared

L	ligand
M	metal
m	middle, multiplet
$M+$	molecular ion
Me	methyl
MeCN	acetonitrile
MeOH	methanol
min.	minute(s)
ml	milliliter
mmol	millimolar
mnt	1,2-maleonitriledithiolato
Moco	molybdenum cofactor
m.p.	melting point
MPT	molybdopterin
MS	mass spectrometry, mass spectra
Mt	Methanobacterium Thermoautotrophicum
Mw	M. wolfei
m/z	mass/charge
NMR	nuclear magnetic resonance
OPPh$_3$	triphenylphosphine oxide
Pa	Pelobacter acertylenicus
Pf	Pyrococcus furiousu
Ph	phenyl
PPh$_3$	triphenyl phosphine
ppm	parts per million
q	quartet
R	organic substituent
rt	room temperature
s	strong, singlet
S$_2$pd	pyranopterin-dithiolate ligand

t	time, triplet
tdt	3,4-toluenedithiol
THF	tetrahydrofuran
Tl	Thermococcus Litoralis
TMS	trimethylsilyl
vs	very strong
w	weak
Z	number of molecules in the unit cell
δ	chemical shift
λ	wavelength
μ	bridging
ν	wave number

Table of Contents

1. Introduction

Molybdenum and tungsten are chemically analogous elements. Although both are relatively scarce in natural environments, they are important metals in many fields [1]. For example, they play a significant role in biological systems as the active site of enzymes [2-3].

1.1. Enzymes containing molybdenum and tungsten

Enzymes containing molybdenum or tungsten are to be found in all forms of life, from ancient archaea to human being. These enzymes catalyze a wide range of reactions in carbon, sulfur, and nitrogen metabolism, and at least 50 enzymes are known already [2]. From the biological perspective, molybdenum and tungsten provide a fascinating study in contrasts and analogies.

The essential role of molybdenum in various fundamental biological conversions carried out by both microorganisms and higher (larger) life forms associates with either of two different basic forms. One form is the FeMo-co-factor, which is as an integral component of the multinuclear M center present exclusively in the nitrogenase MoFe-protein and takes the form of a Fe_7Mo cluster. The other form is the molybdenum cofactor (Moco) which is shown in Fig. 1.1 as the mononuclear active site of a much more diverse group of enzymes that in general catalyses the transfer of an oxygen atom either to or from a physiological acceptor/donor molecule found in a variety of oxotransferases [4-6].

The existence of a molybdenum cofactor was first proposed in 1964 by Pateman et al. as a result of the work on a series of pleiotropic mutant cells in *Aspergillus nidulans* lacking both nitrate reductase and xanthhine oxidase activity. It was proposed that the two enzymes share a common cofactor that is called molybdenum cofactor (Fig. 1.1). Since then much evidence has provided strong indications of the

presence of a wide variety of dithiolene derivatives connecting pterin and phosphate groups as a molybdenum cofactor in xanthine oxidase, sulfite oxidase, trimethylamine *N*-oxide reductase, dimethyl sulfoxide reductase and various molybdenum oxidoreductase [4, 7-8].
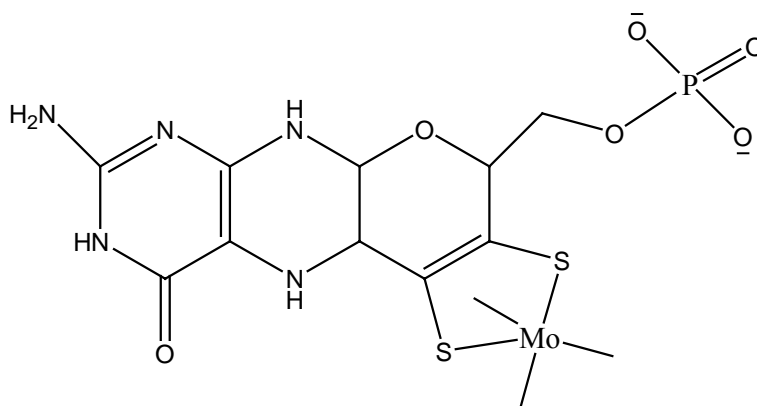
Fig. 1.1. The minimal coordination unit of a molybdenum cofactor, showing the structure of molybdopterin.

Molybdenum-containing enzymes are a broad class of enzymes that are important in both prokaryotic and eukaryotic pathways such as nitrogen assimilation, sulfur and purine metabolism, and hormone biosynthesis, to catalyze the transfer of an oxo-group between the substrate and water in a two-electron redox reaction in a wide variety of organisms. All of the well-characterized molybdoenzymes have been found to have one or two metal-binding pterin-substituted 1,2-enedithiolate ligands (MPT) bound to the molybdenum in the active site. Three oxidation states (6+, 5+, 4+) are available for molybdenum in these enzymes. Along with the MPT ligands there may be zero, one, or two terminal oxo groups, Mo=O, and/or a terminal sulfur group, Mo=S, which functionality may change to Mo-OH or Mo-SH according to solution pH and the oxidation state of molybdenum. In each case, the molybdenum center couples electron-transfer to atom–transfer chemistry, and so there is typically a latent coordination site (a labile Mo-bound ligand X that can be readily displaced by substrate) [9-11].

On the basis of the reaction catalyzed, mononuclear molybdenum enzymes (molybdoenzymes) constitute a fairly large class of enzymes that can be divided into two subcategories [2, 12].

The first class is that of the hydroxylases, which belong to a quite large family of enzymes whose members catalyze the oxidative hydroxylation of a diverse range of aldehydes and aromatic heterocycles in reactions that necessarily involve the process that inserts oxygen derived from water into C-H bonds (Eq. 1.1):

$$RH + H_2O \rightleftharpoons ROH + 2\ H^+ + 2\ e^- \qquad (1.1)$$
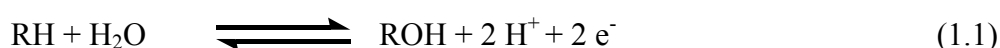
The second category is called oxotransferases, which includes enzymes that typically catalyze proper oxygen atom transfer reactions to or from an available electron lone pair of substrate (Eq. 1.2). In addition, these oxotransferases can be subdivided into two families. The first consists of well-known enzymes such as sulfite oxidase and the assimilatory nitrate reductases (i.e. those enzymes whose physiological function is to reduce nitrate to nitrite in the first step of its reduction to ammonia for utilization by the cell). The second is a family made up of bacterial enzymes such as DMSO reductase and biotin-S-oxide reductase, as well as the bacterial dissimilatory (or respiratory) nitrate reductases: those periplasmic or memberane associated enzymes that function as terminal respiratory oxidases.

$$R + H_2O \rightleftharpoons RO + 2\ H^+ + 2\ e^- \qquad (1.2)$$
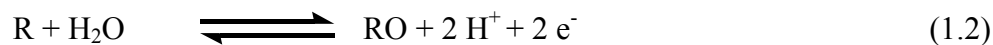
In terms of the protein sequences and their structures and function of oxidized active sites, Hille has divided the molybdoenzymes into three families that are named by their most prominent member, viz. the xanthine oxidase, sulfite oxidase and DMSO reductase families (Fig. 1.2).

Although these three prototypical enzymes are relatively well studied and crystal structures of chicken liver sulfite oxidase, *Rhodobacter sphaeroides* and *R. capsulatus* DMSO reductase as well as *Desulfovibrio gigas*' aldehyde oxidoreductase (a member

of the xanthine oxidase family) have been determined, several unresolved questions remain regarding the structures of the active sites as well as the reaction mechanisms for all three families.

Moco-dependent enzymes

hydroxylases   oxotransferases

Xnathine Oxidase
Family

Sulfite Oxidase
Family

DMSO Reductase
Family
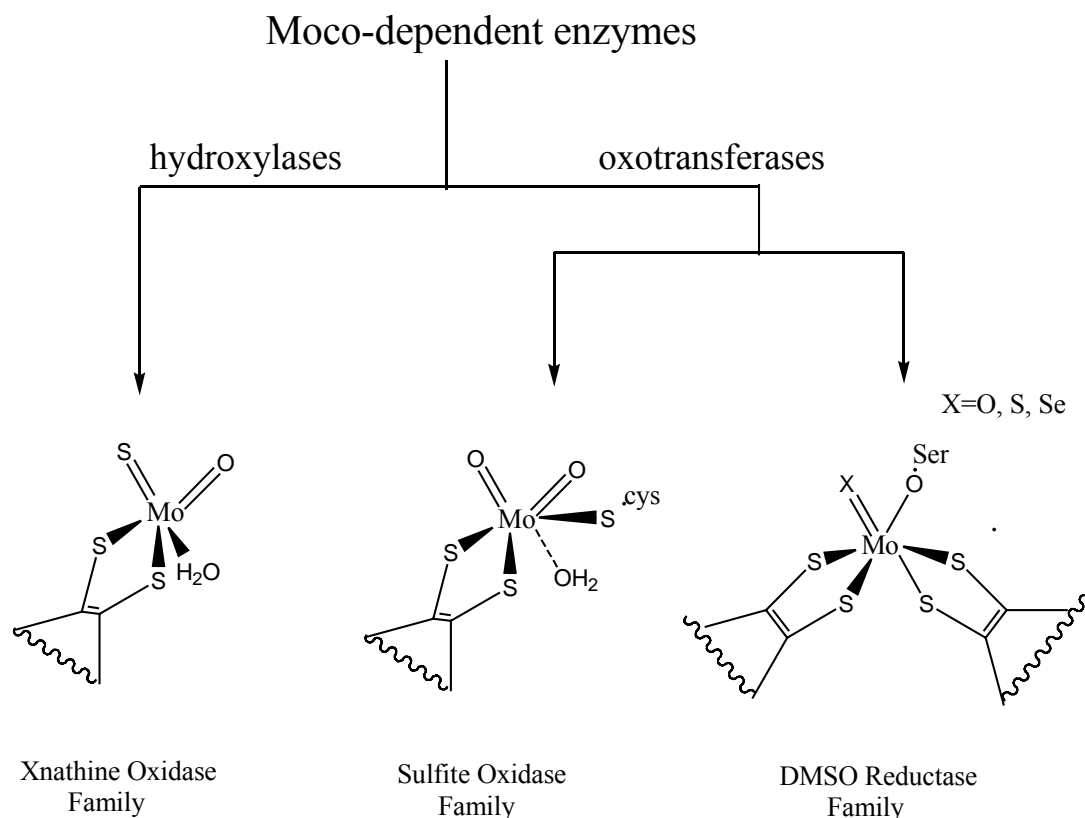
Fig. 1.2. Scheme of mononuclear molybdenum enzymes. The oxidized forms of the cofactors of each class are shown; the molybdopterins are represented as dithiolene moieties.

Tungsten has traditionally been regarded as a biological antagonist of molybdenum; which causes a loss of activity in molybdenum-containing respiration catalysts and is not essential for human beings or animals. In fact the human body normally contains none [13]. But as analogous to molybdenum, it was reasoned that insight into the catalytic role of molybdenum in various enzymes might be provided by replacing molybdenum with tungsten for the great similarities in the properties of these two elements. Recently scientists found that tungsten might have a positive biological role,

which has a very short history compared to that of molybdenum.

A role for tungsten in biology first emerged in the 1970s, when it was reported that tungstate stimulates the growth of certain acetate- and methane-producing microorganisms, and was unequivocally demonstrated in 1983 with the purification of the first tungstoenzyme [3]. By 1990 the stimulatory growth effect of tungstate had been reported with only one other group of microorganisms, the hyperthermophilic archaea, which thrive near 100 ^{o} C, and only two more tungstoenzymes had been purified, a second from an acetogen and one from a hyperthermophile [14-15]. Since then, and particularly in just the last year, rather dramatic progress has been made in the study of tungstoenzymes. Especially after 1995, when the first crystal structure of a tungsten enzyme was detected [16], about 20 X-ray crystal structures of additional molybdenum and tungsten enzymes have been reported [17]. At the present time over a dozen tungstoenzymes have been identified and purified from hyperthermophilic archaea and bacteria. The genes for three of them have been cloned and sequenced, and the crystal structure of one of them has been determined to 2.3 Å resolution [16].

According to the molecular properties, tungstoenzymes have been classified into two major families. The first family is the aldehyde ferredoxin oxidoreductase (AOR) family, which catalyzes the oxidation of aldehydes and uses the redox protein ferredoxin (Fd) as the physiological electron acceptor (Eq. 1.3). This type of enzyme is the major family of tungstoenzymes, and it was detected from hyperthermophilic archaea, such as *Pyrococcus furiousus* (Pf), *Thermococcus* strain ES-1 and *Pyrocusccus* strain ES-4 [16, 18-19]. From all of them, Pf is the most thoroughly studied one.

$$RCHO + H_2O \rightleftharpoons RCO_2^- + 3H^+ + 2e^- \tag{1.3}$$
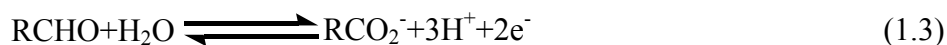
The crystallographic analysis revealed that this enzyme is a homodimeric enzyme wherein each subunit contains a [4Fe-4S] cluster and a single tungsten atom. The two subunits are bridged by a monomeric Fe site, and coordinated by the side chains of a histidine and a glutamate residue from each subunit. A prior study had shown that Pf

AOR contains the so-called mononucleotide form of molybdopterin, where the latter is the pterin cofactor that coordinates the molybdenum atom in all molybdoenzyems, with the notable exception of nitrogenase, and the structural study of Pf AOR revealed that the tungsten atoms were coordinated with two molybdo-pterin molecules [16]. The hyperthermophilic archaea contain two other types of tungstoenzyems besides AOR called fromaldehyde ferredoxin oxidoreductrase (FOR) and glyceraldehydes-3-phosphate ferredoxin oxidoreductasr (GAPOR). The former one has been purified from Pf and *Thermococcus Litoralis* (Tl; T_{max}, 98 °C) [20] and the later one so far has been purified only from Pf [21]. In view of gene encode and from the structural study it was suggested that all these three enzymes arose from an ancestral AOR-type subunit containing the tungstodipterin site and a single [4Fe-4S] cluster [3]. In addition Adams M. W. W. et al. supposed that this AOR subunit was also the evolutionary precursor to all of the tungstoenzymes in the AOR family because to the hyperthermophilic archaea such as species of *Pyrocuccus* and *Thermocuccus* are regarded as the most slowly evolving of all know organisms [22-23].

In addition to the three hyperthermophilic tungsoenzyems the AOR family also includes carboxylic acid reductase (CAR) found in certain acetogenic clostridia [14, 22], which was first identified by its ability to catalyze the reduction of nonactivated carboxylic acids and the aldehyde dehydrogenease (ADH), which was isolated from the sulfate-reducing bacterium *Desulfovibrio gigas* (Dg) [24].

The second family of tungstoenzymes called F(M)DH family includes the first purified tungstoenzyme, formate dehydrogenase (FDH), and N-formylmethanofuran dehydrogenase (FMDH) [25-26]. FDH catalyzes the first step in the conversion of CO_2 to acetate and to methane in acetogens and methanogens, respectively (Eq. 1.4).

$$CO_2 + H^+ + 2\ e^- \rightleftharpoons HCOO^- \tag{1.4}$$

FMDH has been purified from several methanogens and on the basis of sequence data F (M) DH enzymes have similarities to molybdoenzymes including Mo-FDH, biotin S-oxide reductase, and DMSO reductase. It has been suggested that their

tungsten coordination units may be structurally similar to those found from DMSO reductase but with cysteinate or selenocysteinate in place of serinate [3]. Two examples of FMDHs are known from *Methanobacterium thermoautotrophicum* (Mt) and *M. wolfei* (Mw) [27-28]. These FMDH catalyze the first step in the conversion of CO_2 to methane in methanogens where the other substrate is methanofuran (MFR; Eq. 1.5).

$$CO_2 + MFR^+ + H^+ + 2\ e^- \rightleftharpoons CHO\text{-}MFR + H_2O \qquad (1.5)$$

There is another class of tungstoenzyme which has just one member named acetylene hydratase (AH). This enzyme was purified from the acetylene-utilizing anaerobe *Pelobacter acertylenicus* (Pa) and it is the most recently discovered and the least characterized [29]. This AH catalyzes the hydration of acetylene to acetaldehyde, according to Eq. 1.6.

$$HC{\equiv}CH + H_2O \rightleftharpoons CH_3CHO \qquad (1.6)$$

AH represents as a new class of tungstoenzyme because it participates in a reaction called hydration. This is in contrast to the oxidoreductase type reactions catalyzed by all other tungstoenzymes and indeed by all molybdoenzymes [3].

While these tungstoenzymes are undergoing continuing delineation as a class, the complete active site structure of any wild-type enzyme in any physiological oxidation state ($W^{VI,\ V,\ IV}$) remains undefined. The most significant structural feature is the presence of two pyranopterindithiolene cofactor ligands bound in the oxidized mononuclear unit $W^{VI}(S_2pd)_2$ of all enzymes that have been crystallographically examined (Fig. 1.3). Structural data together with other co-ordinations and conjectures have led to the putative oxidized active sites set out in Fig. 1.4.
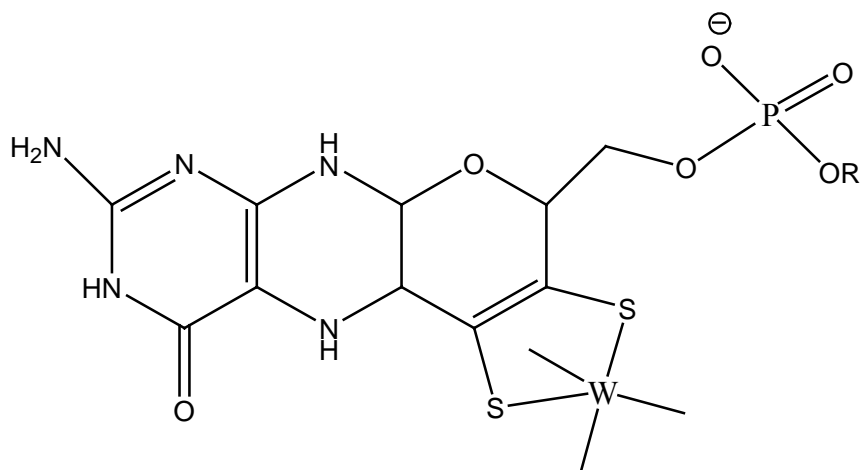
Fig. 1.3. The pyranopterindithiolene cofactor ligand (R absent or a nucleotide) of tungstoenzymes.

As discussed above all molybdenum and tungsten enzymes of the oxotransferase or hydroxylase type contain at least one pterin dithiolene cofactor, sometimes with a nucleotide appended to the phosphate group. The indicated dithiolene chelation mode has been established crystallographically for Pf AOR. Although no bond distances were quoted, the depictions of the cofactor imply tight binding of the metal. In other tunstoenzymes the number of cofactors bound to the metal has not been determined.

Aldehyde Oxidoreductase
AOR

DMSO Reductase
DMSOR

Formate Dehydrogenase
N-formylmethanofuran Dehydrogenase
F (M) DH
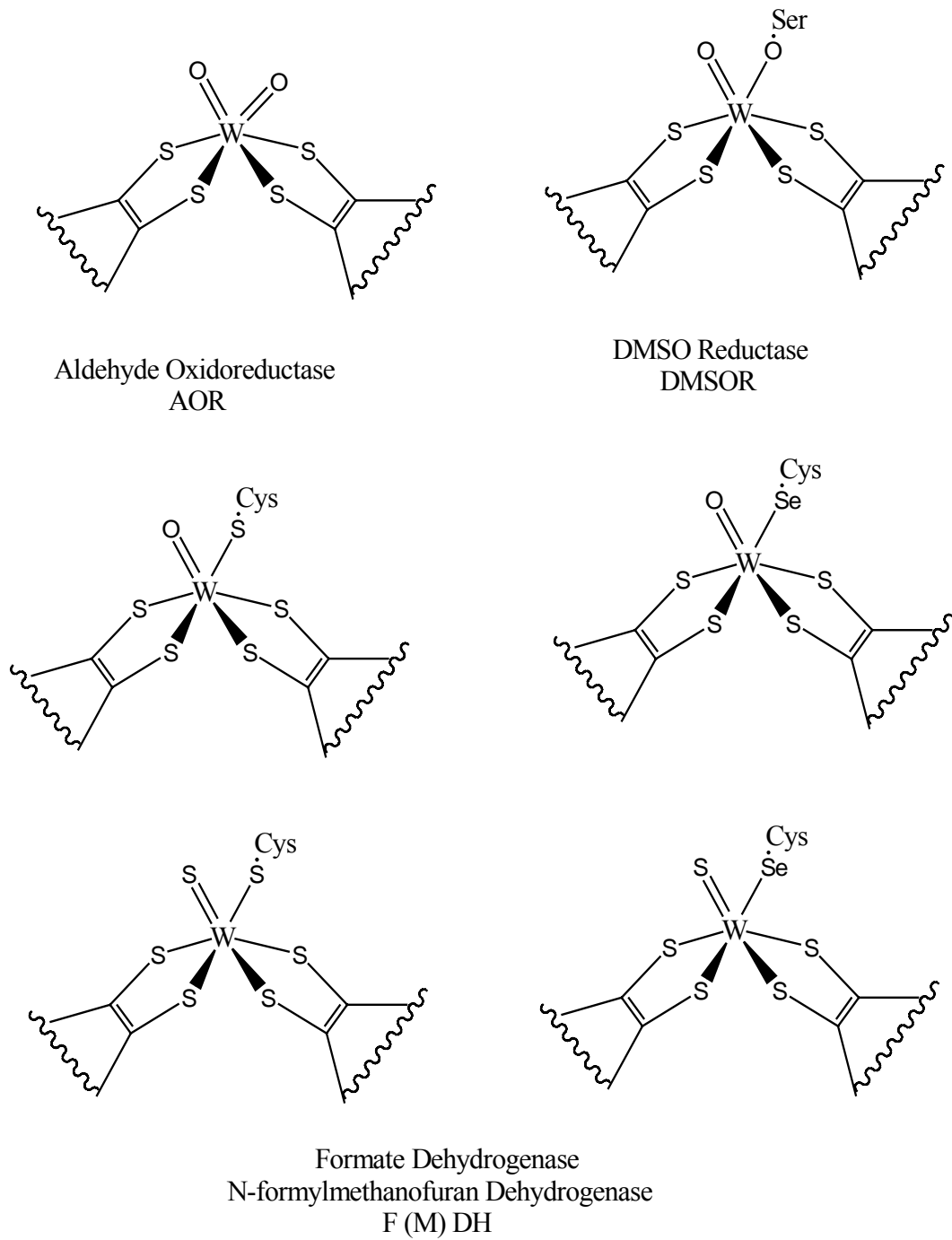
Fig. 1.4. Possible oxidized active sites in tungsten enzymes.

1.2. Synthetic reactions of molybdenum and tungsten dithiolene compounds

The chemistry of molybdenum and tungsten dithiolene compounds is an area of permanent interest that has experienced a remarkable renaissance during the last few years. Much of the attention these compounds attract is due to the importance in industrial and biological catalysis. Based on the molybdenum and tungsten enzyme studies a variety of models of molybdoenzymes and tungstoenzymes have been prepared and reported. A number of dioxomolybdenum complexes with N, S (thiolato, thioether, or thioketone) ligands and oxomolybdenum (V) complexes with S (thiolato) ligands have been synthesized as models of active sites of the enzymes. However, the molecules containing one or two ene-1,2-dithiolate ligands are appropriately simulating the protein ligands and are closer approaches to the active sites of mononuclear molybdenum and tungsten enzymes [30]. The first metal dithiolene complexes were prepared in the early 1960s [31]. Since that time, lots of chemical approaches to molybdenum and tungsten enzyme sites have been directed toward mimicking a portion of the structural center in order to ascertain the role of that particular feature of the center on the chemical reactivity and the spectroscopic properties of the center [30].

Inorganic complexes of molybdenum possessing coordinated pterin species have been a synthetic goal for the past decade or more [32-33]. But while such complexes have interesting chemistry in their own right, it appears unlikely on the basis of the protein structures that this chemistry will prove to be directly relevant to the reaction mechanism of the molybdenum-containing enzymes [3]. As mentioned before, the site analogues of mononuclear molybdenum enzymes require the preparation of mono- or bis- dithiolene species like shown in Fig. 1.2. For models of the active sites in reduced states only a few synthesis of monomeric oxomolybdenum (IV) thiolate complexes have been reported because of the difficulty of the synthesis. The principle routes to these complexes are summarized in Fig.1.5 and Fig. 1. 6 [34-48].
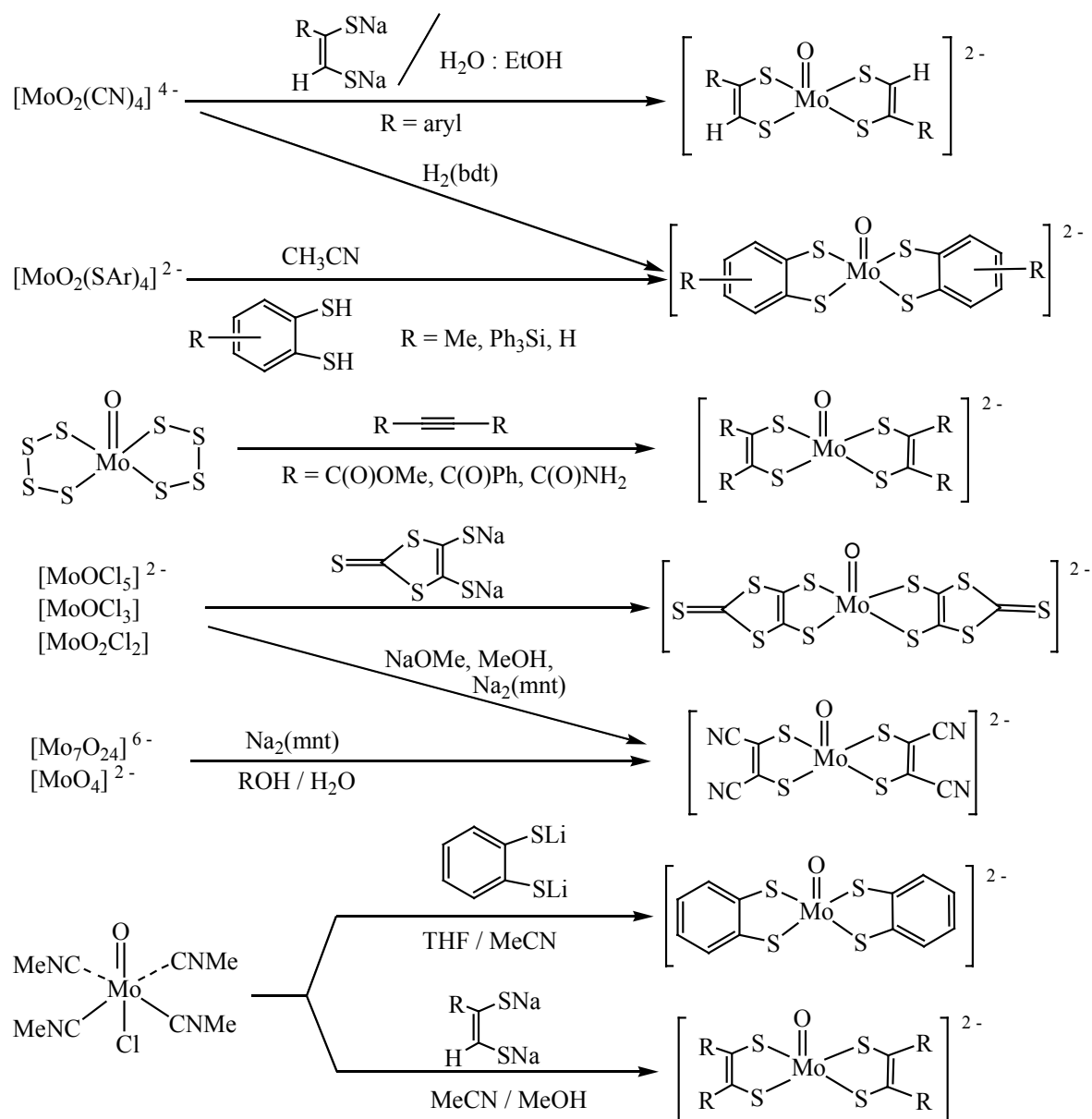
Fig. 1.5. Possible methods of synthesis of bis(dithiolene) molybdenum (IV) complexes (1).

Compared to molybdenum chemistry, the chemistry of tungsten complexes with sulfur donor ligands has developed slowly [3] due to the difficulty in reducing W (VI) species to corresponding W (IV) species. Relevant dithiolene chemistry began in 1992, with the preparation of $[WO(mnt)_2]^{2-}$ and the set $[WO(bdt)_2]^{-, 2-}$ and $[WO_2(bdt)_2]^{2-}$. $[WO_2(mnt)_2]^{2-}$ was reported in 1996 [49-50]. The mnt complexes and $[WO(bdt)_2]^{2-}$ were prepared by methods related to synthesis of molybdenum compounds. Thus all

11

tungsten complexes are isostructural and isoelectronic with their molybdenum counterparts.

$$[MoO(S_2C_2R_2)_2]^{2-} + Me_3NO \longrightarrow [MoO_2(S_2C_2R_2)_2]^{2-} + Me_3N$$

$$[MoO(S_2C_2R_2)_2]^{2-} + R'_3P \longrightarrow [MoO_2(S_2C_2R_2)_2]^{2-} + R'_3PO$$

$$[M(CO)_3(MeCN)_3] + 2\,[Ni(S_2C_2R_2)_2] \longrightarrow [M(S_2C_2R_2)_2(CO)_2] + CO$$
$$+ 2\,[Ni_2(S_2C_2R_2)_2]_X + 3\,MeCN$$

M=Mo, W

$$[M(S_2C_2R_2)_2(CO)_2] + L^- \longrightarrow [M(S_2C_2R_2)_2L(CO)_{2-n}]^- + n\,CO$$

M=Mo, W
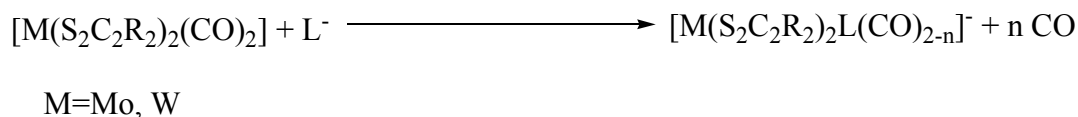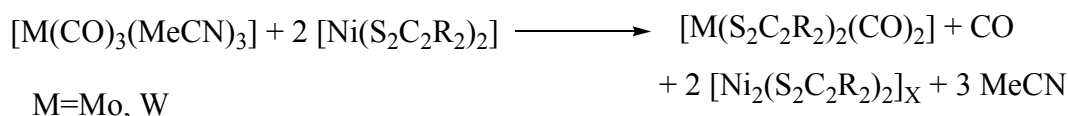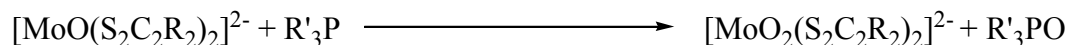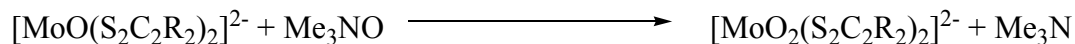
Fig. 1.6. Possible methods of synthesis of bis(dithiolene) molybdenum complexes (2).

1.3. Catalysis of the oxo-transfer

Of all metal-mediated atom and group transfer reactions oxo transfer is by far the most extensively documented and thoroughly investigated [51]. And the oxygen-transfer reactions of molybdenum and tungsten dithiolene compounds have attracted considerable interest in recent years due to the fact that molybdenum and tungsten are found in a class of enzymes that are commonly referred to as mononuclear molybdoenzymes and tungstoenzymes, which catalyze oxygen atom transfer to or from the substrate as shown in Eq. 1.7 [3, 52]. Usually these reactions are accompanied by the dimerization reaction (see Eq. 1.8) [53].

$$M^{VI}O_2L + X \rightleftharpoons M^{IV}OL + XO \qquad\qquad (1.7)$$

$$M^{VI}O_2L + M^{IV}OL \quad \rightleftharpoons \quad L(O=)M^V\text{-}O\text{-}M^V(=O)L \qquad (1.8)$$

M=Mo or W

Moreover coordination compounds of molybdenum can catalyze a variety of important chemical reactions in industry, such as olefine epoxidation [54] and olefine metathesis [55]. In contrast to the oxo-transfer reactions, catalytic oxo-transfer reactions are not hampered by decomposition reaction and the catalytic oxidation reactions of triphenyl phosphine by dimethyl sulphoxide (DMSO) were studied as common models for oxo-trasfer reactions (Eq. 1.9) [52].

$$Ph_3P + Me_2SO \quad \rightleftharpoons \quad Ph_3PO + Me_2S \qquad (1.9)$$

Oxo-transfer occurs from DMSO to the phosphine forming dimethyl sulphide and the oxidized phosphine as shown in Fig. 1. 7. During the procedure the molybdenum and tungsten compounds are catalytic reagents since without these complexes no reactions between triphenyl phosphine and DMSO were observed [56]. This kind of catalytical work helps to understand molybdenum or tungsten-dithiolene chemistry and to investigate the possible mechanisms.

M=Mo or W
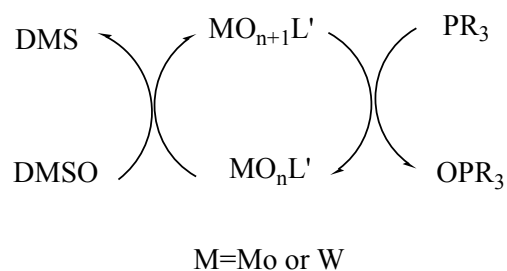
Fig. 1.7. Catalytic oxo-transfer showing the presumed intermediates.

1.4. The selected ligand systems

Two fundamental types of dithiolene ligands ene-1,2-dithiolate and benzene-1,2-dithiolate are depicted in their classical, fully reduced forms (Fig. 1. 8). Both ligands are used in variety of substituents [30]. While ene-1,2-dithiolate ligands have been isolated in substance as alkali metal salts very few, lots of isolated compounds of dianion benzene-1,2-dithiolate and its derivatives are known.

R = H, Me, Ph, CF$_3$,CN, ...

ene-1,2-dithiolate   benzene-1,2-dithiolate
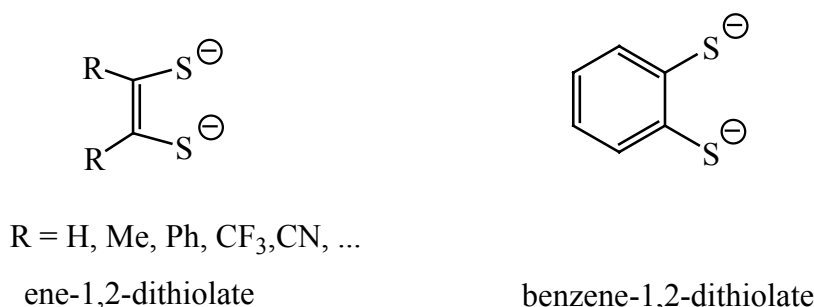
Fig. 1.8. Structures of the two fundamental types of dithiolene ligands in the dithiolate oxidation state.

As mentioned above, the chemistry of molybdenum and tungsten dithiolene compounds is attractive since this type of ligands presents its importance in biology. Indeed, the discovery of the pyranopterindithiolate (Fig. 1.1 and Fig. 1.3) has generated a new imperative in the investigation of molybdenum and tungsten dithiolenes.

In this work benzene-1,2-dithiol and its derivative 3,4-toluenedithiol were used as the ligand precursors. In addition, its related chalcogenide ligands *trans*-1,2-cyclohexanediol and *cis*-1,2-cyclohexanedicarboxylic acid were chosen. The purpose of investigating the related chalcogenide ligands is test the reaction procedure since they have the similar structure with benzene-1,2-dithiol and less expensive than this type of ligands. The selected ligands are shown in Figure 1.9.

benzene-1,2-dithiol

3,4-toluenedithiol

trans-1,2-cyclohexanediol

cis-1,2-cyclohexanedicarboxylic acid
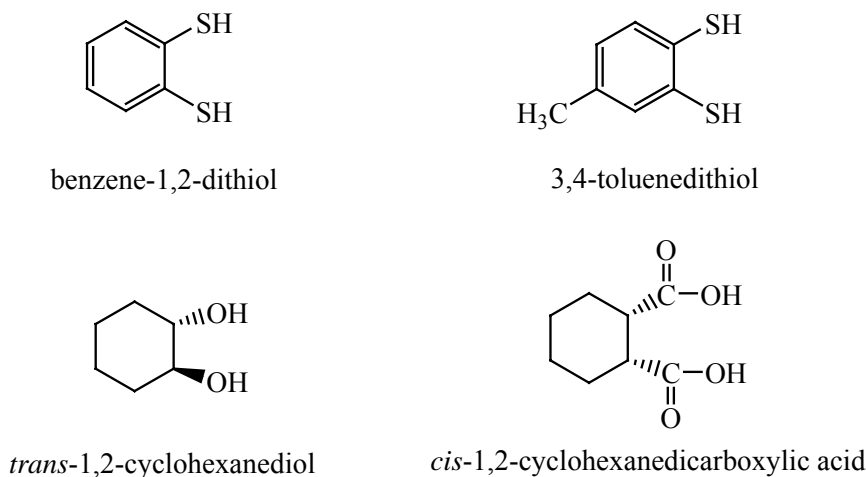
Fig. 1.9. The selected ligand systems.

1.5. Scope and aims of this dissertation

From the above introductions, it can be seen that the studies of model complexes of molybdoenzymes and tungstoenzymes are very interesting and important both in bioinorganic chemistry and industry.

The objective of the present work is to develop new approaches to synthesize model complexes of molybdenum and tungsten enzymes with one or two dithiolene ligands mimicking the natural compounds. Since in general the main product of reactions between dithiolene alkali salts and metal halogenide complexes are the trisdithiolenes, the challenge of the synthetic work is to find proper ways to control the reactions and to obtain the less dithiolene-coordinated complexes. To develop different synthetic approaches to Mo/W dithiolene complexes five reaction systems of $WOCl_4$, $MO_2Cl_2(dme)$, $MO_2(acac)_2$, $(Et_4N)_2[MO_2S_2]$ and $MCl_4(dme)$ (M=Mo, W) were studied. Besides the oxo-transfer model reaction from DMSO to PPh_3 has been used to determine the catalytic properties of the model compounds of some of the molybdenum complexes and their tungsten counterparts.

2. Results and Discussion

Since the existence of a universal pterin dithiolene cofactor ligand for the molybdenum and tungsten oxotransferases shows the biological significance of the fundamental chemistry of mono- and bis(dithiolene) molybdenum and tungsten complexes [57], lots of attention has been paid to the coordination chemistry of molybdenum and tungsten dithiolene compounds, which were referred to as the model complexes of molybdoenzymes and tungstoenzymes. Based on the crystallographic studies the molybdenum oxidoreductases have been classified into two groups. One group has mono-coordination of the pterin-dithiolene ligand to a molybdenum, e.g. aldehyde oxidoreductase and xanthine oxidase. The other group has bis-coordination of the dithiolene ligand, e.g. DMSO reductase [2]. Because of the existence of molybdenum and tungsten isoenzyems, the chemistry of tungsten mono- and bis(dithiolene) complexes has been developed in parallel [58-61]. Among the tungstoenzymes, on the basis of the sequence data, it was suggested that the F(M)DH enzymes have similarities to some molybdoenzymes including Mo-FDH, biotin-S-oxide reductase, and DMSO reductase [3]. A number of molybdenum and tungsten complexes have been synthesized, providing insights into the biological mechanisms by biomimetic oxygen atom transfer reaction systems [62].

2.1. Reactions of WOCl$_4$

2.1.1. Synthesis and Characterization of complexes 1-3

In this research the ligand precursor *trans*-1,2-cyclohexanediol was used to test the reaction procedure since it is a less expensive ligand compared with dithiolene ligands.

Treatment of two equivalents of *trans*-1,2-cyclohexanediol in dichloromethane with

stirred suspension of $WOCl_4$ in dichloromethane at ambient temperature for 6 h gave complex **1**. The reactions proceeded efficiently under these conditions the orange suspension rapidly turning light purple. Complex **1** was isolated in 37 % yield. A byproduct was formed as well, which has the same formula of complex **2** identified by mass spectrometry.

Synthesis of complex **2** was accomplished through the same reaction but change of the temperature from 25 ºC to 0 ºC for 30 min. Compound **2** was isolated in good yield (71 %), and no EI-MS signal of complex **1** was observed in the product. The complex **1** was conveniently isolated by crystallization due to the different solubility of **1** and **2** in dichloromethane and was stable in the air for several hours. Both of the compounds are stable for days under nitrogen atmosphere.
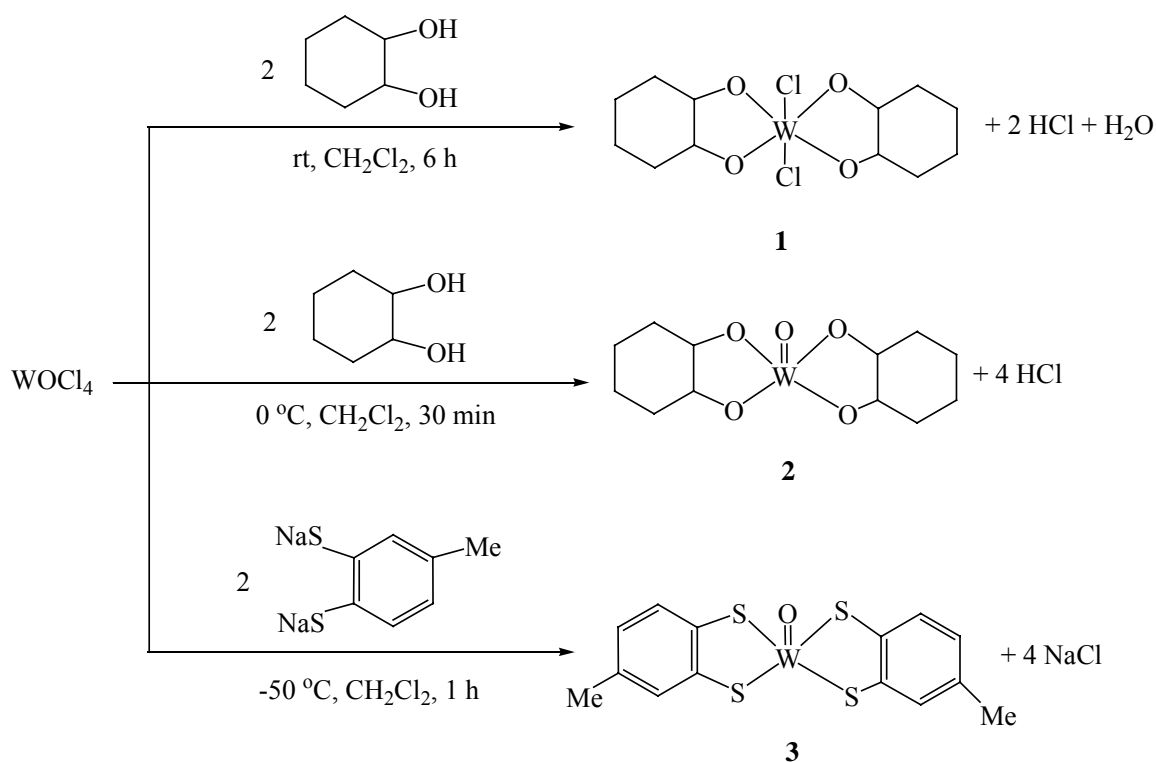
Scheme 2.1. Synthesis of complexes **1-3**.

Analytical and spectroscopic data were consistent with the proposed formulas. The EI mass spectrum of **1** contained a molecular ion peak at *m/z* 483 (25 %) and [*M*-Cl]$^+$

cluster peak at *m/z* 445 (20 %). The EI-MS of **2** contained a molecular ion at *m/z* 427 (100 %). In the infrared spectrum of complex **1** middle to strong bands at 398, 328 and 302 cm^{-1} exhibited and were assigned to the stretching of the W-Cl bond [63]. The spectrum of complex **2** shows strong bands at 980, 927 and 879 cm^{-1}, which are tentatively assigned to the W=O stretching mode [59, 64]. The different synthetic conditions of compounds **1** and **2** by changing the temperature indicate that the W=O bond is less reactive at lower temperature (for example, at 0 ºC). In comparison with the W=O bond the W-Cl bond is more active. Therefore to control the temperature is a proper way to avoid over-reacting of the reactants.

The attempt to prepare the 3,4-toluenedithiolato analogue complex using 3,4-toluenedithiol failed, whatever change of the reaction condition, even at −50 ºC a mixture was always obtained. The 3,4-toluenedithiol seems not strong enough to break all the W-Cl bonds. When treated with two equivalents of sodium 3,4-toluenedithiolato with WOCl$_4$ at −50 ºC for 1 h and then another 1 h at room temperature the desired product **3** was synthesized with 66 % yield with a satisfying elemental analysis results (Scheme 2.1). Sodium 3,4-toluenedithiolato is a stronger Lewis base and the salt NaCl is easy to remove by filtration. The ^{1}H NMR spectrum of complex **3** showed multiple peaks between δ=8-7 ppm for the benzene ring protons. The IR spectrum of complex **3** displays a stretch at 431 cm^{-1} for ν(W-S), which is similar to the W-S (ν=399-451 cm^{-1}) stretch reported by E. I. Stiefel et al. [65], just as expected.

2.1.2. Reactions of WOCl$_4$ with bis(2-hydroxyethyl) ether

The precursor complex **4** was prepared by a procedure analogous to that for the dichloro complexes [WOCl$_2$(L^{Me})] with the use of aminobis(phenolato) [O, N, O] donor ligands [66]. When WOCl$_4$ was treated with one equivalent of bis(2-hydroxyethyl) ether in dichloromethane at room temperature for 1 h, a white powder of **4** precipitated as pure product in 91 % yield (Scheme 2.2). During the

reaction, simple substitution of ligand with chlorine occurred. The volatile HCl is easy to remove by pump. The high yield product was obtained due to the irreversible reaction procedure. The proposed formula was confirmed by elemental analysis result and spectroscopic data. The EI mass spectrum of **4** contained a molecular ion peak at *m/z* 375 (2 %) and [*M*-Cl]$^+$ cluster peak at *m/z* 339 (100 %). The infrared spectra revealed bands assignable to a ν(W=O) vibration at 969, 917 and 861 cm^{-1} [58-59] and a ν(W-Cl) vibration at 340 cm^{-1} [67].
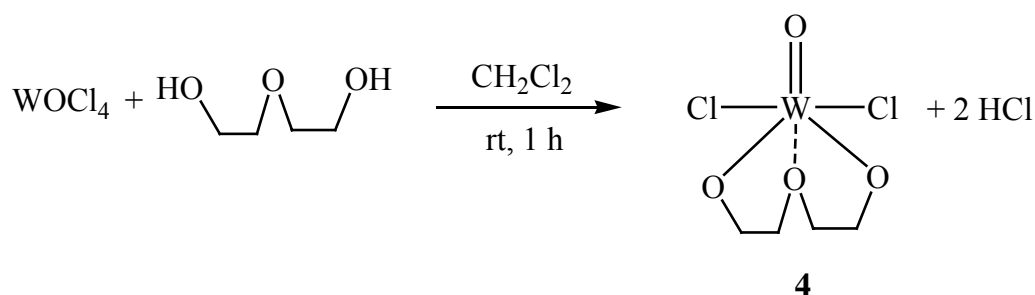
Scheme 2.2. Synthesis of complex **4**.

2.1.3. Synthesis and Characterization of complexes 5-7

The purpose of introducing of the bis(2-hydroxyethyl) ether ligand was to stabilize the tungsten atom. The precursor has two chlorine ligands, which was readily to be removed by substitution reactions. The tungsten complexes with mono-dithiolene and its related mono-chalcogen ligands are the aim of further reactions.

Addition of an equivalent of *trans*-1,2-cyclohexanediol in dichloromethane to a solution of **4** in dichloromethane at room temperature for 2 hours produced a white crystalline solid of **5** (73 %) according to the equation shown in scheme 2.3.

The EI mass spectrum of **5** contains a molecular ion peak at *m/z* 418 (100 %) and a [M-chd]$^+$ cluster peak at *m/z* 304 (48 %). An infrared absorption of **5** was observed at 923 cm^{-1}, which was assigned to ν(W=O) [58]. There was no evidence of the existence of a W-Cl bond both from elemental analysis and IR spectrum, indicating the completion of the reaction.
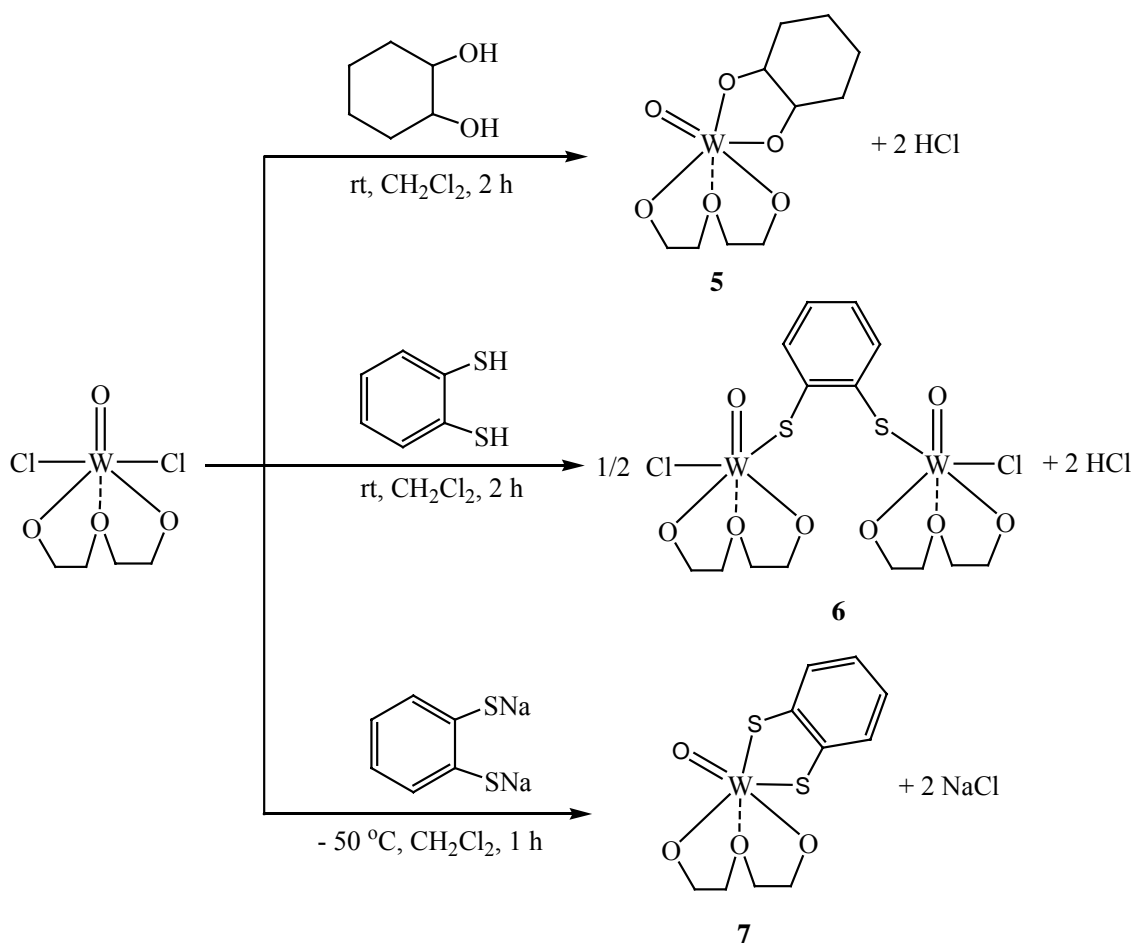
Scheme 2.3. Synthesis of complexes **5-7**.

When changing the ligand to benzene-1,2-dithiol, the proposed compound WO(O(CH$_2$)$_2$O(CH$_2$)$_2$O)(bdt) did not form. The elemental analysis and spectroscopic data indicated the product **6** to be the same or of repeated formula as that shown in scheme 2.3. Satisfactory analysis was obtained for C and H following the proposed formula. The infrared spectra revealed bands assignable to a ν(W=O) vibration at 969, 917 and 863 cm^{-1} [58-59], a ν(W-Cl) vibration at 340 cm^{-1} [67], and a ν(W-S) vibration at 405 cm^{-1} [65].

The reaction by the same procedure at -50 °C was unsuccessful as well and an unidentified byproduct formed.

Treatment of one equivalent of sodium benzene-1,2-dithiolate in dichloromethane with a stirred suspension of **4** in dichloromethane at -50 °C for 1 h and stirring over

night at room temperature gave a dark blue-green powder **7** in 69 % yield with a satisfying elemental analysis result. The EI-MS of **7** contains a [M-O]$^+$ cluster peak at *m/z* 430 (5 %), a [M-O(CH$_2$)$_2$O(CH$_2$)$_2$O]$^+$ cluster peak at *m/z* 339 (100 %) and the ligand [bdt]$^+$ cluster peak at *m/z* 140 (10 %). The IR data for **7** displays a peak at 916 cm^{-1}, which is assigned to the W=O stretching vibration [58]. Although there was no evidence of a W-S bond in the IR spectrum, the elemental analysis result indicates that no chlorine is part of the product and the percentage of sulfur fits the calculated result.

2.2. Reactions of the Molybdenum or Tungsten Dichloro Dioxo Dimethyl-Bispyridine Complexes

In this part we attempted to synthesize [MO$_2$(SPh)$_2$(bipy)] compounds of molybdenum and tungsten that were intended to be used as starting materials for an exchange of the thiophenolate ligands with other thiofunctional ligands. Because [MO(SR)$_4$]$^-$ [68-70] as well as [MO$_2$Cl$_2$(dme)] [71-72] compounds both of molybdenum and tungsten are available we expected the desired complexes to be easily synthesized as well. Unfortunately with molybdenum we were only able to synthesize a dimer with both of the molybdenum atoms reduced to the oxidation state V while tungsten behaved exactly as planned.

2.2.1. Substitution of Thiophenol for Chlorine

Equimolar reactions of 5,5'-dimethyl-2,2'-dipyridyl and MO$_2$Cl$_2$(dme) in dichloromethane at room temperature for 30 min resulted in the preparation of [MO$_2$Cl$_2$(mebipy)] (M=W (**8**), Mo (**10**), mebipy=5,5'-dimethyl-2,2'-dipyridyl) compounds by simple neutral ligand exchange reactions (Scheme 2.4). The nitrogen functional neutral ligand was chosen because it is more strongly bound to the metal center than the dimethoxyethane and therefore a better protector against unwanted

additional coordination of the thiophenol, and because it was expected to help the target complexes to better crystallize. Similar complexes of molybdenum and tungsten with bispyridine and 4,4'-dimethyl-bispyridine are known and their synthesis and some crystal structures are described in the literature [73-79]. The different synthetic approaches include the oxidation of carbonyl complexes [M(CO)$_4$(bipy)] with elemental halogen [73], reaction of solid [MO$_2$Cl$_2$] in molten bipyridyl [74], addition of freshly prepared (from MO$_3$) [MO$_2$Cl$_2$] to bipyridyl in tetrachloromethane [75], as well as the ligand exchange of the bipyridyl for solvent molecules like THF [76] or acetonitrile [77]. The most convenient synthesis probably is the preparation of MO$_2$Cl$_2$ from MOCl$_4$ in the presence of bipyridyl [78]. Recently a procedure was published that reacts tungstate with a bipyridine ligand in presence of trimethyl chlorosilane with the advantage of using rather easy to handle starting materials [79]. However, because we often use the dimethoxyethane adducts [MO$_2$Cl$_2$(dme)] as starting materials both compounds were easily available to us and they also have the advantage of being less sensitive than the [MOCl$_4$] compounds. We therefore simply followed the ligand exchange procedure. The obtained tungsten (**8**) and molybdenum (**10**) compounds were characterized by elemental analysis and infrared spectroscopy showing the characteristic strong bands for the antisymmetric and symmetric OMO valences at 955 cm^{-1}, 913 cm^{-1} (**8**) and 936 cm^{-1}, 904 cm^{-1} (**10**) respectively which is in perfect agreement with previously reported data [73-82].
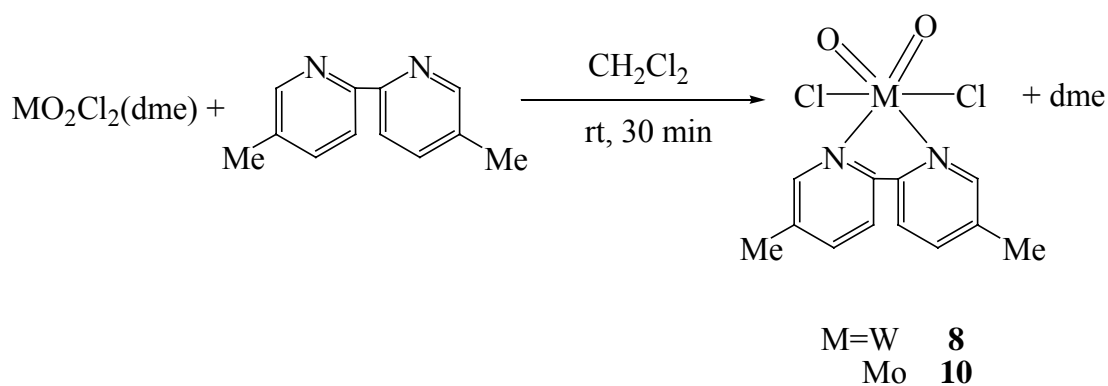
Scheme 2.4. Synthesis of complexes **8** and **10**.

2.2.2. Synthesis of WO$_2$(SPh)$_2$(mebipy) (9), Mo$_2$O$_4$(SPh)$_2$(mebipy)$_2$ (11) and Mo$_2$O$_4$(SPh-Cl)$_2$(mebipy)$_2$ (13) and Structural Characterization of 9 and 11

Treatment of a mixture of two equivalents of thiophenol and two equivalents of triethylamine in acetonitrile with a stirred suspension of **8** in acetonitrile at ambient temperature for 2 hours gave complex **9** in 65 % yield. The same procedure was performed with the ligands thiophenol and 4-chlorothiophenol with **10** for 30 min to afford **11** (52 %) and **13** (79 %), respectively (Scheme 2.5). While the tungsten compound reacted exactly as expected to form WO$_2$(SPh)$_2$(mebipy) (**9**) the molybdenum compound underwent reduction and dimerisation to form Mo$_2$O$_4$(SPh)$_2$(mebipy)$_2$ (**11**) or Mo$_2$O$_4$(SPh-Cl)$_2$(mebipy)$_2$ (**13**) and diphenyldisulfide. The IR spectrum of **9** showed two broad absorption bands at 939 and 859 cm^{-1}. These data are close to the reported vibrations at 935-960 and 900-915 cm^{-1}, which are assigned to the symmetric and antisymmetric stretches of the *cis*-[WO$_2$]$^{2+}$ core [67]. The infrared spectra of **11** and **13** contain bands at 947 and 931 cm^{-1}, respectively, assigned to the terminal Mo=O stretch of the Mo$_2$O$_3$ moiety at 955 cm^{-1} [83]. A sharp band at 728 cm^{-1} of **13** assignable to ν(Mo-O-Mo) was observed [72]. The IR spectra of **13** show bands in the range of 390-313 cm^{-1}, which are distinctive for the Mo-S vibrations [84]. Of both complexes **9** and **11** crystals were obtained that were suitable for X-ray structural analysis. Selected bond lengths and angles are listed in table 2.1 and 2.2.
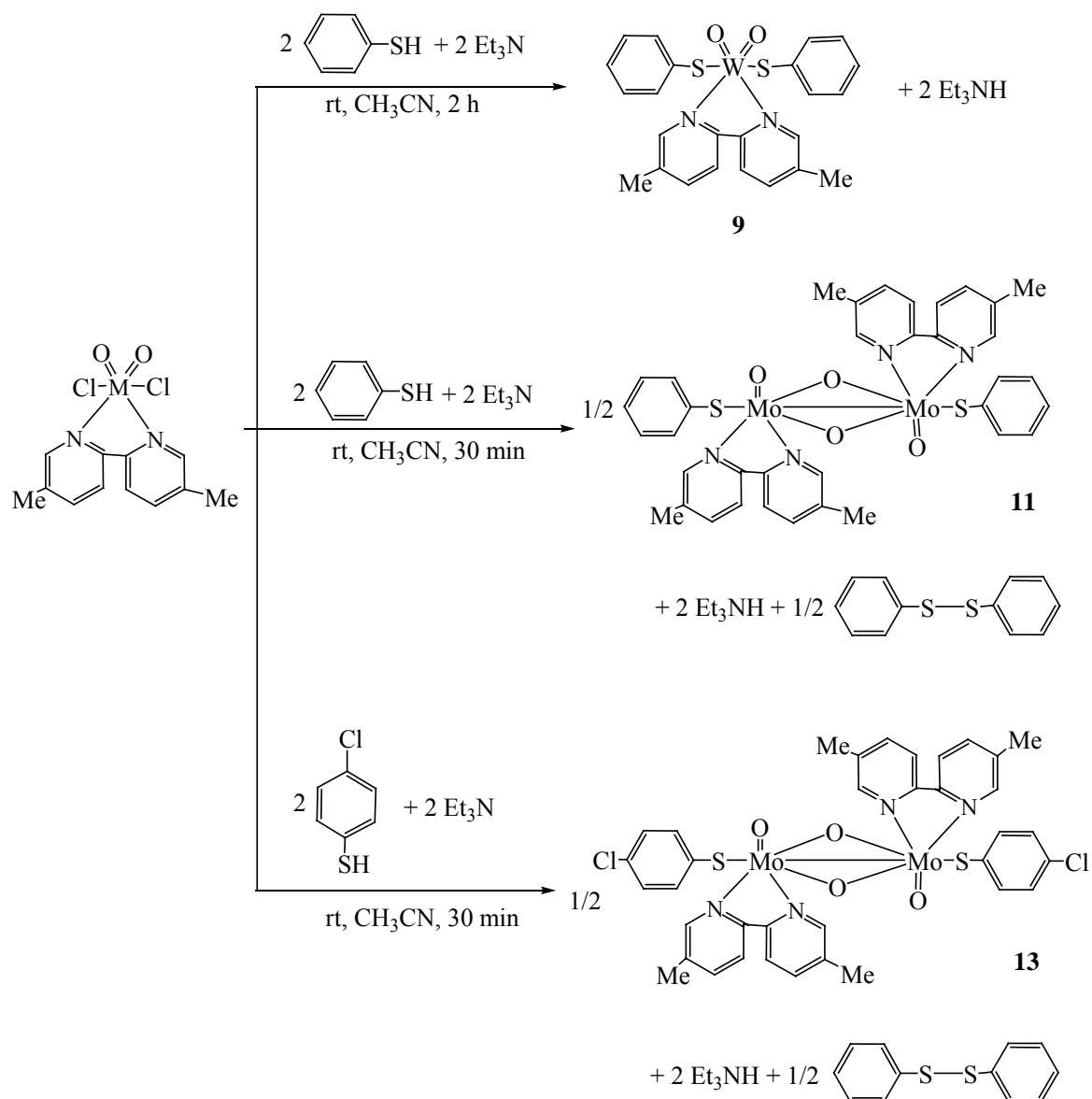
Scheme 2.5. Synthesis of complexes **9**, **11** and **13**.

Table 2.1. Selected bond lengths [Å] and angles [°] for **9**.

W(1)-O(1)	1.721(2)	O(1)-W(1)-O(2)	108.83(11)
W(1)-O(2)	1.729(2)	O(1)-W(1)-N(2)	91.39(10)
W(1)-N(2)	2.278(3)	O(2)-W(1)-N(2)	159.52(10)
W(1)-N(1)	2.300(2)	O(1)-W(1)-N(1)	161.02(10)
W(1)-S(3)	2.444(1)	O(2)-W(1)-N(1)	89.94(10)

W(1)-S(2)	2.453(1)	N(2)-W(1)-N(1)	70.08(9)
O(1)-W(1)-S(3)	100.77(9)	N(1)-W(1)-S(3)	81.24(7)
O(2)-W(1)-S(3)	90.90(8)	O(1)-W(1)-S(2)	91.61(9)
N(2)-W(1)-S(3)	81.90(7)	O(2)-W(1)-S(2)	99.65(8)
N(2)-W(1)-S(2)	82.49(7)	C(13)-S(2)-W(1)	106.32(11)
N(1)-W(1)-S(2)	82.13(7)	C(5)-N(1)-W(1)	121.4(2)
S(3)-W(1)-S(2)	160.26(3)	C(11)-N(2)-W(1)	121.4(2)
C(19)-S(3)-W(1)	110.57(11)	C(1)-N(1)-W(1)	119.45(19)
C(7)-N(2)-W(1)	120.0(2)		
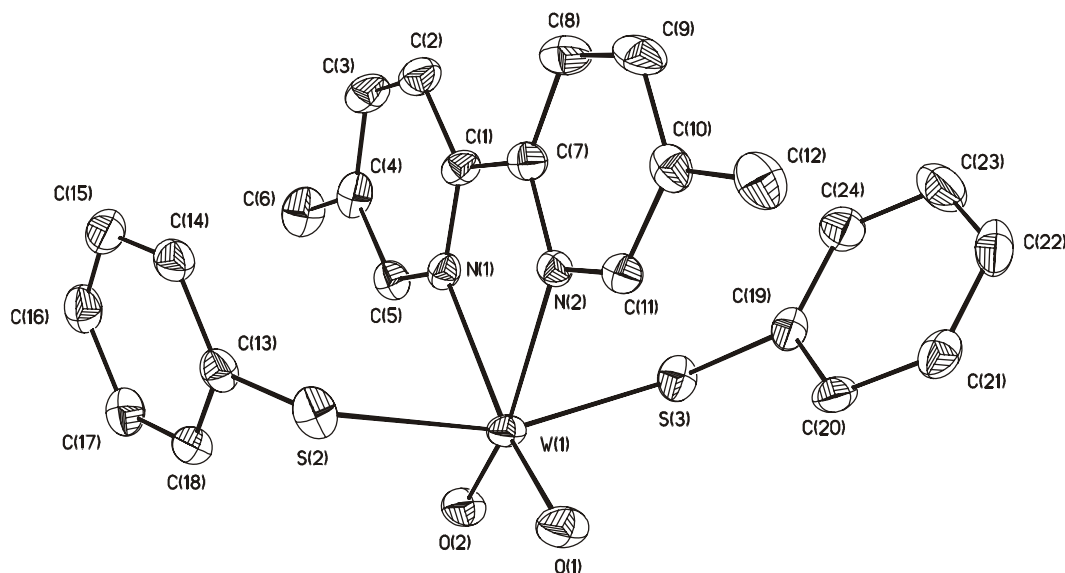
Fig. 2.1. View of the structure of $WO_2(SPh)_2(mebipy)$ (**9**) without hydrogen atoms (with numbering scheme).

The monomeric tungsten compound **9** (Fig. 2.1) exhibits a structure that is very similar to that of $[WO_2Cl_2(bipy)]$ [78] and that of $[WO_2(SPh)_2(phen)]$ [85]. Furthermore the pseudo octahedral geometry with the bending of the mono anionic axial ligands towards the neutral ligangs opposite the *cis*-oxo core is typical for monomeric molybdenum and tungsten *cis*-dioxo compounds. The W=O distances are 1.721 Å and

1.729 Å respectively, which is at the lower end of the so far reported values in the range of 1.702-1.792 Å [76,78,86-88]. The comparatively large distances were reported for the very similar bipy complex with the chloro ligands [78]. The tungsten sulfur distances (2.444 Å, 2.453 Å) are again very close to the reported ones (2.440 Å, 2.464 Å) [78] but more symmetrical. The 5,5'-dimethyl-2,2'-dipyridyl ligand (2.278 Å, 2.300 Å; N-W-N 70.08°) is bound similarly to the phen ligand in $[WO_2(SPh)_2(phen)]$ [85] (2.275 Å, 2.294 Å; 71.3°) although the latter could be regarded as less flexible. Other tungsten (VI) nitrogen distances for ligands derived from the bispyridine system are in the range of 2.263-2.322 Å [76,78,87-88]. Bond angles for O=W=O (108.83°) and X-W-X (with X representing the axial anionic ligands; 160.26°) are each in the upper range compared with similar tungsten and molybdenum structures (O=M=O: 102.2-110.26° [75,76,78,88-89], X-M-X: 148.0-166.71° [75-76,78,31,88,92]). In compounds **9** the distortion from an ideal octahedral geometry is in comparison rather large for the MO$_2$ moiety and rather low for the axial thiolate ligands.

The molybdenum compound **11** (Fig. 2.2) can be compared to several published complexes for the $Mo_2O_2(\mu\text{-O})_2$ core with different ligand systems is not rare and can even be found as part of the polyoxo molybdates. On the other hand only three rather old X-ray structures are known containing this core with thiofunctional ligands: the $[Mo_2O_4(SPh)_4]^{2-}$ anion [93], $[Mo_2O_4(SCH_2CH(NH_2)CO_2Et)_2]$ [94] and the $[Mo_2O_4(SCH_2CH(NH_2)CO_2)_2]^{2-}$ anion [95]. The two former complexes contain molybdenum centers that are coordinated to five ligands in square pyramidal geometry with an additional metal-metal bond. The later complex resembles our structure with six ligand atoms in octahedral geometry with an additional metal-metal bond. Both oxo ligands of the two molybdenum centers are on the same side of the molecule in all cases. The metal-oxo distances are in the range of 1.657 Å to 1.712 Å (compound **11**: 1.691/1.687 Å) with the longer distances for the compounds with six ligands around each molybdenum. The metal-metal distances are between 2.562 Å and 2.627 Å (compound **11**: 2.584 Å) without any observable trend with the coordination number. The $Mo_2O_2(\mu\text{-O})_2$ core of compound **11** is folded along the line between both μ-oxo ligands with a dihedral angle of 143° between the Mo-$(\mu\text{-O})_2$

planes. The $Mo_2O_2(\mu-O)_2$ core itself shows a little un-symmetry meaning that each molybdenum binds one bridging oxo closer (1.917/1.924 Å) than the other (1.963/1.986 Å). O1 is bound closer to Mo1 while O2 is closer to Mo2. This behaviour is typical for that kind of dimeric oxo-bridged molybdenum compounds. The two molybdenum atoms are sitting above the equatorial O_2NS planes by 0.387 Å and 0.425 Å respectively in direction of the terminal oxo ligands.
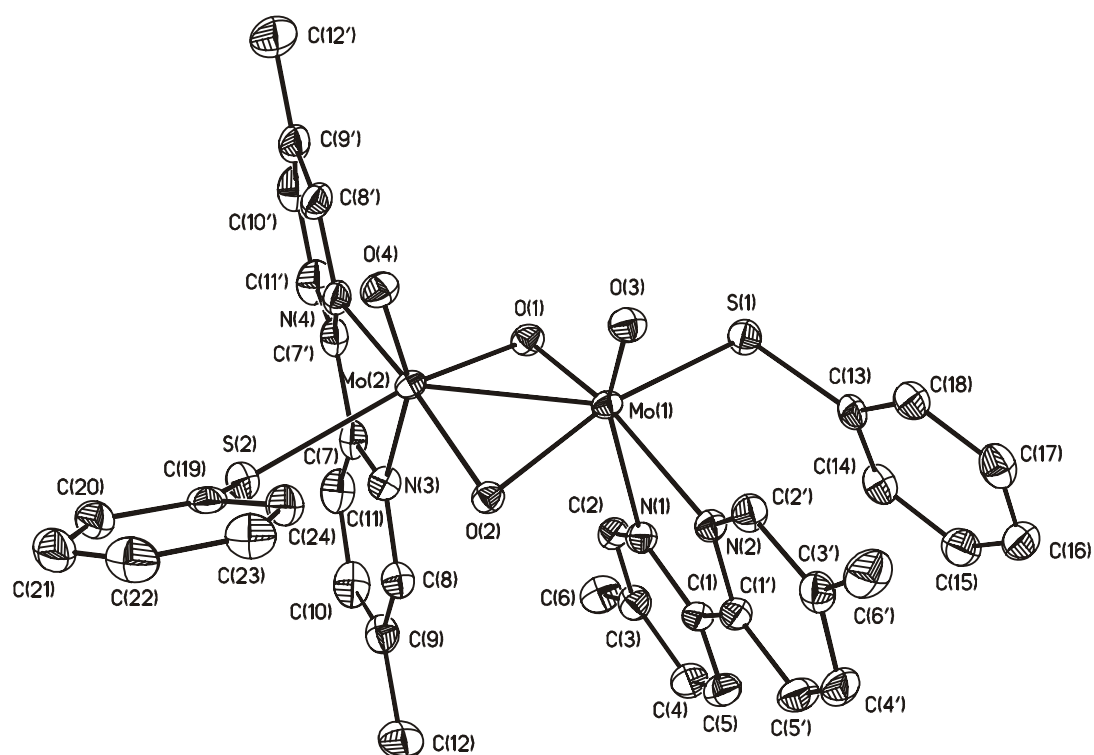
Fig. 2.2. View of the structure of $Mo_2O_4(SPh-Cl)_2(mebipy)_2$ (**11**) without hydrogen atoms (with numbering scheme).

Table 2.2. Selected bond lengths [Å] and angles [°] for **11**.

Mo(1)-O(3)	1.691(2)	O(3)-Mo(1)-O(1)	111.98(7)
Mo(1)-O(1)	1.924(2)	O(3)-Mo(1)-O(2)	106.13(7)
Mo(1)-O(2)	1.986(2)	O(1)-Mo(1)-O(2)	90.74(6)

Mo(1)-N(2)	2.261(2)	O(3)-Mo(1)-N(2)	86.48(7)
Mo(1)-N(1)	2.332(2)	O(1)-Mo(1)-N(2)	161.41(7)
Mo(1)-S(1)	2.497(1)	O(2)-Mo(1)-N(2)	85.86(7)
Mo(1)-Mo(2)	2.584(1)	O(3)-Mo(1)-N(1)	154.95(7)
Mo(2)-O(4)	1.687(2)	O(1)-Mo(1)-N(1)	91.64(7)
Mo(2)-O(2)	1.917(2)	O(2)-Mo(1)-N(1)	80.78(7)
Mo(2)-O(1)	1.963(2)	N(2)-Mo(1)-N(1)	69.78(7)
Mo(2)-N(4)	2.261(2)	O(3)-Mo(1)-S(1)	97.11(6)
Mo(2)-N(3)	2.333(2)	O(1)-Mo(1)-S(1)	81.36(5)
Mo(2)-S(2)	2.518(1)	O(2)-Mo(1)-S(1)	156.74(5)
S(1)-C(13)	1.779(2)	N(2)-Mo(1)-S(1)	94.67(5)
N(1)-Mo(1)-S(1)	77.64(5)	O(3)-Mo(1)-Mo(2)	99.26(6)
O(1)-Mo(1)-Mo(2)	48.98(5)	O(2)-Mo(1)-Mo(2)	47.40(4)
N(2)-Mo(1)-Mo(2)	132.82(5)	N(1)-Mo(1)-Mo(2)	102.73(5)
S(1)-Mo(1)-Mo(2)	130.282(19)	O(4)-Mo(2)-O(2)	112.52(7)
O(4)-Mo(2)-O(1)	108.14(8)	O(2)-Mo(2)-O(1)	91.66(6)
O(2)-Mo(2)-N(4)	156.88(7)	O(1)-Mo(2)-N(4)	79.47(7)
O(2)-Mo(2)-N(3)	88.22(7)	O(1)-Mo(2)-N(3)	83.39(7)
O(2)-Mo(2)-S(2)	90.71(5)	O(1)-Mo(2)-S(2)	155.80(5)
O(4)-Mo(2)-Mo(1)	101.16(6)	O(2)-Mo(2)-Mo(1)	49.70(5)
O(1)-Mo(2)-Mo(1)	47.69(4)	N(4)-Mo(2)-Mo(1)	127.02(5)
N(3)-Mo(2)-Mo(1)	102.57(5)	S(2)-Mo(2)-Mo(1)	140.409(18)
C(13)-S(1)-Mo(1)	104.39(8)	Mo(1)-O(1)-Mo(2)	83.33(6)
Mo(2)-O(2)-Mo(1)	82.90(6)	C(1)-N(1)-C(2)	118.9(2)
C(1)-N(1)-Mo(1)	118.73(15)	C(2)-N(1)-Mo(1)	122.20(15)

Interestingly one benzyl ring of a thiolate ligand is bent towards the bipyridyl ligand at the same molybdenum and oriented parallel to this planar system. The other thiolate ligand is bent away from the methyl-bipyridyl ligand and its plane is more or

less perpendicular to the mbipy plane.

If we compare the tungsten monomer and the molybdenum dimer we note that in the molybdenum's vicinity three oxygen ligand atoms are present and only one sulfur while tungsten is bound to two sulfur and two oxygen atoms. This mirrors the higher oxo philicity of molybdenum and the higher thio philicity of tungsten, which was observed before [96].

2.2.3. Oxygen substitution reaction of 11

In order to obtain compounds analogues to the protein-bound sites of molybdoenzymes, the reaction of silicon electrophiles with the oxo group was investigated. Complex **12** was prepared by a procedure similar to the oxygen substitution reaction of tetraoxometalates reported by R. H. Holm et al. [97]. Reaction of **11** with one equivalent of 1,2-$C_6H_4(SSiMe)_2$ in acetonitrile at -20 ºC for 3 min afforded complex **12** as dark green solid (49 %) with replacement of one oxo ligand by the disilylated version of benzene-1,2-dithiolato ligand (Scheme 2.6).
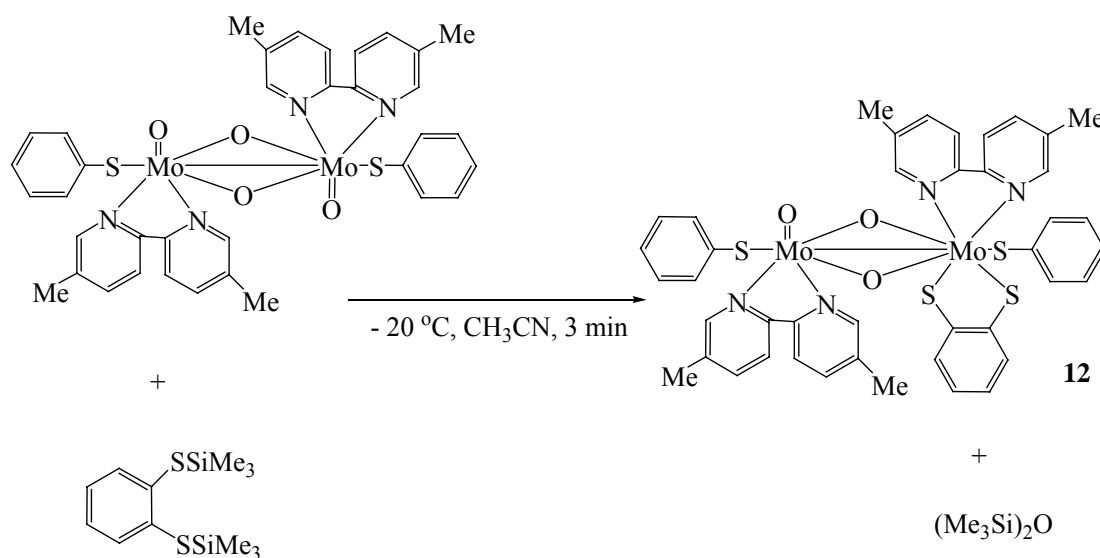
Scheme 2.6. Synthesis of complex **12**.

The obtained complex **12** was characterized by elemental analysis and EI-MS as well as infrared spectroscopy. The infrared spectra revealed bands assignable to the ν(Mo-O) vibration at 461 cm^{-1} [98] and the ν(Mo-O-Mo) vibration at 747 cm^{-1} [72]. The sharp band at 948 cm^{-1} is in agreement with the reported data of the terminal Mo=O stretch of Mo_2O_3 moieties [83,99]. The spectrum also contains peaks at 397 and 351 cm^{-1} fit for the reported 390-313 cm^{-1} for the Mo-S stretching vibration [45,98,100].

The attempts of thiol exchange for **9** by benzene-1,2-dithiol failed, probably due to the steric hinderance of the bulky 5,5'-dimethyl-2,2'-dipyridyl and *cis*-dioxo group.

2.3. Reactions of $MO_2(acac)_2$ (M=Mo, W)

The existence of a universal pterin dithiolene cofactor ligand for the molybdenum and tungsten oxotransferases supports a biological significance of the fundamental chemistry of mono- and bis(dithiolene) complexes of these elements. Members of the DMSO reductase family of enzymes contain two pterin dithiolene ligands; at least one enzyme functions by using the minimal reaction couple $Mo^{IV}+Me_2SO \leftrightarrow Mo^{VI}O+Me_2S$. Accordingly, the synthesis, and reactivity of bis(dithiolene) Mo(VI) complexes of benzene-1,2-dithiolate and related ligands have been investigated. Numerous model complexes for the oxidized state of these molybdenum and tungsten enzymes have been synthesized using a (thiolato, N), (thiolato, thioketone) or (thiolato, thioether) ligand [101-103]. However, few reports on the synthesis of dioxo molybdenum and tungsten (VI) complexes having a dithiolene skeleton have been found [37,39,45,50,104-105] due to this type of complexes is unstable caused by the *trans* influence of a M=O (M=Mo, W) group toward one of the thiolate ligands [106]. Here we report the convenient synthesis of model complexes for the oxidized form of molybdenum and tungsten oxidoraductases (especially, DMSO reductase and F(M)DH enzymes) and similar complexes that have molybdenum or tungsten (VI), two terminal oxo groups, and substituted benzendithiolato ligands as models of the pterin cofactor, $(Ph_3PH)_2[MO_2(bdt)_2]$ (M=Mo, W). Three more related

chalcogenide ligands compounds MoO$_2$(O(CH$_2$)NH(CH$_2$)O)·DMF, MoO$_2$(2-amino-thiophenol)$_2$ and (Ph$_3$PH)$_2$[MoO$_2$(chd)$_2$] are also investigated. In this part, MO$_2$(acac)$_2$ (M=Mo, W) have been used as precursors for M^{VI}O$_2$ (M=Mo, W) complexes in substitution reactions with protonated ligands. The synthetic routs and properties of the products are presented. The reactivity of **17** and **18** with DMSO is shown in Section 3.

2.3.1. Synthesis and Characterization of 14-18

The synthesis of the compound MoO$_2$(O(CH$_2$)$_2$NH(CH$_2$)$_2$O) was reported previously by Mozgin et al. by the reaction of molybdic acid and diethanolamine in water under reflux conditions [107]. Herein, we report a novel synthetic route for the preparation of [MoO$_2$(O(CH$_2$)$_2$NH(CH$_2$)$_2$O)·DMF] (**14**). MoO$_2$(acac)$_2$ reacts with one equivalent of diethanolamine in DMF at room temperature to form the compound **14**. After 12 h, the solvent was concentrated to yield X-ray quality yellow crystals of **14** (49 % yield) at room temperature. The IR spectrum of **14** shows very strong bands in the range of 891-932 cm^{-1}, which are distinctive for the MoO$_2$$^{2+}$ moiety [108]. Other important frequency bands are around 1100 cm^{-1} (O-C stretch), 2960 cm^{-1} (C-H stretch), and 1440 cm^{-1} (C-H bend), which are very similar to the previously reported data as 1080, 2940 and 1480 cm^{-1} [107].

Complex **15** was synthesized by the similar method as that reported for dioxo molybdenum (VI) compounds with N, O-ligands derived from carbohydrates by W. A. Herrmann et al. [109]. The reaction of MoO$_2$(acac)$_2$ with two equivalents of 2'-pyridinyl alcohol in dry methanol at room temperature for 30 min forms the dioxo molybdenum (VI) pyridinyl alcoholate complexes. Under the same conditions, two equivalents of 2-amino-thiophenol were added to the suspension of MoO$_2$(acac)$_2$ in methanol to form the dark dioxo molybdenum complex **15** with 63 % yield and satisfying elemental analysis results. The IR spectra exhibits strong bands at 935 and 905 cm^{-1}, which are near the reported data of 920-940 and 890-910 cm^{-1} by J. H.

Enemark et al., assigned to the symmetric and asymmetric stretches of the MoO_2^{2+} moiety [110 a-b]. Furthermore, two clear medium IR band were observed at 388 and 340 cm^{-1}, which are associated with the vibrations of the Mo-S bonds [98,100].
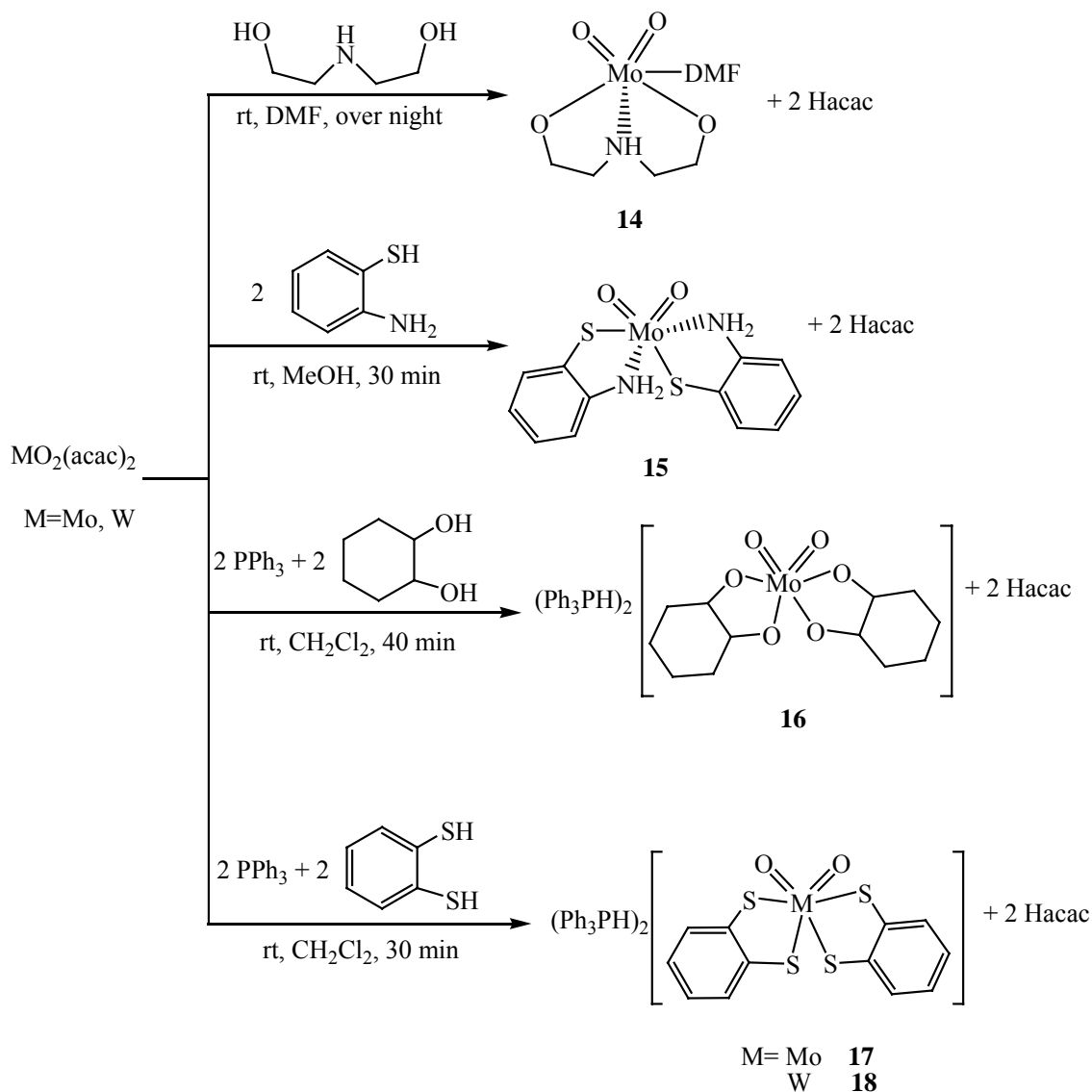
Fig. 2.7. Scheme for the synthesis of complexes **14-18**.

Complexes **16-18** were synthesized by the similar method as that reported for oxovanadium bis(1,2-dithiolate) compounds by J. H. Enemark et al. [111] (Scheme 2.7). When the mixture of two equivalents of PPh_3 and two equivalents of *trans*-1,2-cyclohexanediol in dichloromethane was treated to $MoO_2(acac)_2$ at room temperature, the dark gray solution changed to red-brown gradually. Hacac was

readily removed under vacuo. The product **16** was obtained as brown solid in 66 % yield. Complexes **17** and **18** were formed by the same procedure. The initial color after addition of the reactants changed from dark blue to gray-green (reaction **17**) and from light green to dark blue-green (reaction **18**) after 30 min, respectively. Both products were obtained as dark green solid with 71 % (for **17**) and 63 % (for **18**) yields.

Table 2.3. IR bands (cm^{-1}) of ν(M=O) (M=Mo, W) of complexes **14-18** in KBr disk.

		IR band	
Complex	Ref.	ν_s (M^{VI}=O),	ν_{as} (M^{VI}=O)
$MoO_2(O(CH_2)_2NH(CH_2)_2O)\cdot DMF$	**14**	892	840
MoO_2(2-amino-thiophenol)$_2$	**15**	935	905
$(Ph_3PH)_2[MoO_2(chd)_2]$	**16**	930	855
$(Ph_3PH)_2[MoO_2(bdt)_2]$	**17**	932	865
$(Ph_3PH)_2[WO_2(bdt)_2]$	**18**	903	857
$(Et_4N)_2[W^{VI}O_2(bdt)_2]$	**a**	888	847
$(Et_4N)_2[W^{VI}O_2(1,2-S_2C_2(CN)_2)_2]$	**b**	906	860
$(Et_4N)_2[Mo^{VI}O_2(bdt)_2]$	**c**	858	831

a Ref. 113; b Ref. 49; c Ref. 45.

Analytical and spectroscopic data were consistent with the proposed formulas. In the IR spectra two strong bands were observed at 930, 855 (for **16**), 932, 865 (for **17**), and 903, 857 (for **18**) cm^{-1} assigned to the symmetric and asymmetric [112] stretches of the *cis*-[M^{VI}O$_2$]$^{2+}$ (M=Mo, W) core [102]. The values of the M=O (M=Mo, W) stretches for the products **14-18** in solid state together with those of related compounds are summarized in table 2.3. The infrared spectra of compound **16** exhibits a strong band at 540 cm^{-1} assigned to Mo-O stretching vibration [110]. A very strong band assignable to ν(C-S) [100] was observed at 682 cm^{-1} of complex **17**, while for complex **18** two

bands at 396 and 338 cm^{-1} were observed, which are assigned to the W-S bond [46]. As discussed above, we concluded that the synthesis of **16-18** was achieved via ligand substitution of $MO_2(acac)_2$ (M=Mo, W) using the relevant pro-ligand and properly controlled amount of triphenyl phosphine as a base.

2.3.2. X-ray crystallographic analysis of compounds 14

An X-ray crystal structure analysis has been carried out on **14**. The molecular structure is shown in figure 2.3 while selected important bond lengths and angles are summarized in table 2.4. The X-ray structural analysis revealed that the complex consists of a discrete mononuclear unit in which the diethanolateamine is coordinated to the molybdenum atom as a tridentate ligand to form two five-members rings. Two oxo ligands coordinate to the metal to form a stable *cis*-dioxomolybdenum (VI) core. A DMF molecule trans to one oxo group completes the distorted octahedral coordination sphere.

The metrical parameters are as expected for mononuclear *cis*-dioxomolybdenum (VI) species. The Mo=O distances are 1.7168 Å (O4; trans to DMF) and 1.7225 Å (O3; trans to N). They are common for structures with the *cis*-$[MoO_2]$ unit in the range of 1.66-1.76 Å [114]. The bond lengths of Mo-O$_{alkoxy}$ of 1.9256 Å and 1.9217 Å, are consistent with molybdenum (VI) alkoxide interactions [115-116]. The Mo-N distance of 2.292 Å is long as a consequence of the strong trans influence of an oxo ligand (O3). Again this is in the range of analogous complexes with the $[MoO_2]^{2+}$ core (2.28-2.50 Å) [117-118].

Table 2.4. Selected bond lengths [Å] and angles [°] for **14**.

| Mo(1)-O(4) | 1.7168(17) | O(4)-Mo(1)-O(3) | 106.87(8) |
| Mo(1)-O(3) | 1.7225(17) | O(4)-Mo(1)-O(2) | 100.45(8) |

Mo(1)-O(2)	1.9217(17)	O(3)-Mo(1)-O(2)	100.44(7)
Mo(1)-O(1)	1.9256(17)	O(4)-Mo(1)-O(1)	98.32(8)
Mo(1)-N(1)	2.292(2)	O(3)-Mo(1)-O(1)	100.38(7)
Mo(1)-O(5)	2.4376(18)	O(2)-Mo(1)-O(1)	146.43(7)
O(4)-Mo(1)-N(1)	95.24(8)	O(3)-Mo(1)-N(1)	157.89(8)
O(2)-Mo(1)-N(1)	74.97(7)	O(1)-Mo(1)-N(1)	75.81(7)
N(1)-Mo(1)-O(5)	75.77(7)	C(4)-O(2)-Mo(1)	123.71(14)
C(1)-O(1)-Mo(1)	121.16(14)	C(2)-N(1)-Mo(1)	109.46(14)
C(3)-N(1)-Mo(1)	108.85(14)		
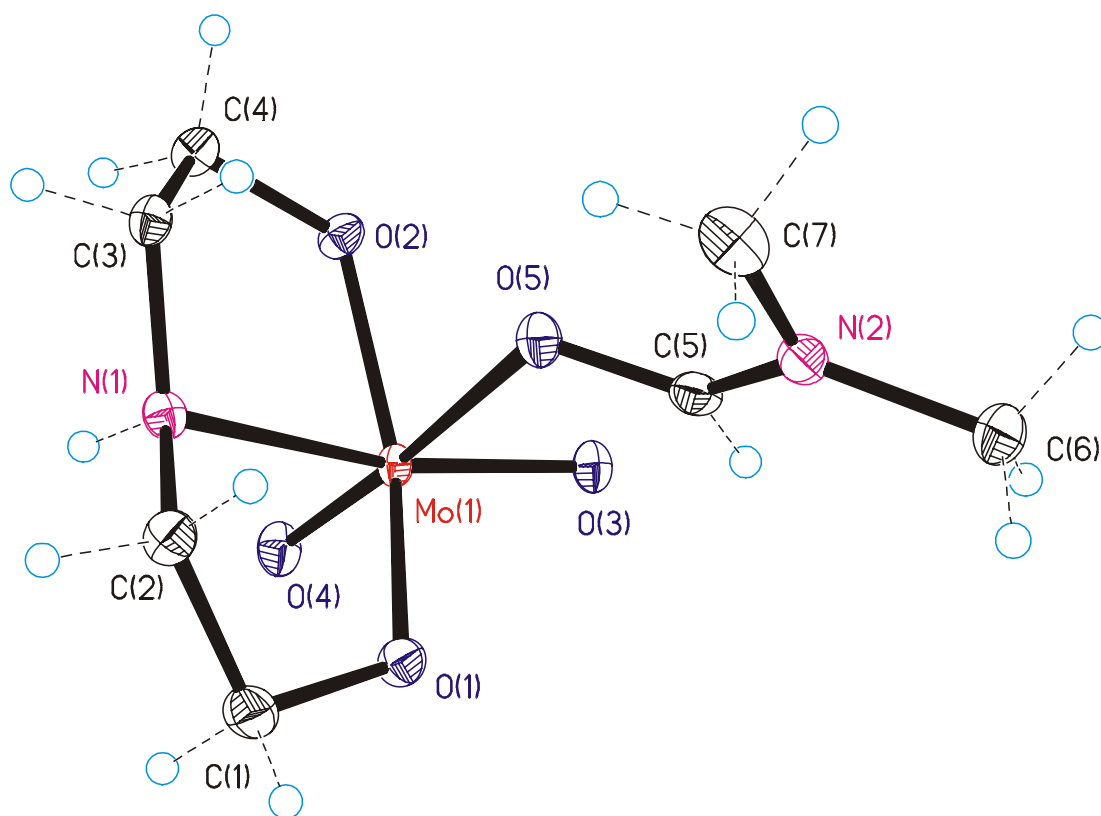
Fig. 2.3. View of the structure of [MoO$_2$(O(CH$_2$)$_2$NH(CH$_2$)$_2$O)·DMF] (**14**) (with numbering scheme). Ellipsoids are drawn at 50% probability.

The length of the Mo-O5 bond is 2.4376 Å, which is rather long, implying a very weak bonding interaction between the molybdenum and the DMF solvent molecule.

This coordination nevertheless allows the molecule to obtain a stable distorted octahedral coordination geometry. The Mo-O (DMF) distance is longer than Mo-O distances formed by other solvent molecules e.g. MeOH with 2.289-2.385 Å [114, 108] or H_2O with 2.255-2.293 Å [119]. The comparably weak bonding interaction indicates that DMF is particularly easy to remove from the molecule. This molecule therefore should be a good starting material for reactions where one oxo group and the solvent will be replaced by a bidentate ligand. The most evident distortions of this structure from the idealized octahedral geometry are defined by the N1-Mo-O1 (75.81°), N1-Mo-O2 (74.97°) and O1-Mo-O2 (146.43°) angles. With the strain of two five-members chelated rings, two alkoxy groups are bent towards the nitrogen atom.
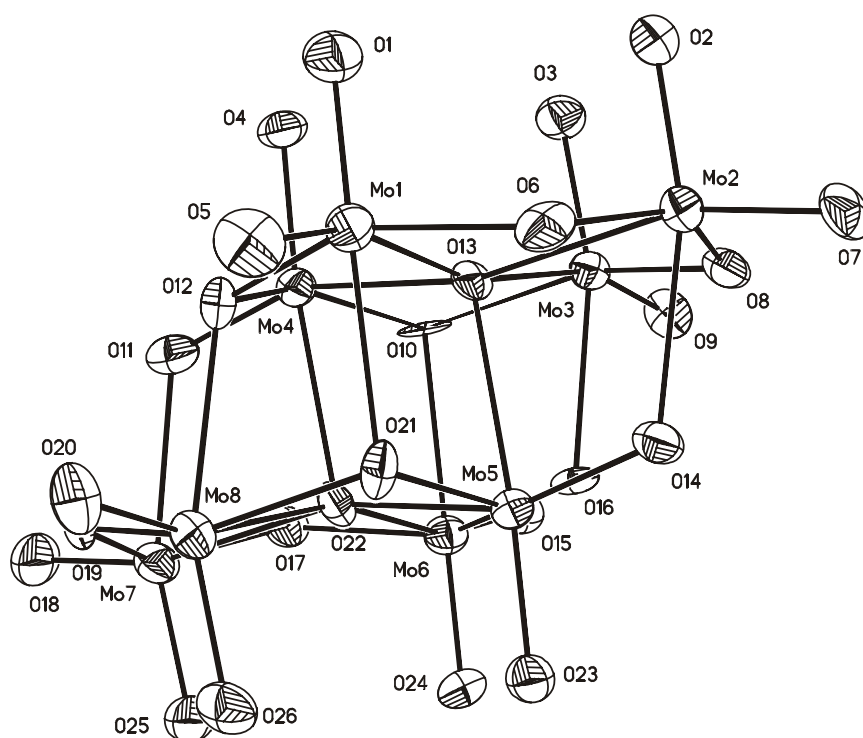
Fig. 2.4. View of the structure of complex **14-1** without hydrogen atoms (with numbering scheme). Ellipsoids are drawn at 50% probability.

The oxygen substitution reaction of 1,2-C_6H_4(SSiMe)$_2$ similar to the reaction of complex **12** was performed with complex **14** as well. Unfortunately here a Mo-O cluster formed. This may have happened because of the existence of traces of water or

air, indicating that the product is extremely sensitive. Since the structure is disordered, details of the bonds and angles will not be discussed, but the structure is displayed here (**14-1**) (Fig. 2.4).

2.4. Reactions of (Et$_4$N)$_2$[MO$_2$S$_2$] (M=Mo, W)

2.4.1. Synthesis and Characterization of complex 19

Transition-metal di- and polysulfide complexes have been found to react with substituted alkynes to yield metallo-1,2-enedithiolate complexes [112,120-124]. The reaction between tetraoxothio metalates (MO$_{4-n}$S$_n$)$^{x-}$ (n=1-4) and electrophiles is a powerful method for preparing sulfur-rich derivatives of transition metals [125]. The related reactions are often complicated by the redox processes concerning metal centers and/or ligands [65]. T. B. Rauchfuss [122] reported on the addition of alkynes to ReS^{4-} through a four-electron reduction leading to (Et$_4$N)$_4$\{Re$_4$S$_{12}$[S$_2$C$_2$(TMS)$_2$]$_2$\} (TMS=trimethylsilyl), a compound containing rhenium sulphide, disulfide groups, and dithiolene ligands.

On the basis of the results of A. A. Eagle et al. [126], similar reaction conditions have been used with phenylacetylene since a reaction involving the formation of Mo/W complexes with unsymmetric dithiolene ligands was expected. Unfortunately no reaction was observed neither under ambient condition nor at higher temperature. One equimolar amount of phenylacetylene was revealed to be not electrophilic enough to react with (Et$_4$N)$_2$[MO$_2$S$_2$] (M=Mo, W). Applying the conditions published by K. Tatsumi et al. [127], five equivalents of phenylacetylene were used. Surprisingly the reaction between (Et$_4$N)$_2$[MoO$_2$S$_2$] and five equivalents of phenylacetylene did not happen. However, when using the tungsten precursor (Et$_4$N)$_2$[WO$_2$S$_2$] instead of the molybdenum one, in acetonitrile at ambient temperature for 4 days, a yellow microcrystalline powder of **19** precipitated in 59 % yield with satisfying elemental

analysis results.
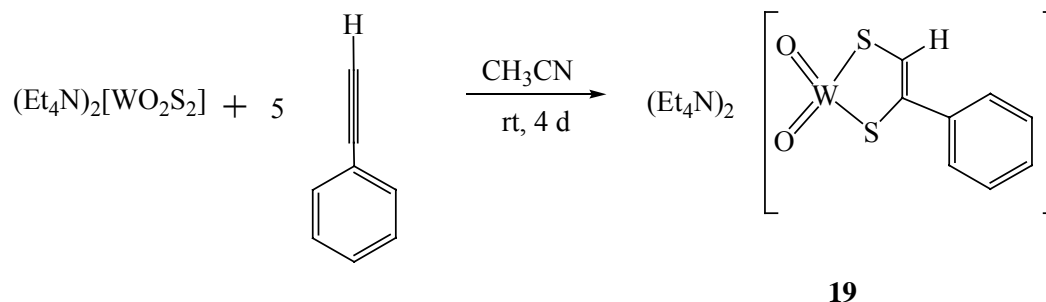
Scheme 2.8. Synthesis of complex **19**.

During the procedure the oxidation state of tungsten changed from VI to IV by cleavage of one bond of alkyne (scheme 2.8). IR spectra give many insights into the W=O bond character of the compound. The complex **19** exhibits a pair of bands at 891 and 850 cm^{-1} which are assigned to the symmetric and antisymmetric W=O stretches [113]. The bands at 765/701 and 536 cm^{-1} are ascribed to mono-substituted aromatic groups and S-S stretching modes, respectively [125]. The band at 351 cm^{-1} is assigned to the vibration of W-S bond [46].

2.4.2. Synthesis and Characterization of complex 20

A variety of reactions which produce stable diamagnetic binuclear di-µ-sulfido bridged M(V) (M=Mo, W) species while each metal atom also is strongly bound to a terminal oxo or sulfido group are well known today [128]. It was emphasized that the additional ligands lead to pseudo-tetragonal coordination geometry about each metal center [129]. Structure A is one of the possibilities for two tetragonal pyramids sharing a basal edge [130]. Several molybdenum and tungsten compounds with structure A have been reported [125,131-133]. However, there is no prior example of tungsten (V) dithiolene complexes with a di-µ-sulfido bridge. Herein we describe the binuclear W(V) complex of A geometry with one benzene-1,2-dithiol ligand per tungsten.
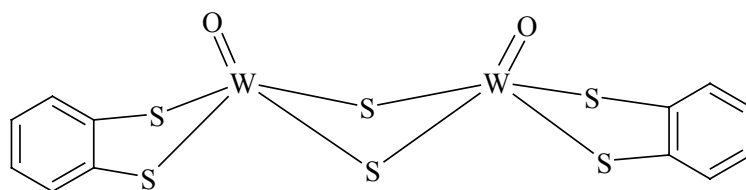
A

The binuclear complex **20** was readily prepared by $(Et_4N)_2[WO_2S_2]$ in the presence of benzene-1,2-dithiol in acetonitrile at room temperature under anaerobic conditions and obtained as red-brown crystals in 30 % yield. However the attempts to prepare $[Mo_2O_2(\mu\text{-}S)_2(bdt)_2]^{2-}$ from $(Et_4N)_2[MoO_2S_2]$ in the presence of benzene-1,2-dithiol failed. The yield of **20** is relatively low due to the simultaneous formation of complex **21** (see chapter 2.4.3.). Complex **21** is easy to be isolated from compound **20** since they have different crystal shapes.

Analytical and spectroscopic data are consistent with the formula of Scheme 2.9 as a dimeric species containing a $[W_2O_2(\mu\text{-}S)_2(bdt)_2]^{2-}$ core. The infrared spectrum of **20** exhibits an intense band at 944 cm^{-1} that is assigned as the W=O stretch [59]. Three additional W-S modes at 437, 362 and 335 cm^{-1} were observed for the compound **20** [65]. The presence of the *syn*-$W_2O_2(\mu\text{-}S)_2{}^{2+}$ core and the complete molecular structure of **20** have been established by single-crystal X-ray diffraction techniques.
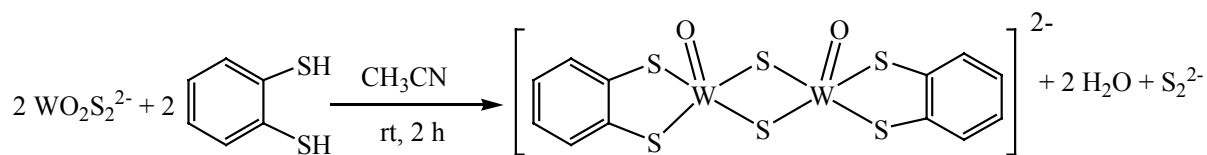
Scheme 2.9. Synthesis of complex **20**.

The crystal structure of **20** consists of the dinuclear tungsten anion

$[W_2O_2(\mu\text{-}S)_2(bdt)_2]^{2-}$ and tetraethylammonium counterions. The view of the molecule is presented in Figure 2.5. Pertinent distances and angles are given in Table 2.5. The $[W_2O_2(\mu\text{-}S)_2(bdt)_2]^{2-}$ anion is formed by two penta-coordinated W (V) atoms, both the five-coordinated W(V) sites possess distorted square pyramidal coordination geometry with S(1)- S(2)- S(3)- S(4) and S(1)- S(2)- S(5)- S(6) based planes for W(1) and W(2), respectively. The apical oxo-tungsten distance observed for **20**, 1.697(3)-1.709(4) Å is in the range of those in $[WO_2(bdt)_2]^{2-}$ [50] and $[WO_2(mnt)_2]^{2-}$ [49]. The W(V) atom lies on a general site, while S(1) and S(2) lie in the equatorial plane. Two sulfide groups doubly bridge the two metal centers. The W-S bonds in the equatorial plane can be divided into two sets. One of which is the W-S_{core} bond. The average distance W-S_{core} is 2.341(2) Å and S_{core}-W-S_{core} angle, 101.31(5)°, being within the ranges observed for related $W_2(\mu\text{-}S)_2$ core structures [132]. The other is W-S_{bdt}, in which the terminal sulfur atoms of the bdt ligand are coordinated to the tungsten center in a nearly symmetrical fashion. The average W-S_{bdt} distance is 2.410(2) Å and the S_{bdt}-W-S_{bdt} angle, 81.49(5)°, agreeing well with the average values of the corresponding parameters found in related tetrasulfido and bdt tungsten complexes [58,131,134]. The W-S bonds of the sulfide bridging atoms are always shorter than the W-S bonds of the organic ligands. Such features were mentioned by D. Coucouvanis et al. [135] already. Of the four C-S distances, the mean C-S distance is 1.759(5) Å, which is shorter than the typical C-S single bond distance 1.81 Å [136]. Therefore, all C-S bonds in the present structures are of partial double bond character as observed in most of the dithiolene ligdans.

Table 2.5. Selected bond lengths [Å] and angles [°] for **20**.

W(1)-O(1)	1.697(3)	O(1)-W(1)-S(1)	108.24(14)
W(2)-O(2)	1.709(4)	O(1)-W(1)-S(2)	109.02(14)
W(1)-S(1)	2.335(2)	S(1)-W(1)-S(2)	101.50(5)
W(1)-S(2)	2.338(2)	S(1)-W(2)-S(2)	101.11(5)

W(2)-S(1)	2.341(2)	O(1)-W(1)-S(4)	103.22(14)
W(2)-S(2)	2.346(2)	O(1)-W(1)-S(3)	106.18(14)
W(1)-S(4)	2.403(2)	O(2)-W(2)-S(1)	108.65(15)
W(1)-S(3)	2.419(2)	O(2)-W(2)-S(2)	108.62(14)
W(2)-S(5)	2.413(1)	S(1)-W(1)-S(3)	78.60(5)
W(2)-S(6)	2.406(2)	S(1)-W(1)-S(4)	146.27(6)
S(2)-W(1)-S(4)	78.96(5)	W(1)-S(1)-W(2)	76.02(5)
S(2)-W(1)-S(3)	142.67(6)	W(1)-S(2)-W(2)	75.88(5)
S(4)-W(1)-S(3)	81.31(5)	S(5)-W(2)-S(6)	81.67(5)
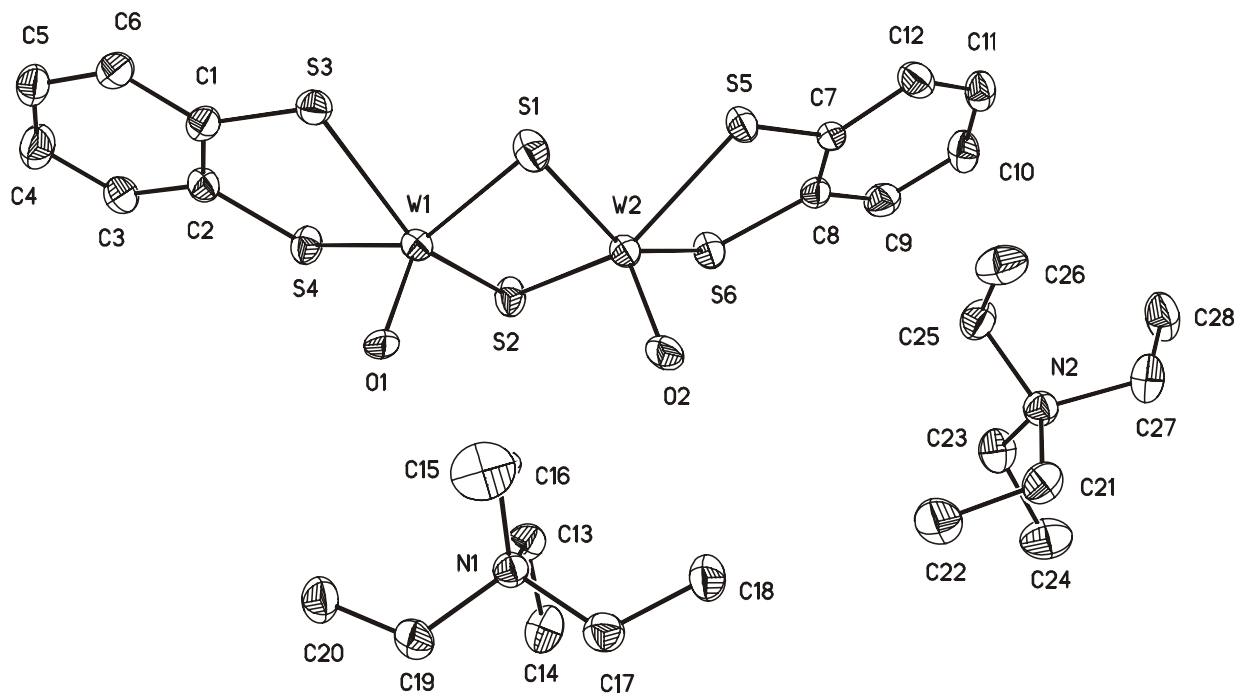
Fig. 2.5. View of the structure of $(Et_4N)_2[W_2O_2(\mu\text{-S})_2(bdt)_2]$ (**20**) without hydrogen atoms (with numbering scheme).

2.4.3. Synthesis and Characterization of complex 21

We have developed an easy access for the preparation of $(Et_4N)[MoO(bdt)_2]$ and $(Et_4N)_2[WO(bdt)_2]$ from $(Et_4N)[MO_2S_2]$ (M=Mo, W) and the benzene-1,2-dithiol ligand. We have synthesized monooxo tungsten (**21**) and molybdenum (**22**) compounds with dithiolene ligands in one step using commercially available reagents and at convenient conditions.

Complex $[W^{IV}O(bdt)_2]^{2-}$ was first prepared by the reduction of $[W^VO(bdt)_2]$ using sodium acenaphthylenide ($Na/C_{10}H_8$) in THF/acetonitrile by R. H. Holm et al. [58]. The precursor compound $[W^VO(bdt)_2]^-$ can be obtained by the ligand substitution reaction by bdtH$_2$ with $[WOSPh_4]^-$ [50], which itself was prepared from $[WOCl_4]^-$ and $Et_3N/PhSH$ [70]; or by the reaction of $[WOCl_3(THF)_2]$ and $Et_3N/PhSH$ in THF/actonitrile [58]. In this work, the complex **21** was synthesized by one step reaction of $(Et_4N)_2[WO_2S_2]$ with two equivalents of bdtH$_2$ in acetonitrile at room temperature and was isolated as tetraethylammonium salt in 67 % yield (Scheme 2.10).

Compounds were identified by elemental analysis, IR and crystal structure determination. In the IR spectra the bands at 948 and 350 cm^{-1} were observed, which are associated with vibrations of the W^{IV}-O and W^{IV}-S bonds, respectively [137].
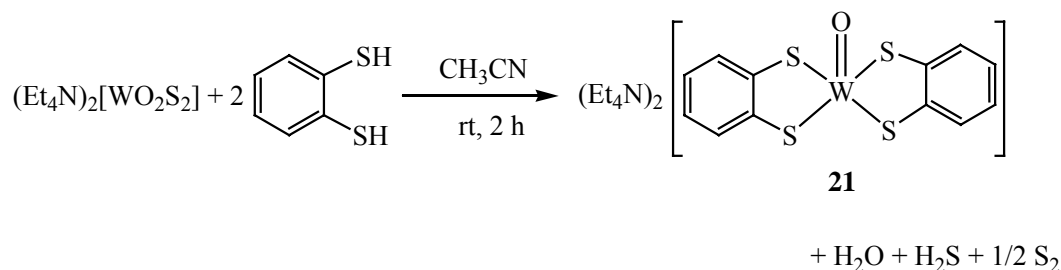
Scheme 2.10. Synthesis of complex **21**.

The molecular structure of the anion moiety of **21** is illustrated in Fig. 2.6. Complex **21** has the same structure as the reported bis(dithiolene)oxotungsten(IV) complex $(Et_4N)_2[W^{IV}O(bdt)_2]$ [50]. Since the structure is disordered, details of the bonds and angles will not be discussed here.
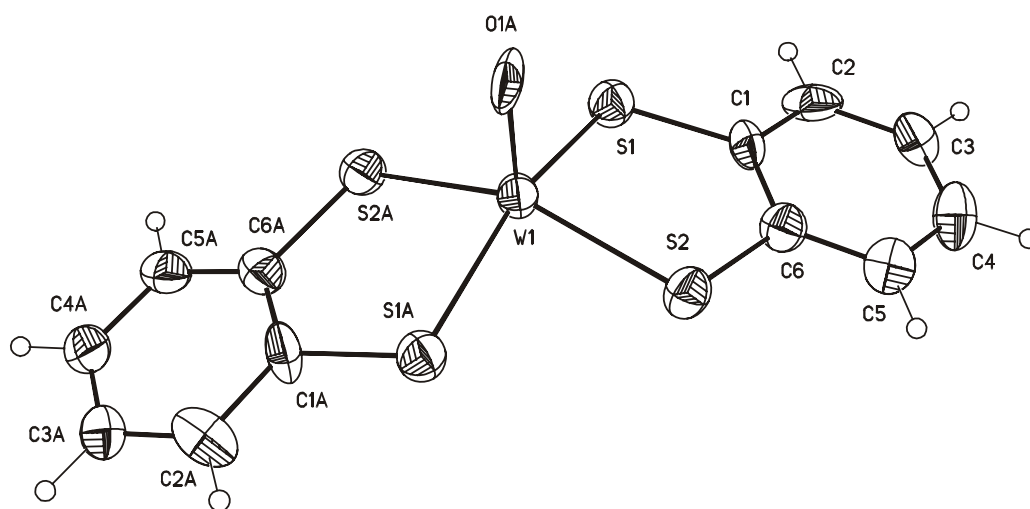
Fig. 2.6. View of the structure of $[WO(bdt)_2]^{2-}$, the anion of **21** (with numbering scheme).

2.4.4. Synthesis and Characterization of complex 22

When $(Et_4N)_2[MoO_2S_2]$ was treated with one equivalent of benzene-1,2-dithiol in DMF at ambient temperature, needle-like red-brown crystals of **22** formed by adding a small amount of diethyl ether in 60 % yield and satisfying elemental analysis results. For reasons not yet clear, the complex $[MoO(bdt)_2]^-$ was formed, whereas the reaction of the tungsten counterpart by the same conditions resulted in the dimeric compound **20**.

The IR data for **22** display an intense peak at 900 cm^{-1}. Strong IR band around 905 cm^{-1} have been reported by S. Boyde et al. [48], and this band has been assigned as the Mo=O stretching vibration. Two observable vibrational bands in the 300-400 cm^{-1} region are at frequencies of 356 and 393 cm^{-1}, which are assigned as the Mo-S stretching vibrations [46,138-139].

Table 2.6. Selected bond lengths [Å] and angles [°] for **22**.

Mo(1)-O(1)	1.686(9)	O(1)-Mo(1)-S(1)	107.23(10)
Mo(1)-S(1)	2.375(3)	S(1)-Mo(1)-S(1A)	145.54(19)
Mo(1)-S(2)	2.383(2)	O(1)-Mo(1)-S(2)	109.11(8)
S(1)-C(1)	1.774(11)	S(1)-Mo(1)-S(2A)	85.60(9)
S(2)-C(2)	1.772(10)	S(1)-Mo(1)-S(2)	83.26(10)
S(2)-Mo(1)-S(2A)	141.78(17)	C(1)-S(1)-Mo(1)	107.2(4)
C(2)-S(2)-Mo(1)	107.3(4)		
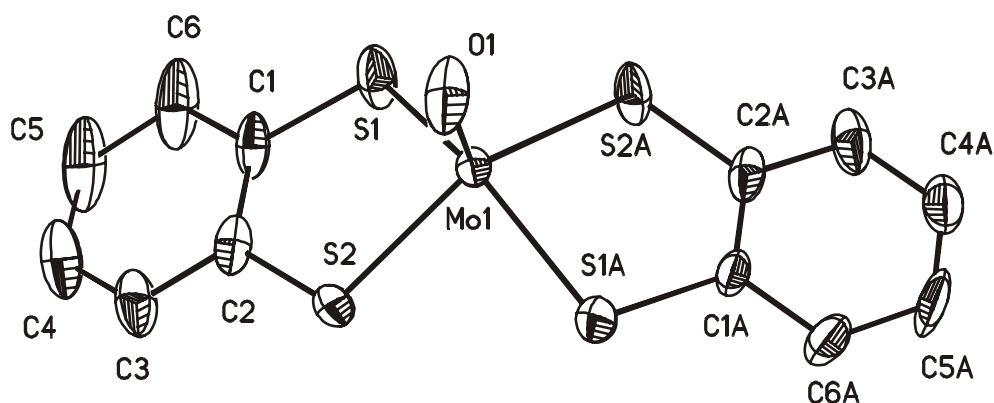
Fig. 2.7. View of the structure of [MoO(bdt)$_2$]⁻, the anion of **22**, without hydrogen atoms (with numbering scheme).

Figure 2.7 shows the crystal structure of the anion of **22** and selected bond distances and angles are listed in Table 2.6. X-ray structure determination shows that the molybdenum (V) center is coordinated with an oxygen atom which is at the apex and four sulfur atoms from the two dithiolene ligands adopting an approximately square pyramidal geometry (C$_{2v}$ symmetry). The coordination geometry is isomorphous with (PPh$_4$)[MoO(bdt)$_2$] [48] and isostructural with reported mononuclear Mo(V) complexes, (Et$_4$N)[MoO(bdtCl$_2$)$_2$] [62], (PPh$_4$)[MoO(SCHCH$_2$S)$_2$] [140],

$(Et_4N)[MoO(S_2C_2H_2)_2]$ [36], and $[MoO(S_2C_2Me_2)_2]^-$ [35]. The average Mo-S distance at 2.386(2) Å is comparable with the common Mo-S bond. The molybdenum atom is raised slightly above the basal S4 plane (S(1)-S(2)-S(1A)-S(2A)) by 0.742 Å. In terms of standard deviations, the terminal Mo=O distance of 1.686(9) Å is similar to that (1.668 Å) of the corresponding Mo(V) complex [48,62]. The mean S-C bond distances at 1.773(9) Å is comparable with the common S-C bonds. The two dithiolates of each bdt ligand in **22** have bite angles of 83.26(10) and 85.60(9)°, which closely correspond to the values obtained from $(PPh_4)[MoO(bdt)_2]$ [48]. The Mo-S-C angle, 107.2(4)- 107.3(4) °, is similar to that (106.8(2)-107.3(2) °) of the related Mo(V) complex [62].

2.5. Reactions of MCl$_4$(dme) (M=Mo, W)

All molybdenum DMSO reductase enzymes are now recognized to contain a universal cofactor (Moco) in which a $Mo^{VI}X$ unit (X=O, S) is tightly coordinated by two pterin dithiolene ligands (S_2pd) [2]. Recently the X-ray crystallographic and EXAFS analysis results for *Rhodobacter Sphaeroides* (Rs) DMSO reductase indicate one $Mo^{VI}=O$ group in the oxidized form, the absence of this group in the reduced form, and serinate ligation in both forms, but are in apparent nonconformity in other structural aspects [11,141-143]. In the case of F(M)DH enzymes, based on amino acid sequence data, it has been implicated that their coordination units may be structurally similar to those found for DMSO reductase but with cysteinate or selenocysteinate in place of serinate [3]. The desoxo M^{IV} and monooxo M^{VI} (M=Mo, W) centers were not addressed in all earlier oxo transfer systems developed as models for enzymatic reactions.

In the course of a program directed towards the development of new synthetic approaches for the molybdenum and tungsten dithiolene compounds, we have considered the complexes of molybdenum and tungsten with valent state IV as suitable starting materials for further synthesis since the metal center of lower valence

IV is not as easy as valence V or VI to be reduced by dithiolene ligands (or thiolate ligands in general), and the proposed products will be proper model complexes of the reduced form of DMSO reductase. Here we aim to prepare analogues of these sites for structural and reactivity investigations and disclose new synthetic routes to bis(dithiolene) desoxo M^{IV} (M=Mo, W) complexes related to the metal centers in these enzymes.

2.5.1. Synthesis and Characterization of complexes 23-26

Treatment of one equivalent of sodium *trans*-1,2-cyclohexanediolate in dimethoxyethane with a stirred suspension of WCl_4(dme) in dimethoxyethane at -50 ºC for 30 min and another 1 hour at room temperature gave the compound **23**. Scheme2.11 shows the reaction procedure while the two mol of the starting material were oxidized from valance IV to valence V, and three chlorine atoms were replaced by *trans*-1,2-cyclohexanediolato ligands due to the steric hinderance. At the same time, another two mol of the metal precursor were reduced to valance III. After one week, the solvent was concentrated to yield X-ray quality dark red crystals of **23** (26 % yield) at room temperature with satisfying elemental analysis and EI-MS results.
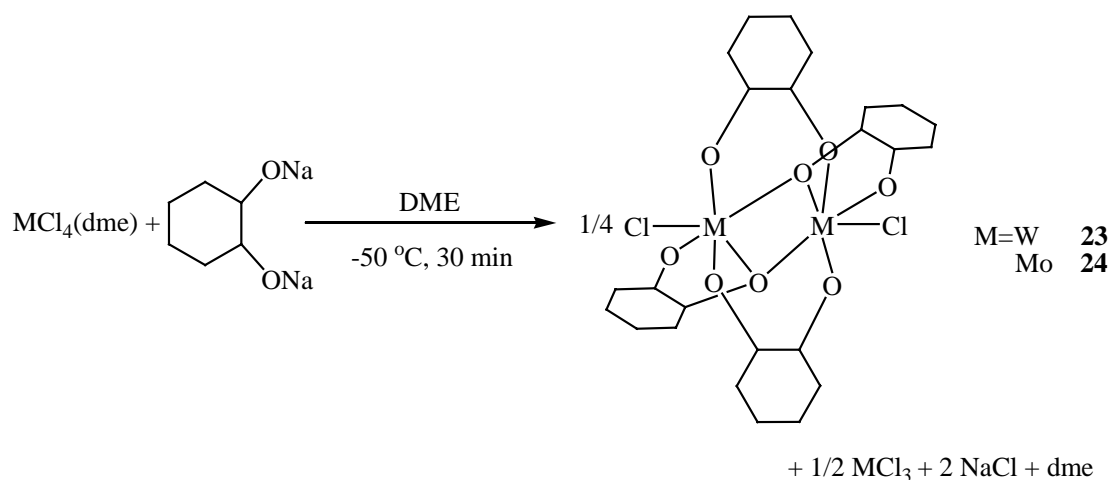
Scheme 2.11. Synthesis of complexes **23** and **24**.

The same procedure was performed with MoCl$_4$(dme) giving a dark-green solid **24** with 63 % yield. The EI-MS and elemental analysis results show **24** has the same formula as **23** except for the metal. The IR spectrum of **24** contains a peak of middle intensity at 548 cm^{-1}, which is assigned to the Mo-O stretch [110]. Other important frequency bands are around 1088 cm^{-1} (O-C stretch), 2953 cm^{-1} (C-H stretch) and 1450 cm^{-1} (C-H bend), which are very similar to previously reported data (1080, 2940 and 1480 cm^{-1}) [107].

When the mixture of WCl$_4$(dme) in dimethoxyethane was treated with one equivalent of sodium *cis*-1,2-cyclohexanedicarboxylate in dimethoxyethane at -50 ºC for 30 min and another 1 hour at room temperature, the product **25** was obtained as brown solid in 58 % yield. The molybdenum complex **26** was prepared by the same procedure in 56 % yield. Both the proposed formulas were confirmed by elemental analysis results and spectroscopic data. Scheme 2.12 shows the reaction procedure. In these reactions, the redox reaction did not happen probably due to the steric hinderence of *cis*-1,2-cyclohexanedicarboxyliate.
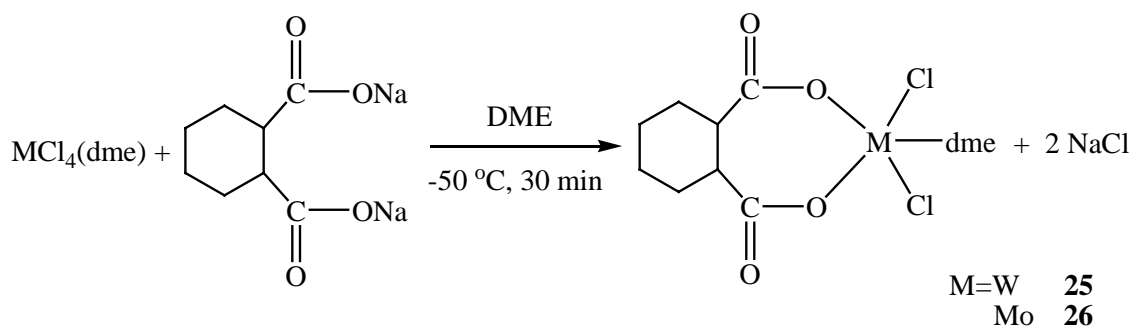
Scheme 2.12. Synthesis of complexes **25** and **26**.

The EI-MS of **25** contains a [M-dme]$^+$ cluster peak at *m/z* 429 (4 %), when the EI mass spectrum of **26** contains a molecular ion peak at *m/z* 429 (5 %) and [M-dme]$^+$ cluster peak at *m/z* 335 (66 %). The IR spectra exhibited bands of middle intensity at 852 cm^{-1} (**25**) and 472 cm^{-1} (**26**), respectively, assigned to the M-O (M=W, Mo) stretches [63,110]. The infrared spectra of both the tungsten and molybdenum complexes contain the bands at 1088 cm^{-1} (**25**) and 1100 cm^{-1} (**26**), respectively, assigned to the

C-O stretch. The bands at 2936 and 1452 cm^{-1} of **25** and 2964 and 1420 cm^{-1} of **26** are distinctive for the C-H stretch and bend [107]. Furthermore, the peaks at 1713 cm^{-1} of **25** and 1701 cm^{-1} of **26** are assigned to the C=O stretch.

The attempts to obtain mono-dithiolene molybdenum and tungsten compounds by the same procedure with one equivalent of sodium benzene-1,2-dithiolato or sodium 3,4-toluenedithiolato to substitute two chlorine ligands failed since the tris(dithiolene) metal complexes always were the main products.

2.5.2. X-ray crystallographic analysis of compound 23

View of the molecule structure of compound **23** is shown in Fig. 2.8 and Fig. 2.9. Selected bond distances and angles are given in Table 2.7. Compound **23** crystallizes in the triclinic system in the *P-1* symmetry space group. The asymmetric unit comprises one half of the dimer, the other half being generated by the center of symmetry. Thus the overall molecule is crystallographically constrained to possess D_{2d} point group symmetry. The intermolecular contacts between dimers are observed and shown in Fig. 2.8.

The tungsten atom in complex **23** is six-coordinate and the geometry of the coordination sphere can be described as two edge-sharing distorted octahedra, which closely resembles $W_2Cl_4(\mu\text{-}OEt)_2(OEt)_4$ [144], $W_2Cl_4(\mu\text{-}OEt)_2(Me_2C(O)C(O)Me_2)_4$ [145] and $W_2Cl_4(\mu\text{-}OR)_2(OR)_2(ROH)_2$ [146]. The molecular structure viewed at right angles to the metal-metal vector is presented in Figure 2.9, where the atomic numbering scheme is also defined.

The tungsten atoms are coordinated to a planar arrangement of two chlorine atoms and two bridging *trans*-1,2-cyclohexanediolate groups. The two axial positions of the octahedron are occupied by half of the *trans*-1,2-cyclohexanediolate groups. The chlorine atoms are bound to the tungsten atoms with W-Cl distances equal to 2.394(6) Å. For the similar complexes described in the literature the W-Cl bond lengths vary from 2.355 [146] to 2.410 Å [144] with the mean equal being 2.383 Å.

Table 2.7. Selected bond lengths [Å] and angles [°] for **23**.

W(1A)-O(3A)	1.847(5)	O(3A)-W(1A)-Cl(1)	89.09(17)
W(1A)-O(4)#1	1.848(5)	O(3A)-W(1A)-O(4)#1	172.8(2)
W(1A)-O(1)	1.910(5)	Cl(1)-W(1A)-O(4)#1	89.10(17)
W(1A)-O(2)	2.042(5)	O(3A)-W(1A)-O(2)	92.3(2)
W(1A)-O(2)#1	2.127(5)	Cl(1)-W(1A)-O(2)	171.37(16)
W(1A)-Cl(1)	2.394(2)	O(4)#1-W(1A)-O(2)	90.5(2)
W(1A)-W(1A)#1	2.762(1)	O(3A)-W(1A)-O(1)	93.5(2)
O(4)-C(12)	1.426(9)	C(1)-O(1)-W(1A)	116.5(5)
O(3A)-C(7)	1.403(10)	C(2)-O(2)-W(1A)#1	159.0(5)
O(1)-C(1)	1.431(10)	Cl(1)-W(1A)-O(1)	92.31(16)
O(2)-C(2)	1.421(10)	W(1A)-O(2)-W(1A)#1	82.95(18)
O(2)-W(1A)-O(2)# 1	97.05(18)	O(2)-W(1A)-O(1)	79.1(2)
O(3A)-W(1A)-W(1A)#1	88.17(17)	O(4)#1-W(1A)-W(1A)#1	88.62(17)
O(2)-W(1A)-W(1A)#1	49.85(15)	O(2)#1-W(1A)-W(1A)#1	47.19(14)

The confirmation of the $\overline{WWOCCO}$ rings is unusual and indicative of steric strain. The W-O-C angle of 159.0(5) ° is within the reported angles of 155.9(6) to 160.4(6) ° [145] indicating the existence of the $\overline{WWOCCO}$ ring. The mean W-O(bridge) and W-O(terminal) distances are 2.085(5) and 1.868(5) Å, respectively, which is consistent with the reported data of W-O_B and W-O_T [144-147]. The mean W-O_B distance is ca. 0.217 Å longer than the mean W-O_T distance, which is similar with the difference of reported compound $W_2Cl_4(\mu\text{-}OEt)_2(Me_2C(O)C(O)Me_2)_4$ [145]. The W(1A)-O(1) and W(1A)-O(2) distance is longer than the normal W-O_T distance due to the *trans*-1,2-cyclohexanediolate group (O(1) and O(2) atoms) participating in the formation of the bridge.
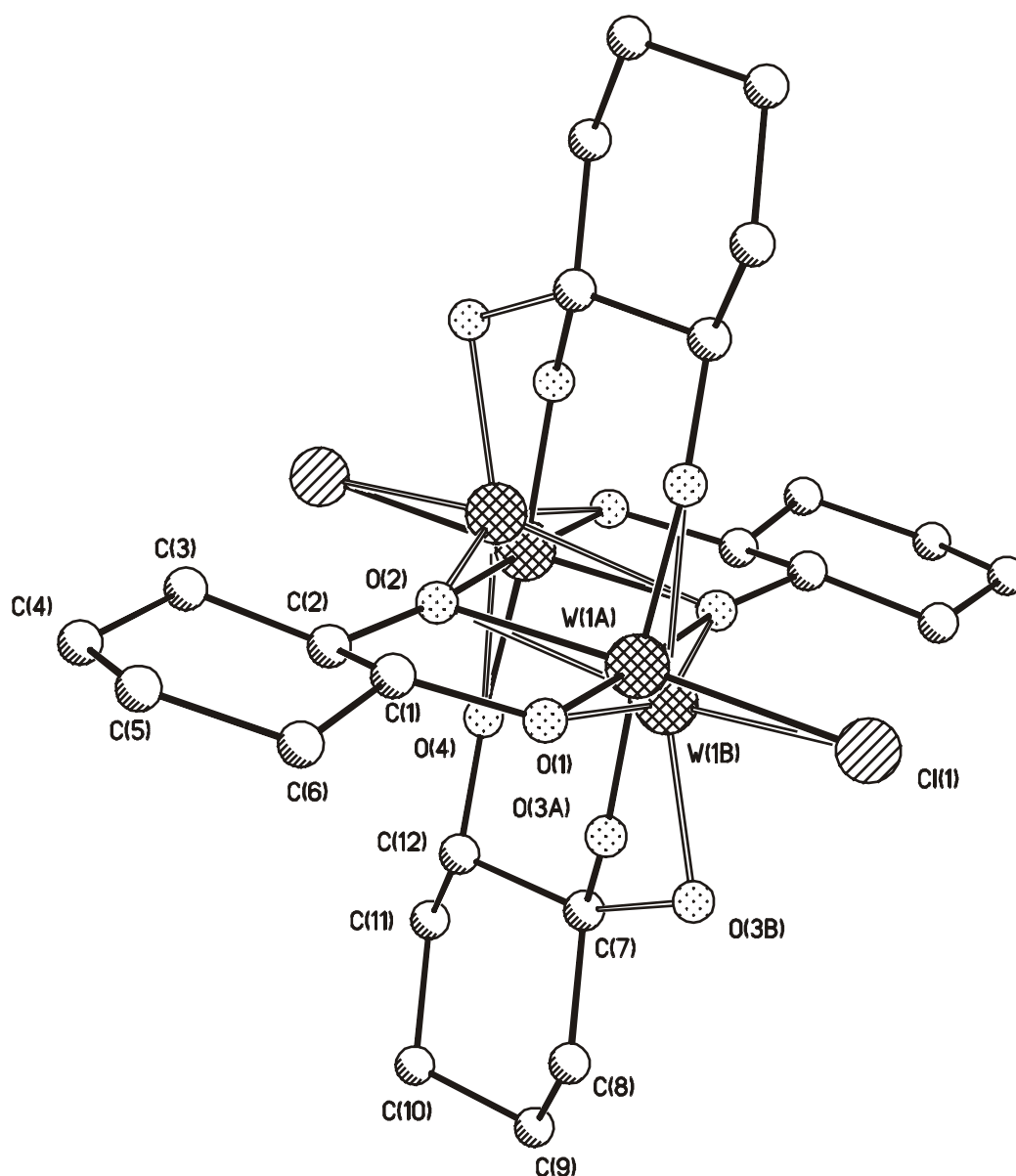
Fig. 2.8. View of the intermolecular contacts between dimers of **23** (with numbering scheme).

The W-W distance in the molecule of 2.762(2) Å is within the range of 2.691(1) to 2.791(1) Å of reported W-W single bond distances between two W^V atoms [144,147-148], which indicates that the W-W single bond probably exists. Moreover, the (μ-O)-W-(μ-O) angle is 97.05(18) ° and the W-(μ-O)-W angle is 82.95(18) °, which are similar to the reported data of F. A. Cotton et al. [146-147]. The W-W distance of

2.762(1) Å is slightly shorter than that expected for a rectangular bridge system with the observed W-(μ-O) bond lengths, viz., 2.85 Å [147]. These results are evidence for the presence of the W-W bond.

The O(3A)-W(1A)-W(1A)' and O(4)'-W(1A)-W(1A)' angles are 88.17(17) and 88.62(17) °, respectively, due to distortion of the octahedron introduced by the closeness of the tungsten atoms.
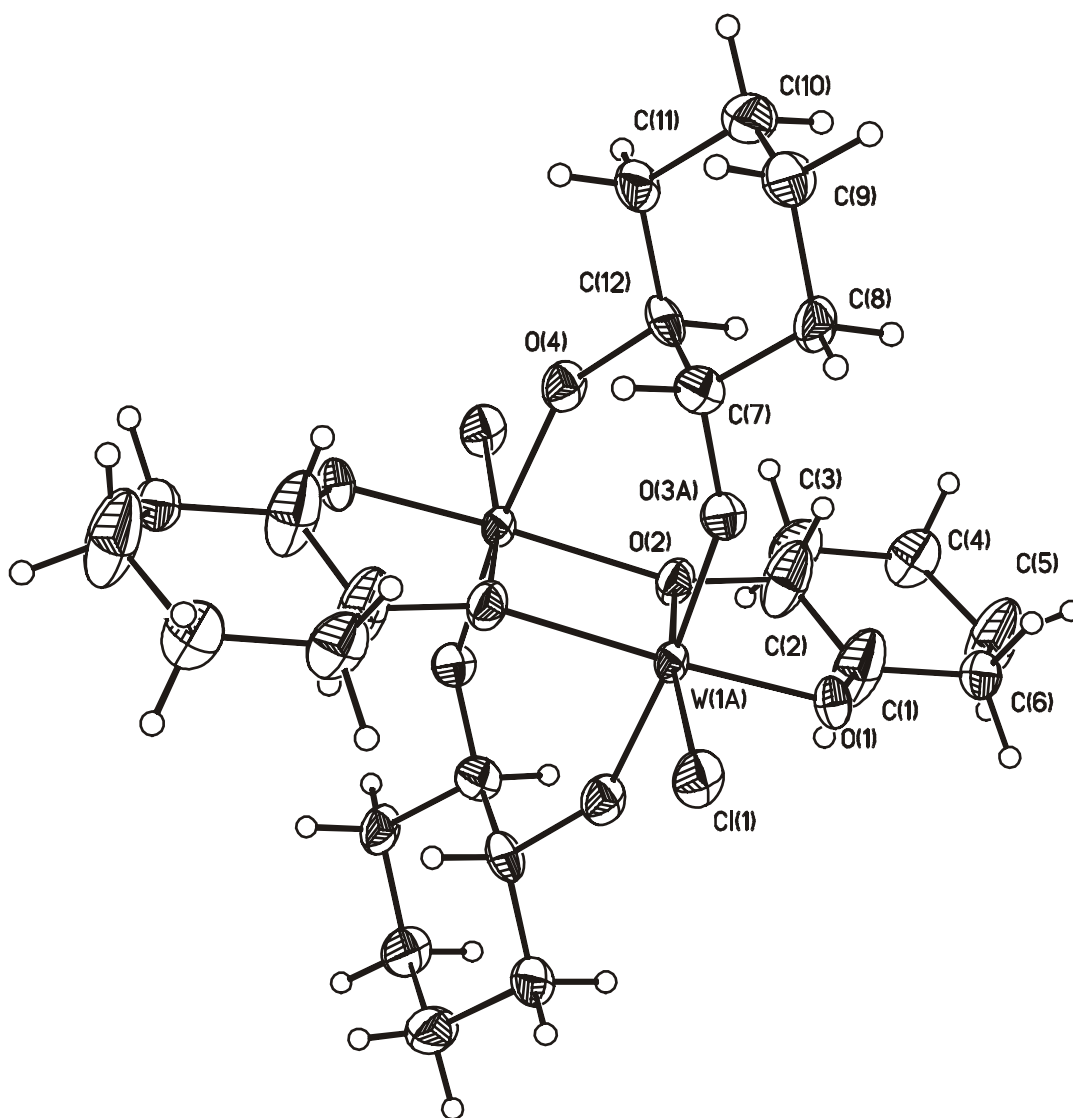
Fig. 2.9. View of the structure of **23** (with numbering scheme).

2.5.3. Synthesis and Characterization of complexes 27-30

In the past there were some reports of procedures employing the synthesis to obtain desoxo molybdenum bis(dithiolene) compounds since the reduced desoxo site $[Mo^{IV}O(O^.Ser)(S_2pd)_2]$ for *Rs* DMSO reductase was established by protein crystallography [11] and XAS [141,143]. With respect to the existence of molybdenum and tungsten isoenzymes, the desoxo tungsten dithiolene chemistry was developed in parallel with that of molybdenum dithiolenes [47,60-61,149-150]. One synthetic example is $[M^{IV}(bdt)_2(OSiBu^tPh_2)]^{1-}$ (M=Mo, W), which was synthesized by the silylation reaction of $[M^{IV}O(bdt)_2]^{2-}$ [142]. The desoxo molybdenum and tungsten complexes were also obtained by ligands substitution reaction of $Li_2(bdt)$ or $Na_2(S_2C_2R_2)$ with $[MCl_4(R'NC)_2]$ or $[MCl_4(PmePh_2)_2]$, which formed by reaction of $[MCl_4(MeCN)_2]$ and $R'CN$ or $PMePh_2$ [47,60].

With respect to desoxo molybdenum and tungsten compounds containing bis(dithiolene) ligands, they were obtained after several steps $(WCl_6 \rightarrow WOCl_3(THF)_2 \rightarrow (Et_4N)[WO(bdt)_2] \rightarrow (Et_4N)[W(bdt)_2(OSiMe_3)])$ [58]. Here we have synthesized desoxo molybdenum and tungsten complexes with sodium 3,4-toluenedithiolato and sodium benzene-1,2-dithiolato in one step by simple ligand substitution of dithiolene for chlorine using commercially available reagents as shown in Fig. 2.13. When $MoCl_4(dme)$ was treated with two equivalents of sodium 3,4-toluenedithiolato in dimethoxyethane at -50 ºC, a dark-green microcrystalline powder of **27** was afforded by reducing the filtrate under vacuum in 61 % yield and with satisfying elemental analysis results. This method was applied in the preparation of $Mo(dme)(bdt)_2$ (**28**), $W(dme)(tdt)_2$ (**29**) and $W(dme)(bdt)_2$ (**30**) in 65 %, 63 % and 78 % yield, respectively, again with satisfying elemental analysis results.
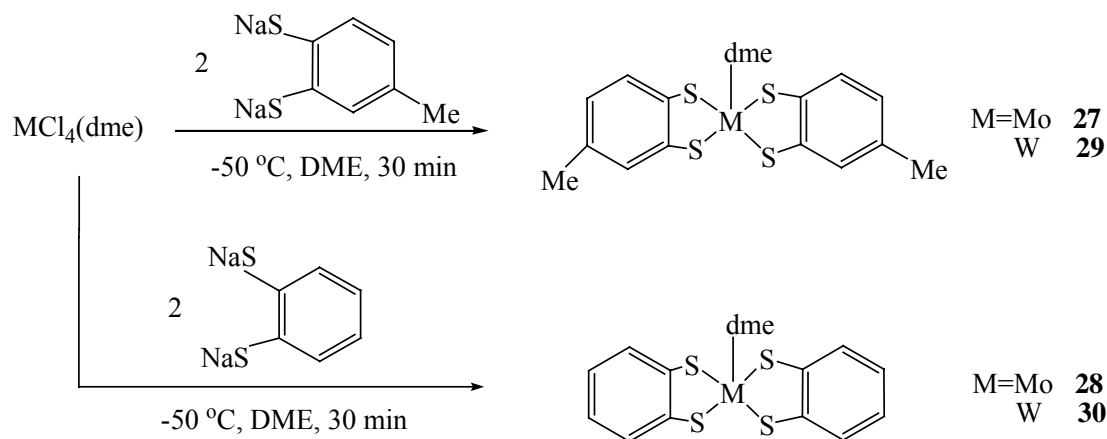
Fig. 2.13. Scheme for the synthesis of complexes **27-30**.

The IR data for **27** and **28** display peaks at 302, 336, 354, 390 and 327, 348 cm^{-1}, respectively. Vibrational bands in the 300-400 cm^{-1} region of transition metal 1,2-ene-dithiolates have been collectively assigned as Mo-S stretching vibrations [46,138,151]. Comparably, the IR spectra of **29** and **30** contained bands at 441, 390, 334 and 434, 393, 364 cm^{-1} which are distinctive for the W-S stretching mode [65]. Other important frequency bands are around 1578 and 1454 cm^{-1} (**27**), 1555 and 1440 cm^{-1} (**28**), 1585 and 1456 cm^{-1} (**29**), and 1559 and 1442 cm^{-1} (**30**), which were assigned to the existence of the benzene ring. Moreover, the bands at 2964 and 1375 cm^{-1} of **27** and 2964 and 1380 cm^{-1} of **29** can be ascribed to the C-H stretch and bend of the CH$_3$ group.

In conclusion the reaction of MCl$_4$(dme) (M=Mo, W) with sodium 3,4-toluenedithiolato or sodium benzene-1,2-dithiolato yields the bis(dithiolene) desoxo molybdenum and tungsten complexes, which present the minimal site representations for reduced *Rs* DMSO reductase.

3. Catalytic oxygen atom transfer reaction

Oxo-transfer chemistry of molybdenum is of topical interest owing to the biological relevance of the model reaction (Eq. 3.1) involving molybdoenzymes [117,152-160].

$$Mo^{VI}O_2(ligand)_n + X \rightleftharpoons Mo^{IV}O(ligand)_n + XO \qquad (3.1)$$

Among various molybdoenzymes *Rs* and *Rc* DMSO reductases have afforded descriptions of the monooxo $[Mo^{VI}O(S_2pd)_2(O^.Ser)]$ and desoxo $[Mo^{IV}(S_2pd)_2(O^.Ser)]$ active sites, which catalyze the *minimal* oxo-transfer reactions showed in Eq. 3.2 [154, 161]. Indeed, the study of oxo-transfer reactions of these types of species is far less developed than that of $Mo^{IV}O$ and $M^{VI}O_2$ dithiolene complexes [37,39,45,48,142], which catalyze the oxo-transfer reactions shown in Eq. 3.3.

$$Mo^{IV} + Me_2SO \rightleftharpoons Mo^{VI}O + Me_2S \qquad (3.2)$$

$$Mo^{IV}O + Me_2SO \rightleftharpoons Mo^{VI}O_2 + Me_2S \qquad (3.3)$$

Some of the tungstoenzymes also participate in oxo-transfer reactions. For example, *Pyrococcus furiosus* aldehyde oxidoreductase (AOR) catalyzes oxygen atom transfer reactions following the same way shown in Eq. 3.3.

In contrast to the oxo-transfer reactions, catalytic oxo-transfer reactions occur from DMSO to the phosphine forming dimethyl sulphide and the oxidized phosphine as shown in Eq. 3.4. During the procedure the molybdenum and tungsten compounds are catalytic reagents since without these complexes no reactions between triphenyl phosphine and DMSO were observed [56]. This kind of catalytic work helps to understand molybdenum or tungsten-dithiolene chemistry and to investigate the possible mechanisms.

$$Ph_3P + Me_2SO \quad \rightleftharpoons \quad Ph_3PO + Me_2S \qquad (3.4)$$

As for related systems a feasible reaction pathway involves attack of the nucleophilic phosphine on the vacant π^* orbitals of a $M^{VI}=O$ group followed by development of a transition state with M^{IV} character and reduction of the M-O bond order of the reacting group to near one in the course of forming a P-O bond [152]. This transition state is depicted in Fig. 3.1.

Oxo Transfer from Substrate
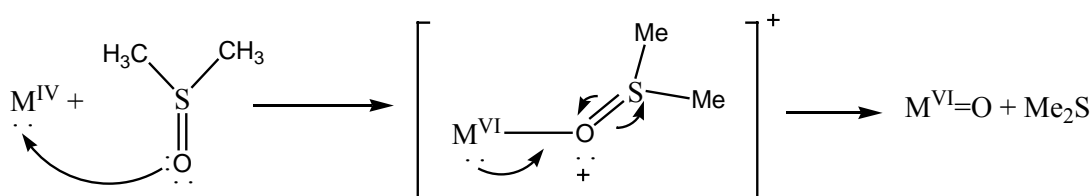
Oxo Transfer to Substrate
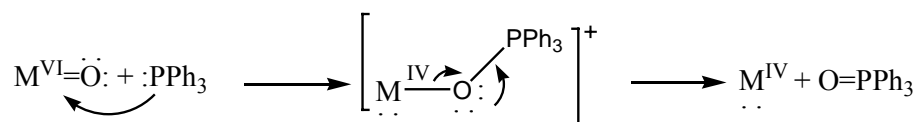
M=Mo, W

Fig. 3.1. Proposed transition states for the oxo-transfer from DMSO to PR_3 catalyzed by molybdenum and tungsten compounds.

In this study, the oxo-transfer model reaction from DMSO to PPh_3 has been used to test the catalytic properties of some of the dioxo compounds $(Ph_3PH)_2[MoO_2(bdt)_2]$ (**17**) and $(Ph_3PH)_2[WO_2(bdt)_2]$ (**18**)).

The oxo-transfer ability of two pairs of desoxo molybdenum and tungsten complexes (**27/29** and **28/30**) was investigated as well. The purpose is to determine the influence of a ligand exchange tdt *vs.* bdt on redox behavior and the oxygen atom transfer properties of molybdenum and its tungsten counterpart with respect to the fact that in nature the molybdenum and tungsten containing oxidoreductases are exist in

parallel. The procedure and results are described herein.

3.1. General procedure

In this work, the catalytic oxygen atom transfer reaction was investigated with three pairs of molybdenum and tungsten complexes which shown in Scheme 3.1.
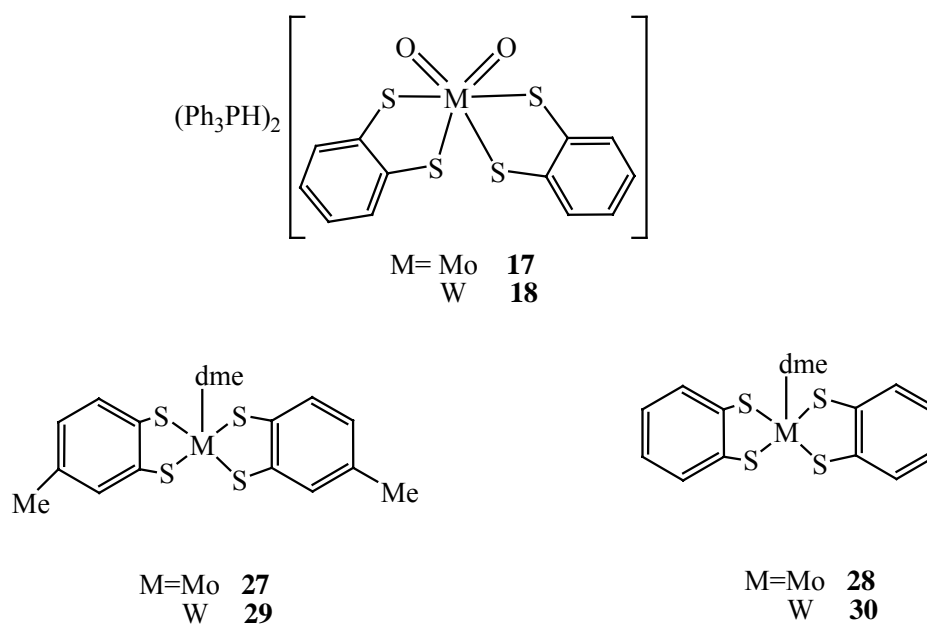
Scheme 3.1. The scheme of molybdenum and tungsten complexes used in catalytic oxygen atom transfer reaction.

3.1.1. Catalytic oxo-transfer reactions of dioxo molybdenum and tungsten complexes 17 and 18

In a sealed NMR tube, over a mixture of **17** (ca. 0.02 mmol) and an excess of PPh$_3$ (0.11 mmol) was added DMSO (0.6 ml, 8 mmol). The reaction was monitored immediately by ^{31}P NMR spectroscopy at room temperature. The color of the solution initially changed from colorless to light green and back to colorless. After 330 min, total conversion to OPPh$_3$ was achieved. The presence of DMSO in the reaction

mixture was detected by isolating Me$_2$S as (Me$_2$S)(HgCl$_2$)$_3$ [162]. The same procedure was applied to complex **18** with no color change observed during the reaction.

3.1.2. Catalytic oxo-transfer reactions of desoxo molybdenum and tungsten complexes 27-30

In sealed NMR tubes the reactions of a mixtures of **27** (0.02 mmol) and PPh3 in different quantities (0.06-2.00 mmol) in degassed, dry DMSO (0.6 ml, 8 mmol) were monitored by ^{31}P NMR spectroscopy. The color of the solution remained unchanged. The presence of DMSO in the reaction mixture was detected by isolating Me$_2$S as (Me$_2$S)(HgCl$_2$)$_3$ [162]. Similar experiments were carried out with complexes **28**, **29** and **30** at room temperature, and no color changes were observed in all these reactions.

3. 2. Results and Discussion

The oxidations of PPh$_3$ by molybdenum and tungsten complexes were carried out in DMSO at room temperature (Scheme 3.2) and the solutions were analyzed by ^{31}P NMR spectroscopy using chloroform-d as an internal reference.

$$PPh_3 \xrightarrow[\text{Cat.}]{\text{DMSO}} OPPh_3$$
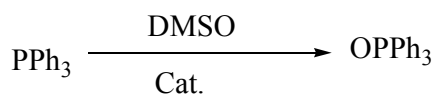
Scheme 3.2. The catalyzed oxygen atom transfer from DMSO to phosphine.

The reduction of complexes **17** and **18** by oxo-transfer can be coupled to its reoxidation by the reaction with DMSO leading to catalytic transfers. The oxidations of complexes **27-30** were following the same way. The occurrence of catalytic oxo transfer reactions involving oxygen atom transfer to and from substrate, suggests that the process could be coupled in form of a catalytic reaction (Eq. 3.2 and Eq. 3.3). The reaction is very effectively monitored by ^{31}P NMR spectroscopy, because of the

base-line resolution of the two signals in each system (δ, PPh$_3$, 5.135 and OPPh$_3$, 29.104 ppm) and no additional ^{31}P resonances were observed in the range of 80 to -140 ppm. Chemical shifts of products agreed with those of authentic samples; the total sum of integrated intensities was constant; systems remained homogeneous over the entire course of monitoring. Concentrations at various times were determined by signal integration.

In these systems, excess of PPh$_3$ in DMSO in the presence of catalysts was completely converted to OPPh$_3$. Without catalyst no reaction occurs between PPh$_3$ and DMSO under these conditions [162].

3.2.1. Catalytic oxo-transfer reactivity of complexes 17 and 18

In deoxygenated DMSO solution complexes **17** and **18** react with 5-fold excess of PPh$_3$ (pseudo-first-order conditions) to give OPPh$_3$ in 100 % conversion in a few hours at room temperature. At the end of the catalytic reaction colorless solutions were obtained from which all the starting molybdenum and tungsten complexes can be recovered intact.

The reactions were monitored with ^{31}P NMR spectroscopy. Demonstration of the catalysis of complexes **17** and **18** is provided in Fig. 3.2. In Fig. 3.2 (left), representing catalysis with complex **17**, PPh$_3$ (5.135 ppm) is consumed while OPPh$_3$ (29.104 ppm) is produced in precisely equal amounts. In Figure 3.2 (right), depicting catalysis with complex **18**, the situation is completely analogous: PPh$_3$ (5.135 ppm) is consumed and OPPh$_3$ (29.104 ppm) is generated in equimolar amounts. Both systems were very well behaved.

In the examples shown, catalysis with complex **17** produced the complete conversion from PPh$_3$ to OPPh$_3$ in 135 min, and the catalysis with complex **18** is less active under these conditions (100 % of PPh$_3$ was converted to OPPh$_3$ after 155 min). During catalysis for complex **17** as catalyst the color of the solution initially changed from colorless to light green and back to colorless whilst for complex **18** as catalyst

no color change was observed at all. Although no detailed kinetic experiments were carried out, the rate constant observed for the oxidation of PPh_3 in the presence of compounds **17** and **18** is about one to two orders.
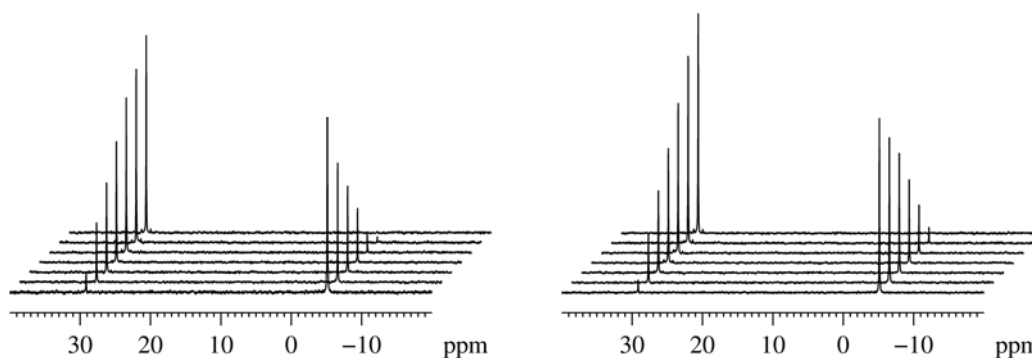
Fig. 3.2. The ^{31}P NMR spectroscopy studies of oxo-transfer reactions of $(Ph_3PH)_2[MoO_2(bdt)_2]$ (**17**, left) and $(Ph_3PH)_2[WO_2(bdt)_2]$ (**18**, right), every 20 min.

3.2.2. Catalytic oxo-transfer reactivity of complexes 27-30

Since the proposed formulas of complexes **27** and **28** identify them as minimal site representations for reduced *Rs* DMSO reductase, we have examined their catalytic oxygen atom transfer properties in the intended reaction couple (Eq. 3.2) in DMSO by mixing the catalysts with PPh_3 in different ratios. The reactions of the analogue tungsten compounds **29** and **30** with different ratios of PPh_3 in DMSO were performed under the same conditions.

The reaction of complexes **27-30** by oxo-transfer can be coupled to its oxidation by the reaction with DMSO leading to the catalytic transfers. Reaction solutions show no color change during the entire catalysis. The NMR spectra show the decrease of the resonance of the phosphorus in PPh_3 and the increase of that in $OPPh_3$ (Fig. 3.3 and Fig. 3.4). These results demonstrate the operation of catalytic cycle in Scheme 3. 3.
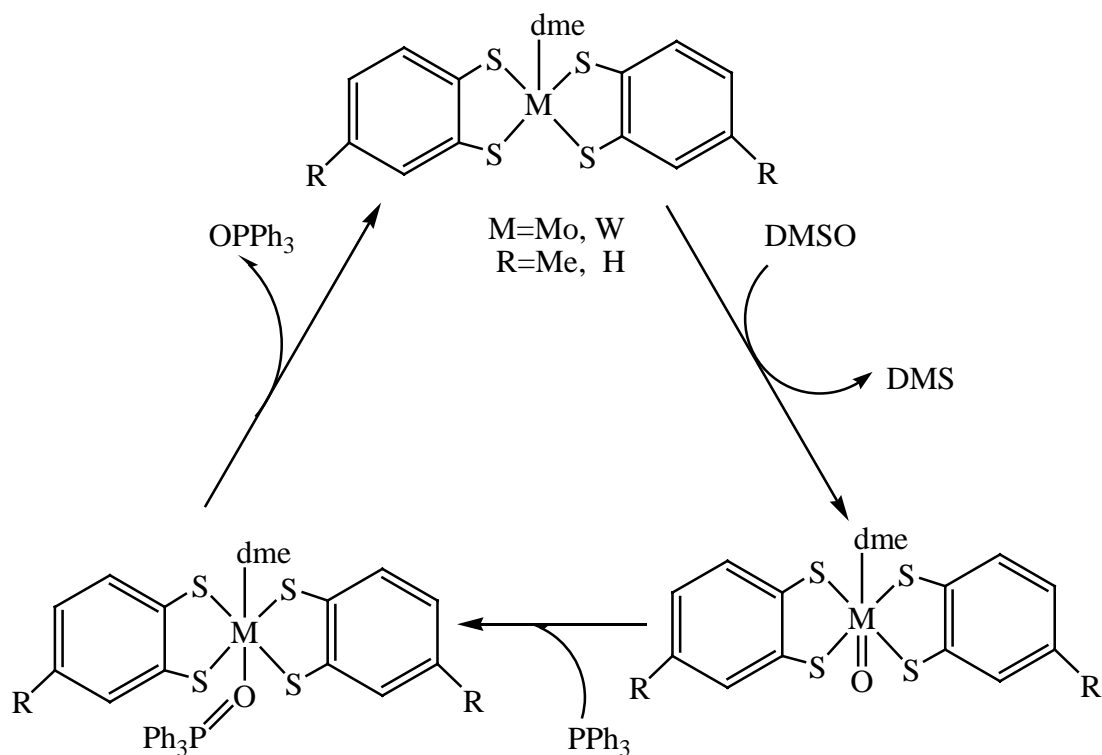
Scheme 3.3. Catalytic oxo-transfer showing the presumed intermediates.
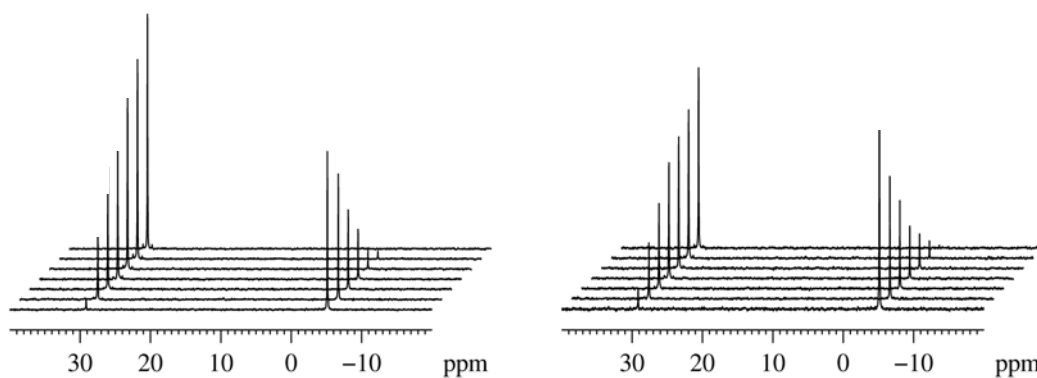
Fig. 3.3. The ^{31}P NMR spectroscopy studies of oxo-transfer reactions of Mo(dme)(tdt)$_2$ (**27**, left) and Mo(dme)(bdt)$_2$ (**28**, right) with PPh$_3$ in DMSO in a ratio of 1:20 cat. : PPh$_3$. For clarity only seven spectra are displayed for each compound.
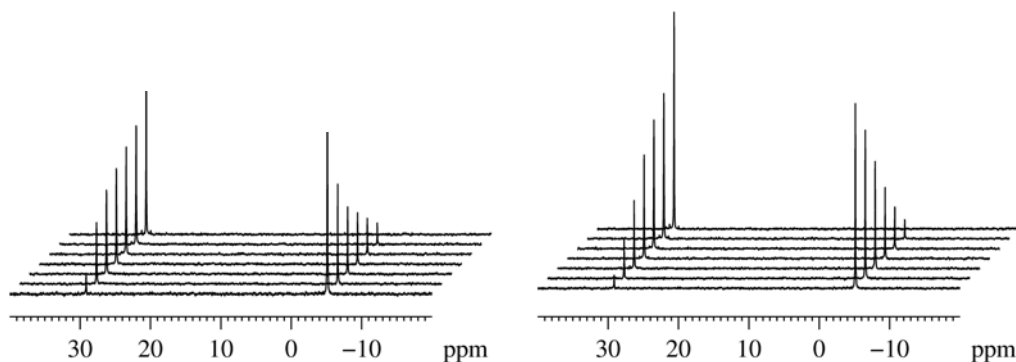
Fig. 3.4. The ^{31}P NMR spectroscopy studies of oxo-transfer reactions of W(dme)(tdt)$_2$ (**29**, left) and W(dme)(bdt)$_2$ (**30**, right) with PPh$_3$ in DMSO in a ratio of 1:20 cat. : PPh$_3$. For clarity only seven spectra are displayed for each compound.
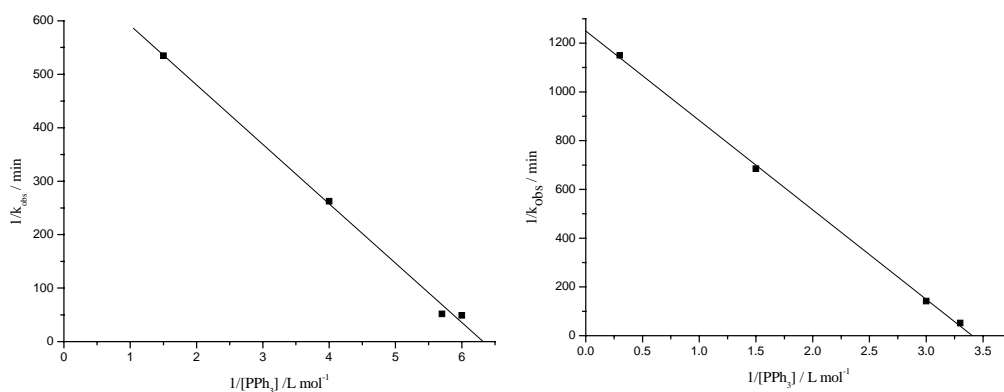
Fig. 3.5. Graphs for the $1/k_{obs}$ dependency on $1/[PPh_3]$ for Mo(dme)(tdt)$_2$ (**27**, left) and Mo(dme)(bdt)$_2$ (**28**, right) as catalysts.

Because DMSO was used in large excess over PPh$_3$ and the catalysts, the reaction should be first-order with respect to the phosphine. Phosphine oxidation is the rate-limiting step, so that re-oxidation of the catalysts is probably fast and its concentration maybe assumed constant [52]. The k_{obs} determined from exponential fits ([OPPh$_3$]$_t$/[PPh$_3$]$_0$=1-exp(-k$_{obs}$t)) show a reverse behavior and are decreasing with the

substrate concentration (Fig. 3.5 and Fig. 3.6). This indicates that with high PPh$_3$ (and/or DMS) concentration these complete with DMSO for binding to the molybdenum or tungsten center even though the intermediate could not observed with ^{31}P NMR [163].
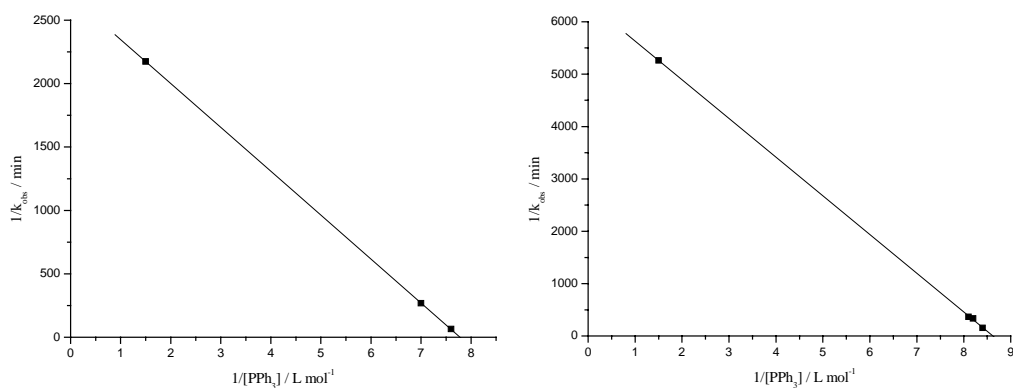
Fig. 3.6. Graphs for the 1/k$_{obs}$ dependency on 1/[PPh$_3$] for W(dme)(tdt)$_2$ (**29**, left) and W(dme)(bdt)$_2$ (**30**, right) as catalysts.
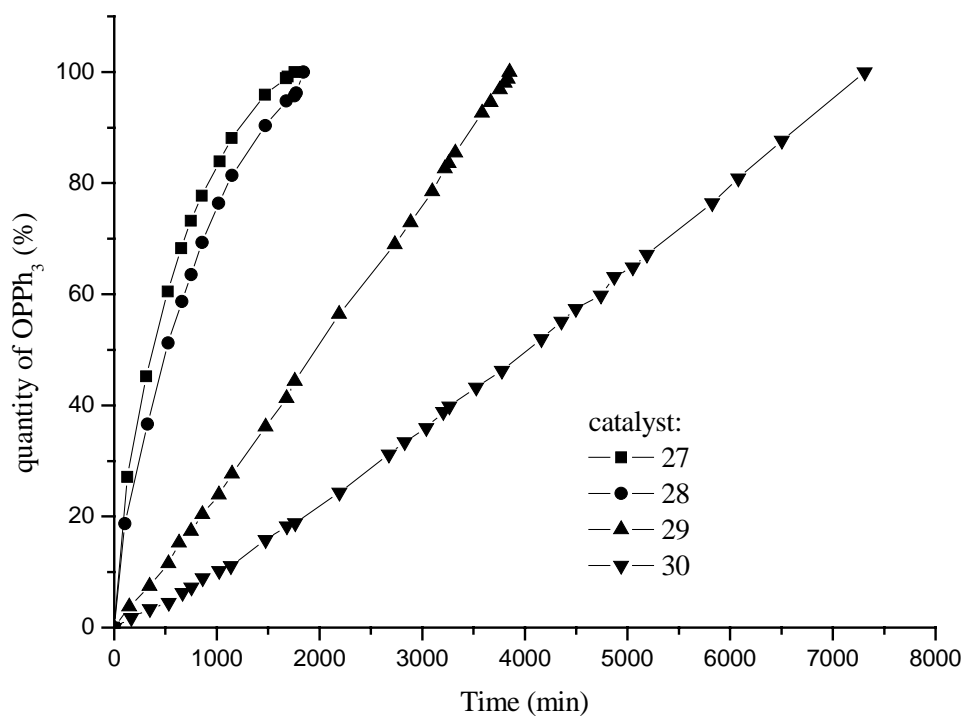
Fig. 3.7. Development of OPPh$_3$ with time for 1:20 of cat. : PPh$_3$ ratio over time with different catalysts in DMSO.

The development of OPPh$_3$ for 1:20 of catalyst : PPh$_3$ ratio over time with different catalysts is shown in Figure 3.7. The curves for the reactions with molybdenum compounds (**27** and **28**) as catalysts are normal curved lines [52, 163]. In contrast the behavior observed for the reaction with their tungsten counterparts (**29** and **30**) is almost linear. This phenomena occurs probably due to the slow reaction velocity of catalyzed oxygen atom transfer reactions by tungsten complexes.

The analogous reaction of the tungsten compounds **29** and **30** with PPh$_3$ in DMSO at room temperature led also to the oxidation of the phosphine, although significantly slower than its molybdenum analogue. This might explain why tungsten usually is not found in organisms living at ambient temperature. In thermophilic and hyperthemophilic organisms their reactivity should be much greater [164].

Interestingly the catalytic oxo-transfer reaction with the 3,4-toluenedithiolato complex is faster than with its benzene-1,2-dithiolato counterpart. This maybe because the oxygen atom is easier to transfer from the catalyst to substrate since the methyl group in the 3,4-toluenedithiolato ligand can increase the electron density of the metal center.

Notably, the catalytic oxygen atom transfer reactions of tungsten compounds are worse compared to the molybdenum complexes [30,61,126,165-166]. The reactions usually are very sluggish or do not occur at all. For one sample of the [WO(OSiPh$_2$Bu^T)(bdt)$_2$]$^{1-}$ complex, the catalytic conversion in DMSO is less than 8 % even at higher temperature (60-80 °C) for 3 days [142]. But in this work the oxygen atom transfer reactions catalyzed by tungsten complexes W(dme)(tdt)$_2$ (**29**) and W(dme)(bdt)$_2$ (**30**) are completed at room temperature in 64.17 and 121.87 hours, respectively. These represent examples of bis(dithiolene) tungsten systems that catalyze the oxidation of phosphines. The good catalytic results also present new aspect of the oxo-transfer chemistry of tungsten.

4. Summary and Outlook

4.1 Summary

The focus of the work reported here has been on the synthesis, structures and reactions of molybdenum and tungsten compounds with dithiolene and its related chalcogenide ligands. In this thesis, four bidentate ligands 3,4-toluenedithiolato, benzene-1,2-dithiolato, *cis*-1,2-cyclohexanedicarboxylate, and *trans*-1,2-cyclohexanediolate have been mainly employed as supporting moieties for molybdenum and tungsten complexes. The experimental results demonstrate that the different synthetic approaches presented here might be proper ways to control the reactions and to obtain the less dithiolene-coordinated complexes.

The oxo-transfer model reaction from DMSO to PPh_3 has been used to test the catalytic properties of some of the molybdenum complexes and their tungsten counterparts. The kinetics of the catalytic processes were measured. The complexes act as good catalysts of the oxygen atom transfer reaction indicating their biological relevance to DMSO reductases, which are able to utilise a variety of dialkyl and alkyl aryl sulphoxides as oxidizing substrates.

Reaction of $WOCl_4$ with *trans*-1,2-cyclohexanediol at room temperature forms $WCl_2(chd)_2$ (**1**). When controlling the reaction at 0 ºC, the desired product $WO(chd)_2$ (**2**) is obtained. In analogy $WOCl_4$ reacts with sodium 3,4-toluenedithiolato to afford the bis(dithiolene) complex $WO(tdt)_2$ (**3**). When $WOCl_4$ is treated with bis(2-hydroxyethyl) ether, the proposed precursor complex $WOCl_2(O(CH_2)_2O(CH_2)_2O)$ (**4**) is obtained. **4** reacts with *trans*-1,2-cyclohexanediol and sodium benzene-1,2-dithiolato to afford the desired products $WO(O(CH_2)_2O(CH_2)_2O)(chd)$ (**5**) and $WO(O(CH_2)_2O(CH_2)_2O)(bdt)$ (**7**), respectively. During the procedures simple elimination reactions occurred. Attempts to obtain complex **7** from the reaction of **4** and benzene-1,2-dithiol was unsuccessful, but form the same or repeated formula as $W_2O_2Cl_2(O(CH_2)_2O(CH_2)_2O)_2(bdt)$ (**6**). The reaction

mechanism is not clear so far due to the fact that the exact formula is not identified yet.

Treatment of mixture of two equivalents of thiophenol and two equivalents of triethylamine with formula **8** and formula **10** by the same procedure leads to the monomeric tungsten complex $WO_2(SPh)_2(mebipy)$ (**9**) and the dimeric molybdenum compound $Mo_2O_4(SPh)_2(mebipy)_2$ (**11**), respectively. Ligand 4-chlorothiophenol was used instead of thiophenol to react with **10** because the chlorine atom introduced to thiophenol can work as electron withdrawing group and decrease the electron density of the benzene ring to affect the coordinative nature of the thiophenol. But the product $Mo_2O_4(SPh-Cl)_2(mebipy)_2$ (**13**) was identified to be of the similar formula of **11**.
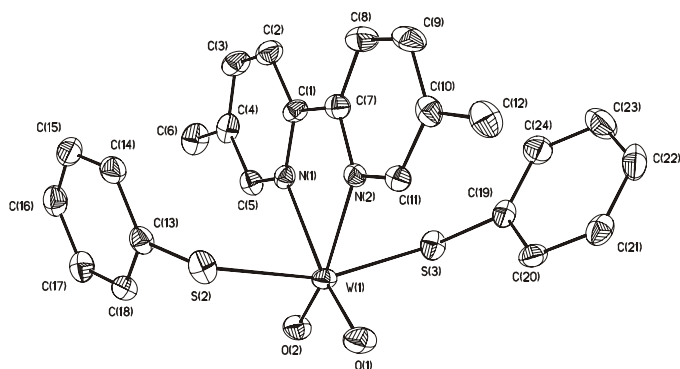
Structure of 9
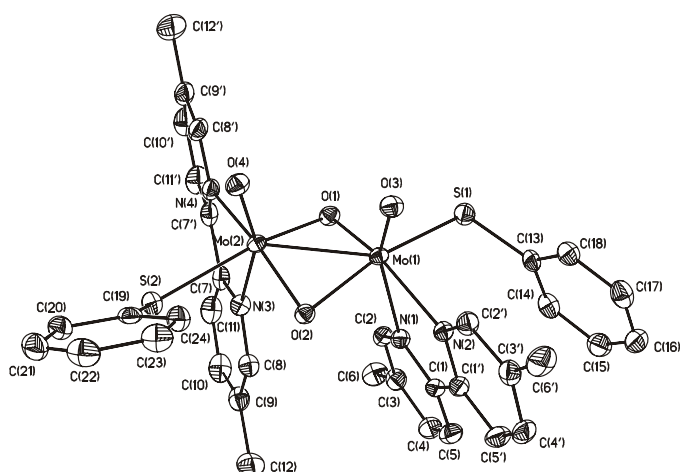
Structure of 11

In order to obtain compounds analogues to the protein-bound sites of molybdoenzymes, the reaction of silicon electrophiles with the oxo group of the metal

precursors was investigated. Reaction of **11** with one equivalent of 1,2-C$_6$H$_4$(SSiMe)$_2$ affords complex Mo$_2$O$_3$(SPh)(bdt)(mebipy)$_2$ (**12**), which was characterized by elemental analysis and EI-MS as well as infrared spectroscopy. The attempt of thiol exchange for **9** by benzene-1,2-dithiol failed, probably due to the steric hinderence of the bulky 5,5'-dimethyl-2,2'-dipyridyl and *cis*-dioxo group. The intended substitution of benzene-1,2-dithiol for chlorine of **8** and **10** was unsuccessful as well, the steric hinderence mentioned above may be the reason.

MoO$_2$(acac)$_2$ reacts with diethanolamine in DMF at room temperature to form the compound MoO$_2$(O(CH$_2$)$_2$NH(CH$_2$)$_2$O)·DMF (**14**). Complex **14** was characterized by elemental analysis and IR spectroscopy as well as X-ray structural analysis. The oxygen substitution reaction with 1,2-C$_6$H$_4$(SSiMe)$_2$ similar to the reaction of **12** was performed with **14**. Unfortunately some Mo-O cluster formed (**14-1**). This may be because of the existence of traces of water or air.
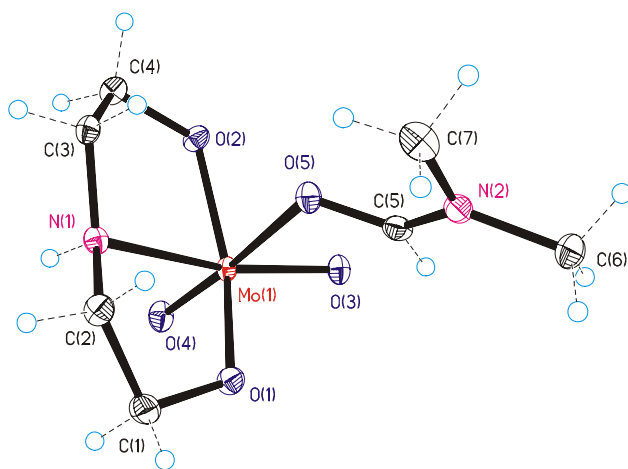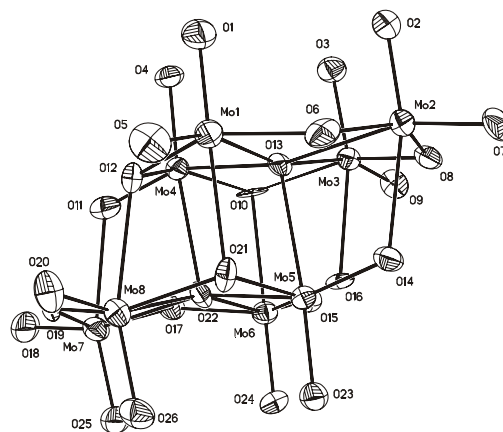
Structure of 14   **Structure of 14-1**

Complex **15** was synthesized from the reaction of MoO$_2$(acac)$_2$ with 2-amino-thiophenol in methanol in 1:2 ratio. When the mixture of two equivalents of PPh$_3$ and two equivalents of *trans*-1,2-cyclohexanediol in dichloromethane was treated to MoO$_2$(acac)$_2$ in dichloromethane the product (Ph$_3$PH)$_2$[MoO$_2$(chd)$_2$] (**16**)

was obtained. $MoO_2(acac)_2$ and $WO_2(acac)_2$ react with PPh_3 and benzene-1,2-dithiol by the same ratio as **16** to form $(Ph_3PH)_2[MoO_2(bdt)_2]$ (**17**) and $(Ph_3PH)_2[WO_2(bdt)_2]$ (**18**), respectively. During the reaction, the elimination product Hacac was readily removed under vacuo. Complexes **15-18** were characterized by elemental analysis and mass spectrometry as well as IR spectroscopy. The catalytic properties of **17** and **18** were examined by the reaction of DMSO and PPh_3 at room temperature. The results show that **17** and **18** can catalyze oxygen atom transfer reactions.
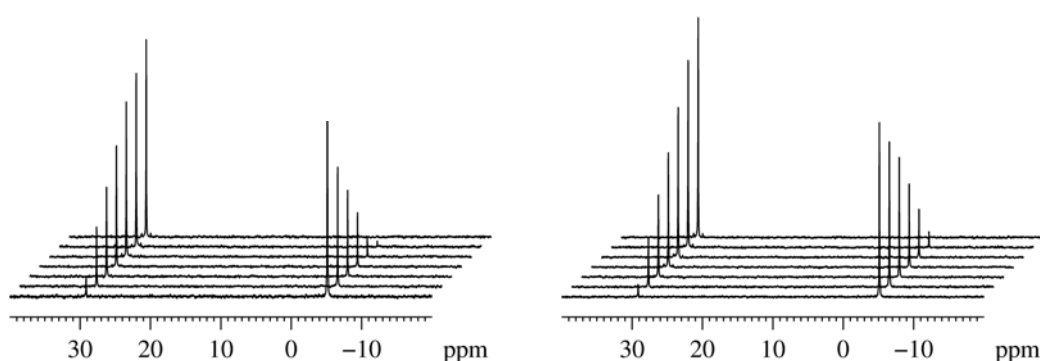
^{31}P NMR spectroscopy studies of oxo-transfer reaction of 17 and 18.

$(Et_4N)_2[WO_2S_2]$ and five equivalents of phenylacetylene in acetonitrile at ambient temperature react for 4 days to afford $(Et_4N)_2[WO_2(S_2C_2PhH)]$ (**19**). Complex **19** was characterized by ^{1}H NMR spectroscopy, elemental analysis as well as IR spectroscopy. During the procedure the oxidation state of tungsten induced from VI to IV by cleavage of one bond of alkyne. However, the attempts to obtain the molybdenum counterpart of **19** were unsuccessful.

The reaction of $(Et_4N)_2[WO_2S_2]$ and benzene-1,2-dithiol in acetonitrile by 1:1 ratio formed the first tungsten (V) dithiolene complex with a di-μ-sulfido bridge, $(Et_4N)_2[W_2O_2(\mu\text{-}S)_2(bdt)_2]$ (**20**). When treating $(Et_4N)_2[WO_2S_2]$ with two equivalents of benzene-1,2-dithiol under the same conditions, $(Et_4N)_2[WO(bdt)_2]$ (**21**) is obtained. Unexpectedly, treatment of one equivalent of $(Et_4N)_2[MoO_2S_2]$ with benzene-1,2-dithiol in acetonitrile did not produce $[Mo_2O_2(\mu\text{-}S)_2(bdt)_2]^{2-}$. Instead

$(Et_4N)[MoO(bdt)_2]$ (**22**) was obtained as the product. The reaction mechanism is not clear yet.
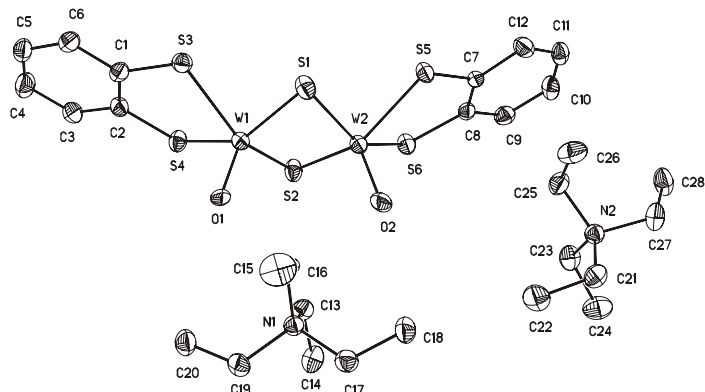
Structure of 20
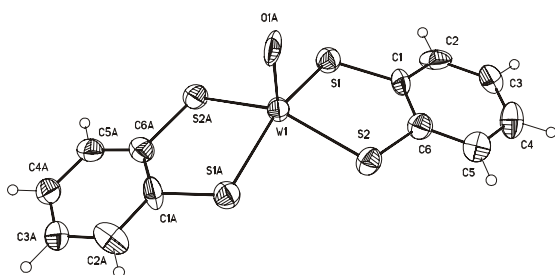
Structure of 21
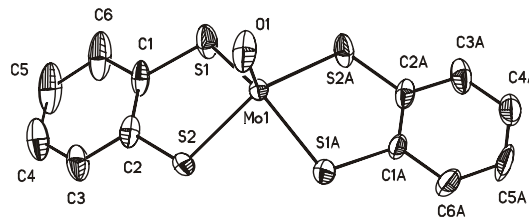
Structure of 22

Treatment of one equivalent of $WCl_4(dme)$ or $MoCl_4(dme)$ with sodium *trans*-1,2-cyclohexanediolate in dimethoxyethane at -50 ºC for 30 min afforded the new complexes $W_2Cl_2(chd)_2$ (**23**) and $Mo_2Cl_2(chd)_2$ (**24**), respectively. The proposed reaction procedure is that during the reaction two mol of the starting material were oxidized from valance IV to valence V and at the same time another two mol of the starting complex were reduced to valance III. Both the complexes **23** and **24** were characterized by elemental analysis and mass spectrometry. Complex **23** was identified by X-ray structural analysis while **24** was characterized by IR spectroscopy in addition.
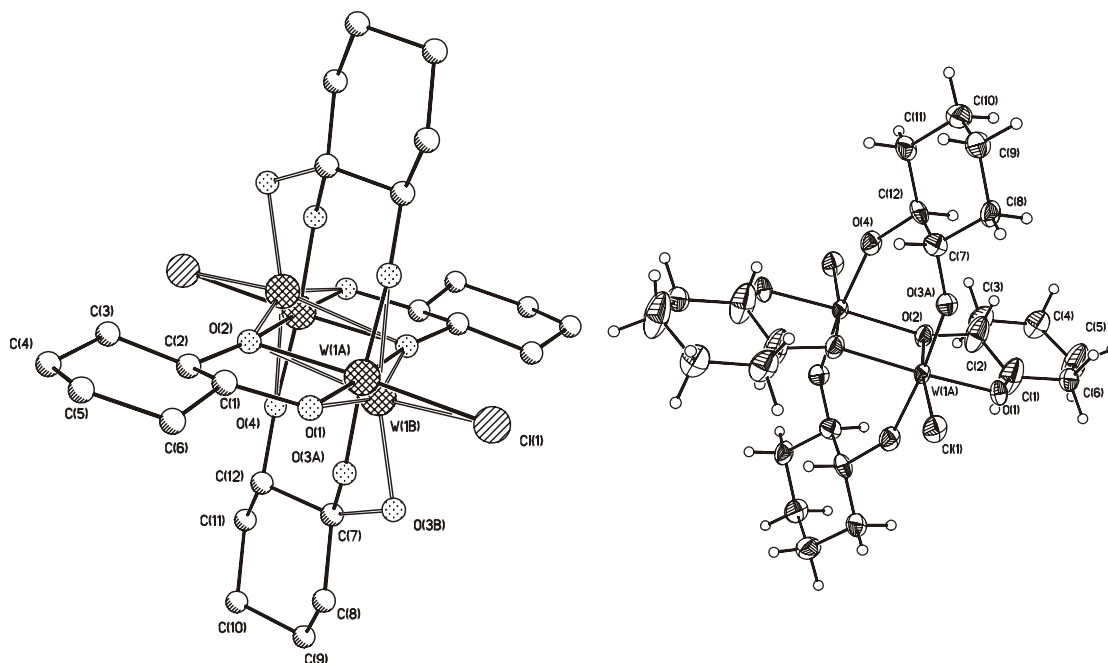
Structure of 23

When the mixture of WCl$_4$(dme) and MoCl$_4$(dme) in dimethoxyethane was treated with one equivalent of sodium *cis*-1,2-cyclohexanedicarboxylate in dimethoxyethane at -50 ºC for 30 min, WCl$_2$(dme)(*cis*-1,2-cyclohexanedicarboxylate) (**25**) and MoCl$_2$(dme)(*cis*-1,2-cyclohexanedicarboxylate) (**26**) were obtained, respectively. During the procedures the byproduct sodium chloride formed and was easily removed by filtration. In these reactions, the redox reaction did not occur probably due to the steric hinderence of *cis*-1,2-cyclohexanedicarboxylate. The attempts to obtain mono(dithiolene) molybdenum and tungsten compounds by the same procedure failed since the tris(dithiolene) metal complexes always were the main products.

Desoxo molybdenum complexes with 3,4-toluenedithiolato and benzene-1,2-dithiolato ligands Mo(dme)(tdt)$_2$ (**27**) and Mo(dme)(bdt)$_2$ (**28**) were synthesized in one step by simple ligand substitution of dithiolene for chlorine by the reaction of MoCl$_4$(dme) and two equivalents of sodium 3,4-toluenedithiolato or sodium benzene-1,2-dithiolato at -50 ºC for 30 min. W(dme)(tdt)$_2$ (**29**) and

W(dme)(bdt)$_2$ **(30)** were synthesized by the same procedure. All products were characterized by elemental analysis and EI-MS as well as IR spectroscopy. The catalytic properties of **27** and **28** were examined by the reaction of DMSO and PPh$_3$ at room temperature. The results show that **27** and **28** can catalyze oxygen atom transfer reactions in analogy to the desoxo forms of the DMSO reductases. The same oxygen atom transfer reactions of their tungsten counterparts **29** and **30** were examined in parallel. The results suggest that complexes **29** and **30** can by used as proper catalysts in oxo transfer reactions as well.
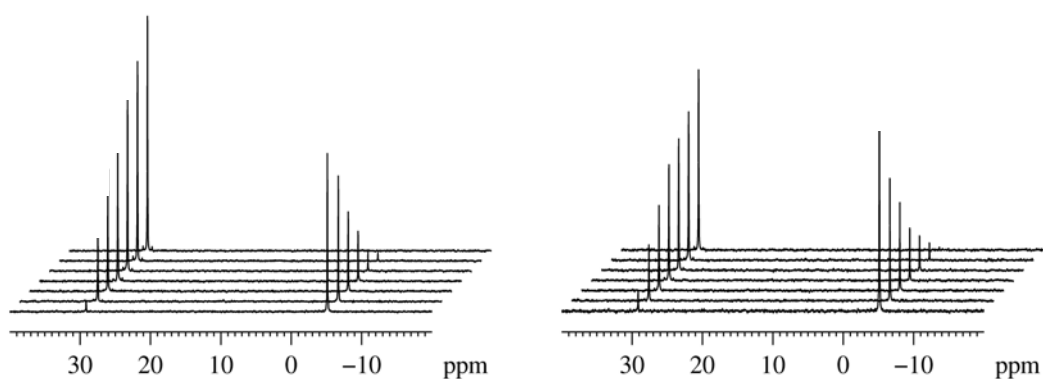
^{31}P NMR spectroscopy studies of oxo-transfer reaction of 27 and 28.
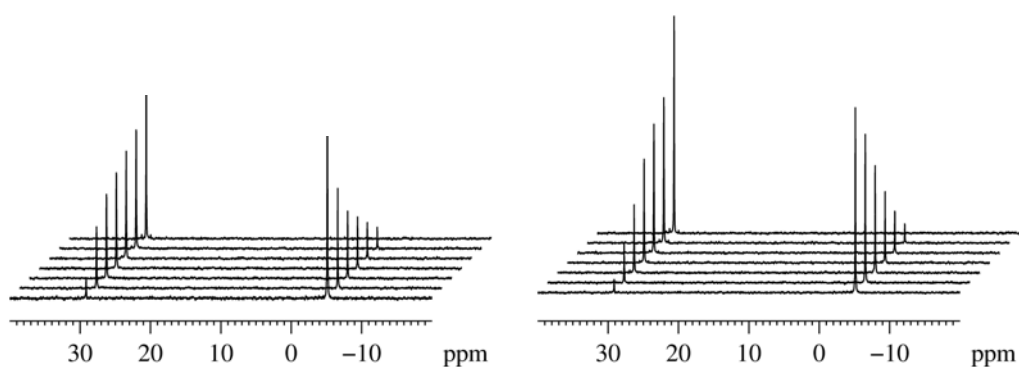
^{31}P NMR spectroscopy studies of oxo-transfer reaction of 29 and 30.

4.2. Outlook

This thesis reports the synthesis and characterization of molybdenum and tungsten compounds with dithiolene and its related chalcogenide ligands. A more general extension of this work would be:

1. The mono- and bis(dithiolene) molybdenum and tungsten compounds can be used to mimic the natural compounds with the aim to explore the properties of molybdoenzymes and tungstoenzymes.

2. Molybdenum and tungsten compounds with related chalcogenide ligands as well as dioxomolybdenum (VI) species stabilized by nitrogen and oxygen donor ligands may have the ability to catalyze a variety of industrially important chemical reactions such as olefin epoxidation and isomerization of alcohols.

3. The desoxo bis(dithiolene) molybdenum and tungsten complexes can catalyze oxygen atom transfer reactions, which provides the possibility for the synthesis of analogues of desoxo molybdenum and tungsten sites in the DMSOR and AOR family and the comparison of molybdenum and tungsten isoenzymes.

5. Experimental Section

5.1. General procedures

All manipulations, unless otherwise stated, were carried out in oxygen-free dry dinitrogen or argon atmosphere using Schlenk glassware and techniques [167]. The glassware used in all the manipulations were oven-dried at 150 ºC for a minimum of 14 h, assembled hot and cooled under high vacuum prior use. Commercial grade solvents were purified and freshly distilled following conventional procedures before use [168].

5.2. Physical measurements

Melting points were measured on a Büchi B-540 melting point apparatus in sealed capillaries and are uncorrected.

IR spectra were recorded on a Bio-Rad Digilab FTS-7 spectrometer in the range of 4000-300 cm^{-1} and the samples were prepared as KBr pellets.

NMR spectra were recorded on Bruker Avance 200, Bruker Avance 300, and Bruker Avance 500 NMR spectrometers. Chemical shifts are reported in ppm external referenced by $SiMe_4$ for ^1H, ^{13}C nuclei and 85 % H_3PO_4 for ^{31}P nuclei. Downfield shifts from the reference are quoted positive, upfield shifts are assigned negative values. The NMR grade deuterated solvents were dried prior use and in following manners: $CDCl_3$-3 min stirring with P_4O_{10} followed by filtration. CD_2Cl_2-storing over freshly activated molecular sieves for one week.

Mass spectra were obtained on Finnigan MAT system 8230 or Varian MAT CH5 mass spectrometers by EI- and ESI-MS methods.

Elemental analysis were performed at the Analytisches Chemisches Laboratorium des Instituts für Anorganische Chemie der Universität Göttingen.

Crystal structure determination: Intensity data for compounds **14** and **23** were collected on a Stoe-IPDS II two-circle diffractometer, and **9**, **11**, **20**, **21** and **22** were collected on a Bruker AXS array detector system. The data for all the compounds were collected at low temperatures. All structures were solved by direct methods (SHELXS-97) [169] and refined with all data by full-matrix least-squares methods on F^2 [170]. All non-hydrogen atoms were refined anisotropically, and hydrogen atoms were attached at idealized positions on carbon atom and were refined as riding atoms with uniform isotropic thermal parameters. Crystal data, data collection details, structural solution and refinement procedures for all compounds are summarized in the tables of section 7.

5.3. Starting Materials

Commercially available chemicals, $MoCl_5$ (Aldrich), WCl_6 (Aldrich), benzene-1,2-dithiol (Fluka), 3,4-toluenedithiol (Alfa Aesar), NaH (Aldrich), 5,5'-dimethyl-2,2'-bipyridyl (Aldrich), *trans*-1,2-cyclohexanediol (Acros), *cis*-1,2-cyclohexanedicarboxylic acid (Acros), triphenyl phosphine (Acros), dimethyl sulfoxide (Grüssing), 4-chlorothiophenol (Alfa Aesar), diethanolamine (Acros) and 2-aminothiophenol (Alfa Aesar) were used as received. Allyltrimethylsilane (Acros), cyclopentene (Aldrich), phenylacetylene (Acros), hexamethyldisiloxane (Aldrich), Me_3SiCl (Aldrich), thiophenol (Fluka), triethylamine (BASF), acetylacetone (Fluka), bis(2-hydroxyethyl) ether (Acros) were freshly distilled prior to use. $MoCl_4$(dme) and WCl_4(dme) [171-173], $WOCl_4$ [63], MoO_2(acac)$_2$ [83] and WO_2(acac)$_2$ [36], MoO_2Cl_2(DME) [72] and WO_2Cl_2(DME) [174], $(Et_4N)_2[MoO_2S_2]$ and $(Et_4N)_2[WO_2S_2]$ [175], benzene-1,2-dithiolate derivatives, o-$C_6H_4(SSiMe_3)_2$ [176] were prepared according to literature procedures.

5.4. Synthesis of compounds 1-30

5.4.1. Synthesis of $WCl_2(chd)_2$ (1)

A solution of *trans*-1,2-cyclohexanediol (0.54 g, 4.6 mmol) in 20 ml dichloromethane was added to a solution of $WOCl_4$ (0.80 g, 2.3 mmol) in 20ml dichloromethane with stirring at room temperature. After stirred for 6 h, the solution was filtered and then reduced to 5 ml under vacuum. The solution was allowed to stand overnight to give colorless crystals of $WCl_2(chd)_2$. Yield: 0.41 g (37 %). IR (KBr) (cm^{-1}): 2948(s), 2863(m), 1653(w), 1454(s), 1419(w), 1347(m), 1238(m), 1089(m), 1067(s), 1042(vs), 1025(vs), 972(vs), 925(m), 880(w), 862(m), 784(m), 712(s), 694(vs), 534(m), 419(m), 398(m), 328(s), 302(s); EI-MS: *m/z* (%) 483 (25) M^+, 445 (20) $(M\text{-}Cl)^+$, 367 (6) $(M\text{-}chd)^+$; *Anal. Calc.* for $C_{12}H_{20}WO_4Cl_2$ (483.04 g/mol): C, 29.84; H, 4.17; Cl, 14.68; found: C, 29.57; H, 4.45; Cl, 14.70.

5.4.2. Synthesis of $WO(chd)_2$ (2)

A solution of *trans*-1,2-cyclohexanediol (0.44 g, 3.8 mmol) in 20 ml dichloromethane was added to a solution of $WOCl_4$ (0.64 g, 1.9 mmol) in 20ml dichloromethane at 0 ºC with stirring. After stirred for 0.5 h, the solution was filtered and the solvent was removed under vacuum. The product was obtained as white powder. Yield: 0.57 g (71 %). IR (KBr) (cm^{-1}): 2939(s), 2863(m), 1653(w), 1451(s), 1342(m), 1262(s), 1240(s), 1199(w), 1135(w), 1062(vs), 1041(vs), 980(vs), 927(s), 879(s), 854(s), 791(w), 736(w), 676(vs), 574(s), 529(m); EI-MS: *m/z* (%) 427 (100) M^+; *Anal. Calc.* for $C_{12}H_{20}WO_5$ (428.14 g/mol): C, 33.66; H, 4.71; found: C, 33.65; H, 5.17.

5.4.3. Synthesis of WO(tdt)$_2$ (3)

A solution of sodium 3,4-toluenedithiolate (0.55 g, 2.8 mmol) was added to a solution of WOCl$_4$ (0.47 g, 1.4 mmol) in 40 ml dichloromethane at -50 ºC with stirring. The color changed from orange to dark green immediately. The reactants were stirred for 1 h at -50 ºC and then another 1 h at room temperature to give a dark green mixture. After filtration, the solvent of the filtrate was removed and the product was obtained as dark green powder. Yield: 0.46 g (66 %). ^{1}H NMR (300.13 MHz, CD$_2$Cl$_2$): δ 2.37 (s, 6H, CH$_3$), 7.22-3.24 (m, 2H, Ar-H), 7.96-7.99 (m, 4H, Ar-H); (KBr) (cm^{-1}): 1583(m), 1518(m), 1453(m), 1374(m), 1307(w), 1261(vs), 1204(m), 1152(w), 1096(vs), 1080(vs), 1022(vs), 865(m), 800(vs), 689(m), 542(s), 483(w), 431(m); *Anal. Calc.* for C$_{14}$H$_{12}$WOS$_4$ (508.34 g/mol): C, 33.08; H, 2.38; S, 25.23; found: C, 32.98; H, 2.48; S, 25.34.

5.4.4. Synthesis of WOCl$_2$(O(CH$_2$)$_2$O(CH$_2$)$_2$O) (4)

A solution of bis(2-hydroxyethyl) ether (0.39 g, 3.7 mmol) was added to a solution of WOCl$_4$ (1.25 g, 3.7 mmol) in 40 ml dichloromethane with stirring at room temperature. The mixture was stirred for 1 h to give a light purple solution. After filtration, the solvent of the filtrate was removed and the product was obtained as white powder. Yield: 1.11 g (80 %). IR (KBr) (cm^{-1}): 1472(vs), 1445(vs), 1395(m), 1359(s), 1353(s), 1330(s), 1253(vs), 1237(vs), 1227(vs), 1085(vs), 1050(vs), 1023(vs), 1003(s), 969(vs), 917(vs), 861(s), 807(s), 612(vs), 404(vs), 340(s); EI-MS: *m/z* (%) 375 (2) M^+, 339 (100) (*M*-Cl)$^+$; *Anal. Calc.* for C$_4$H$_8$WO$_4$Cl$_2$ (374.86 g/mol): C, 12.82; H, 2.15; Cl, 18.92; found: C, 13.62; H, 2.43; Cl, 18.76.

5.4.5. Synthesis of WO(O(CH$_2$)$_2$O(CH$_2$)$_2$O)(chd) (5)

A solution of *trans*-1,2-cyclohexanediol (0.14 g, 1.2 mmol) in 20 ml dichloromethane was added to a solution of WCl$_2$(O(CH$_2$)$_2$O(CH$_2$)$_2$O) (0.46 g, 1.2 mmol) in 15ml dichloromethane with stirring at room temperature. The color of the solution changed from light purple to colorless immediately. After 2 h, the solution was filtered and the filtrate was dried under vacuum to afford white crystalline solid. Yield: 0.36 g (73 %). IR (KBr) (cm^{-1}): 1457(m), 1352(w), 1262(vs), 1092(vs), 1023(vs), 982(m), 923(w), 863(m), 799(vs), 613(m), 574(m), 524(w), 397(m); EI-MS: *m/z* (%) 418 (100) *M*$^+$, 304 (48) (*M*-chd)$^+$; *Anal. Calc.* for C$_{10}$H$_{18}$WO$_6$ (418.06 g/mol): C, 28.73; H, 4.34; found: C, 27.09; H, 3.97.

5.4.6. Synthesis of W$_2$O$_2$Cl$_2$(O(CH$_2$)$_2$O(CH$_2$)$_2$O)$_2$(bdt) (6)

0.22 g (1.5 mmol) benzene-1,2-dithiol was added to a solution of WCl$_2$(O(CH$_2$)$_2$O(CH$_2$)$_2$O) (0.57 g, 1.5 mmol) in 15ml dichloromethane with stirring at room temperature. The color of the solution changed from light purple to blue-green immediately. After 2 h, the solution was filtered and the filtrate was dried under vacuum to afford dark-blue solid. Yield: 0.68 g (57 %). ^{1}H NMR (300.13 MHz, CDCl$_3$): δ 4.57 (t, 8H, CH$_2$), 4.70 (t, 8H, CH$_3$), 6.86-6.99 (m, 4H, Ar-H); IR (KBr) (cm^{-1}): 1472(s), 1446(s), 1359(m), 1330(m), 1260(s), 1237(s), 1228(s), 1086(vs), 1049(vs), 1023(vs), 1004(vs), 969(vs), 917(vs), 863(s), 803(vs), 744(m), 706(m), 616(vs), 599(vs), 405(s), 340(s), 297(vs); *Anal. Calc.* for C$_{14}$H$_{20}$W$_2$O$_8$S$_2$Cl$_2$ (819.03 g/mol): C, 20.53; H, 2.46; found: C, 20.74; H, 2.70.

5.4.7. Synthesis of WO(O(CH$_2$)$_2$O(CH$_2$)$_2$O)(bdt) (7)

A solution of sodium benzene-1,2-dithiolato (0.17 g, 0.9 mmol) in 10ml dichloromethane was added to a solution of $WCl_2(O(CH_2)_2O(CH_2)_2O)$ (0.34 g, 0.9 mmol) in 10 ml dichloromethane at -50 ºC with stirring. The color changed from cream to blue-green. The reactants were stirred for 1 h at -50 ºC and then stirred at room temperature overnight to give a dark blue-green mixture. After filtration, the solvent of the filtrate was removed under vacuum and the product was obtained as dark blue-green powder. Yield: 0.28 g (69 %). IR (KBr) (cm^{-1}): 1447(w), 1309(vs), 1238(vs), 1184(vs), 1127(vs), 1065(m), 1022(m), 984(vs), 916(m), 862(w), 805(s), 746(s), 717(w), 666(w), 618(w), 584(m), 562(m), 532(m); EI-MS: *m/z* (%) 430 (5) (*M*-O)$^{+}$, 339 (100) (*M*-O(CH$_2$)$_2$O(CH$_2$)$_2$O)$^{+}$, 140 (10) (bdt)$^{+}$; *Anal. Calc.* for $C_{10}H_{12}WO_4S_2$ (444.17 g/mol): C, 27.04; H, 2.72; S, 14.44; found: C, 26.97; H, 2.71; S, 14.04.

5.4.8. Synthesis of WO$_2$Cl$_2$ (mebipy) (8)

WO$_2$Cl$_2$ (DME) (1.27 g, 3.7 mmol) and 5, 5`-dimethyl-2, 2`-dipyridyl (0.68 g, 3.7 mmol) were suspended in 40 ml dichloromethane at room temperature. The cream color mixture was stirred for 30 min. White precipitate was formed. The solvent was decanted and the precipitate was dried under vacuum for 1 h. The solid was washed with dichloromethane 3×30ml and diethyl ether 3×30ml, and then dried under vacuum for 2 h. Yield: 1.12 g (65 %). IR (KBr) (cm^{-1}): 1635(s), 1602(s), 1506 (m), 1484(s), 1476(s), 1448(w), 1386(s), 1319(s), 1266(w), 1242(s), 1165(m), 1153(m), 1052(s), 1039(w), 1002(w), 955(vs), 913(vs), 846(vs), 824(m), 730(m), 693(m), 656(m), 489(w), 428(w), 365(m), 333(s); A*nal. Calc.* For $WO_2N_2Cl_2C_{12}H_{12}$ (471.00 g/mol): C, 30.60; H, 2.57; N, 5.95. Found: C, 30.25; H, 2.60; N, 5.94.

5.4.9. Synthesis of WO$_2$(SPh)$_2$(mebipy) (9)

The mixture of thiophenol (0.46 g, 4.2 mmol) and triethylamine (0.42 g, 4.2 mmol)

in acetonitrile (20 ml) was added to the solution of WO$_2$Cl$_2$(mebipy) (0.99 g, 2.1 mmol) in acetonitrile (30 ml) at room temperature. The mixture was stirred for 2 h and yellow solution was isolated by filtration. The solvent was reduced to 20 ml under vacuum. The solution was allowed to stand overnight to afford golden crystals of WO$_2$(SPh)$_2$(mebipy). Yield: 0.84 g (65 %). Melting point: 182-183 °C (decomp.). IR (KBr) (cm^{-1}): 1600(m), 1577(s), 1502(w), 1476(vs), 1434(m), 1398(w), 1384(m), 1317(m), 1262(s), 1156(m), 1096(s), 1080(s) 1050(s), 1023(s), 939(vs), 895(vs), 844(vs), 801(vs), 737(vs), 690(vs), 654(m), 505(w), 480(m), 429(m), 393(w), 355(s); *Anal. Calc.* For WO$_2$S$_2$N$_2$C$_{24}$H$_{22}$ (618.42 g/mol): C, 46.61; H, 3.59; N, 4.53. Found: C, 46.43; H, 3.76; N, 4.58.

5.4.10. Synthesis of MoO$_2$Cl$_2$(mebipy) (10)

Mixture of MoO$_2$Cl$_2$(DME) (1.98 g, 6.9 mmol) and 5, 5`-dimethyl-2, 2`-dipyridyl (1.26 g, 6.8 mmol) were suspended in 70 ml dichloromethane at room temperature. The cream color mixture was stirred for 30 min. Light green precipitate was formed. The solvent was decanted, and the residue was dried under vacuum for 1 h. The solid was washed with dichloromethane 3×30ml and diethyl ether 3×30ml, and then dried under vacuum for 2 h. Yield: 1.99 g (76 %). IR (KBr) (cm^{-1}): 1638(w), 1600(s), 1505(m), 1484(s), 1476(s), 1450(m), 1385(s), 1319(s), 1241(s), 1164(m), 1152(m), 1052(s), 936(vs), 904(vs), 842(vs), 822(w), 729(m), 692(m), 655(m), 496(w), 487(w), 427(m), 385(m), 373(m), 346(s); *Anal. Calc.* For MoO$_2$N$_2$Cl$_2$C$_{12}$H$_{12}$ (383.09 g/mol): C, 37.62; H, 3.16; N, 7.31. Found: C, 37.43; H, 3.26; N, 7.26.

5.4.11. Synthesis of Mo$_2$O$_4$(SPh)$_2$(mebipy)$_2$ (11)

The mixture of thiophenol (0.17 g, 1.5 mmol) and triethylamine (0.15 g, 1.5 mmol) in acetonitrile (10 ml) was added to the solution of MoO$_2$Cl$_2$(mebipy) (0.29 g, 0.8 mmol) in acetonitrile (20 ml) at room temperature. The mixture was stirred for 30 min

and dark brown solution was isolated by filtration. The solvent was reduced to 10 ml under vacuum. The solution was allowed to stand overnight to afford dark red crystals of $Mo_2O_4(SPh)_2(mebipy)_2$. Yield: 0.33 g (52 %). Melting point: 250 °C (decomp.). IR (KBr) (cm^{-1}): 1669(m), 1601(s), 1575(s), 1505(m), 1479(vs), 1434 (s), 1387(s), 1314(s), 1260(m), 1245(s), 1158(m), 1083(m), 1048(s), 1023(m), 947(m), 923(vs), 897(vs), 886(vs), 838(vs), 748(vs), 706(vs), 698(vs), 676(vs), 650(vs), 488(m), 460(w), 423(s), 365(w), 328(m); *Anal. Calc.* For $Mo_2O_4S_2N_4C_{36}H_{34}$ (842.69 g/mol): C, 51.31; H, 4.07; N, 6.65. Found: C, 50.99; H, 4.19; N, 6.96.

5.4.12. Synthesis of $Mo_2O_3(SPh)(bdt)(mebipy)_2$ (12)

To a solution of $Mo_2O_4(SPh)_2(mebipy)_2$ (0.23 g, 0.3 mmol) in acetonitrile (10 ml) at -20 ºC was added dropwise a solution of 1,2-$C_6H_4(SSiMe_3)$ (0.08 g, 0.3 mmol) in acetonitrile (2 ml). The color changed to dark blue immediately. After stirring for 3 min, N, N-Dimethylacetamide (0.48 ml) in acetonitrile (0.5 ml) was added, then the reaction mixture was dried under vacuum to afford dark green solid. Yield: 0.12 g (49 %). IR (KBr) (cm^{-1}): 1653(w), 1575(m), 1559(w), 1477(m), 1437(w), 1312(w), 1262(vs), 1100(vs), 1021(vs), 948(s), 928(s), 800(vs), 747(s), 695(m), 489(m), 461(m), 397(m), 351(w), 327(m); EI-MS: *m/z* (%) 566 (5) (*M*-2SPh-mebipy)$^+$, 518 (100) (*M*-2mebipy-Ph)$^+$; *Anal. Calc.* For $Mo_2O_3S_4N_4C_{42}H_{38}$ (966.91 g/mol): C, 52.17; H, 3.96; N, 5.79; S, 13.26. Found: C, 51.92; H, 4.60; N, 6.31; S, 13.28.

5.4.13. Synthesis of $Mo_2O_4(SPh-Cl)_2(mebipy)_2$ (13)

The mixture of 4-chlorothiophenol (0.82 g, 5.7 mmol) and triethylamine (0.57 g, 5.7 mmol) in acetonitrile (20 ml) was added to the solution of $MoO_2Cl_2(mebipy)$ (1.09 g, 2.8 mmol) in acetonitrile (30 ml) at room temperature. The mixture was stirred for 30 min and dark green solution was isolated by filtration. The solvent of the filtrate was removed and the product was obtained as dark powder. Yield: 1.68 g (65

%). IR (KBr) (cm^{-1}): 1601(s), 1575(m), 1504(s), 1479(s), 1471(vs), 1385(s), 1316(s), 1261(m), 1245(s), 1153(m), 1090(vs), 1050(s), 1011(s), 931(vs), 895(vs), 845(vs), 813(vs), 761(vs), 728(vs), 688(s), 652(s), 543(s), 493(s), 428(s), 378(s), 367(s), 351(w), 320(m), 299(w); *Anal. Calc.* For $Mo_2O_4S_2N_4Cl_2C_{36}H_{32}$ (911.58 g/mol): C, 47.43; H, 3.54; N, 6.15. Found: C, 47.00; H, 3.85; N, 6.15.

5.4.14. Synthesis of $MoO_2(O(CH_2)_2NH(CH_2)_2O)\cdot DMF$ (14)

A solution of diethanolamine (0.46 g, 1.4 mmol) in DMF (20 ml) was added to a solution of $MoO_2(acac)_2$ (0.45 g, 1.4 mmol) in DMF (20 ml) at room temperature. The mixture was stirred overnight and the resulting yellow solution was isolated by filtration. Half of the solvent was removed under vacuum. The solution was allowed to stand overnight to give 0.16 g yellow crystals of $MoO_2(O(CH_2)_2NH(CH_2)_2O)\cdot DMF$ (49 % yield). Melting point: 257-259°C (decomp.). IR (KBr) (cm^{-1}): 1661(vs), 1559(w), 1442(s), 1414(s), 1380(s), 1292(w), 1254(s), 1230(m), 1193(w), 1098(s), 1064(s), 1040(s), 892(vs), 840(s), 662(s), 555(m), 484(w), 400(w), 363(m), 333(m); *Anal. Calc.* for $C_7H_{16}MoN_2O_5$ (304.16 g/mol): C, 27.63; H, 5.27; N, 9.13; found: C, 27.75; H, 5.32; N, 8.91.

5.4.15. Synthesis of $MoO_2(2-amino-thiophenol)_2$ (15)

A solution of 2-amino-thiophenol (0.86 g, 6.9 mmol) was added to a suspension of $MoO_2(acac)_2$ (1.12 g, 3.4 mmol) in 30ml methanol. After stirring for 30 min at room temperature the solution was dried under vacuum to afford dark solid. Yield: 0.81 g (63 %). IR (KBr) (cm^{-1}): 1575(m), 1540(m), 1434(m), 1343(m), 1315(w), 1248(m), 1159(m), 1124(s), 1060(s), 1017(m), 935(m), 905(m), 845(m), 759(s), 724(s), 690(s), 643(s), 566(vs), 530(m), 454(s), 435(s), 388(s), 340(vs), 297(vs), 280(vs); EI-MS: *m/z* (%) 375 (16) *M*$^+$, 343 (46) (*M*-2O)$^+$; *Anal. Calc.* for $MoO_2S_2N2C_{12}H_{12}$ (376.30 g/mol):

C, 38.30; H, 3.21; N, 7.44; found: C, 38.20; H, 3.64; N, 6.77.

5.4.16. Synthesis of $(Ph_3PH)_2[MoO_2(chd)_2]$ (16)

To a suspension of $MoO_2(acac)_2$ (0.45 g, 1.4 mmol) in 20 ml dichloromethane, the mixture of PPh_3 (0.72 g, 2.8 mmol) and *trans*-1,2-cyclohexanediol (0.32 g, 2.8 mmol) in 10 ml dichloromethane was added. The mixture was allowed to stir for 40min. The white precipitate was removed by filtration and the filtrate was dried under vacuum to afford brown solid. Yield: 0.80 g (66 %). IR (KBr) (cm^{-1}): 1582(m), 1563(m), 1520(s), 1475(s), 1434(s), 1354(s), 1307(w), 1262(s), 1243(m), 1201(m), 1177(w), 1154(m), 11189m), 1088(s), 1068(s), 1044(w), 1025(s), 996(m), 958(m), 930(m), 855(m), 806(s), 742(vs), 722(m), 693(vs), 618(w), 596(w), 568(w), 540(s), 512(s), 490(s), 446(m), 419(m), 397(w); ESI-MS: *m/z* (%) 357 (4) $(M_a+H)^+$, 325 (4) $(M_a-2O+H)^+$; *Anal. Calc.* for $MoO_6P_2C_{48}H_{52}$ (882.82 g/mol): C, 65.30; H, 5.94; found: C, 65.28; H, 5.96.

5.4.17. Synthesis of $(Ph_3PH)_2[MoO_2(bdt)_2]$ (17)

To a suspension of $MoO_2(acac)_2$ (0.42g, 1.3mmol) in 20 ml dichloromethane, the mixture of PPh_3 (0.67 g, 2.6 mmol) and benzene-1,2-dithiol (0.35 g, 2.5 mmol) in 10 ml dichloromethane was added. The mixture was allowed to stir for 30min. After filtration the filtrate was dried under vacuum to afford dark green solid. Yield: 0.85 g (71 %). Melting point: 82.4 °C (decomp.). IR (KBr) (cm^{-1}): 1559(m), 1521(m), 1476(m), 1435(s), 1359(w), 1307(w), 1261(s), 1198(m), 1154(w), 1118(vs), 1089(vs), 1070(m), 1034(m), 997(w), 932(s), 865(s), 800(s), 742(s), 720(s), 692(vs), 665(s), 617(w), 539(vs), 511(m), 490(m); ESI-MS: *m/z* (%) 403 (2) $(M_a+H)^+$, 301 (100) $(M_a$-Ar-S+H)$^+$; *Anal. Calc.* for $MoO_2S_4P_2C_{48}H_{40}$ (934.97 g/mol): C, 61.66; H, 4.31; found: C, 61.71; H, 4.66.

5.4.18. Synthesis of (Ph$_3$PH)$_2$[WO$_2$(bdt)$_2$] (18)

To a suspension of WO$_2$(acac)$_2$ (0.53 g, 1.3 mmol) in 20 ml dichloromethane, the mixture of PPh$_3$ (0.67 g, 2.6 mmol) and benzene-1,2-dithiol (0.36 g, 2.5 mmol) in 10 ml dichloromethane was added. The mixture was allowed to stir for 30min. After filtration the filtrate was dried under vacuum to afford dark green solid. Yield: 0.82 g (63 %). Melting point: 79 °C (decomp.). IR (KBr) (cm^{-1}): 1560(w), 1475(w), 1436(m), 1308(m), 1239(vs), 1154(s), 1121(s), 1091(s), 1024(m), 985(w), 903(s), 857(s), 802(s), 741(vs), 692(vs), 666(s), 616(w), 537(m), 498(m), 429(w), 396(w), 338(m); ESI-MS: *m/z* (%) 497 (2) (M_a+H)$^+$, 479 (5) (M_a-O+H)$^+$, 463 (15) (M_a-2O+H)$^+$, 279 (100) (M_a-bdt-Ar+H)$^+$; *Anal. Calc.* for WO$_2$S$_4$P$_2$C$_{48}$H$_{40}$ (1022.88 g/mol): C, 56.36; H, 3.94; found: C, 56.36; H, 4.10.

5.4.19. Synthesis of (Et$_4$N)$_2$[WO$_2$(S$_2$C$_2$PhH)] (19)

A solution of phenylacetylene (0.36 g, 3.5 mmol) was added to a solution of (Et$_4$N)$_2$[WO$_2$S$_2$] (0.36 g, 0.7 mmol) in 10 ml acetonitrile with stirring at room temperature. After 4 days stirring the yellow mixture was filtered and the solvent was removed under vacuum. The product was obtained as yellow precipitate. Yield: 0.25 g (59 %). ^{1}H NMR (300.13 MHz, CDCl$_3$): δ 1.15-1.40 (m, 24H, CH$_3$), 1.99 (s, 1H, S$_2$C$_2$PhH-H), 3.38-3.64 (m, 16H, CH2), 7.3-7.5 (m, 5H, Ar-H); IR (KBr) (cm^{-1}): 1458(s), 1401(m), 1374(w), 1310(m), 1183(vs), 1121(w), 1081(m), 1034(s), 1009(s), 891(vs), 850(vs), 798(s), 765(m), 702(w), 618(w), 556(w), 536(w), 451(vs), 435(vs), 351(w), 314(w); *Anal. Calc.* for C$_{24}$H$_{46}$WO$_2$N$_2$S$_2$ (642.61 g/mol): C, 44.86; H, 7.22; N, 4.36; found: C, 43.15; H, 7.28; N, 4.97.

5.4.20. Synthesis of   (Et$_4$N)$_2$[W$_2$O$_2$(μ-S)$_2$(bdt)$_2$] (20)

A solution of benzene-1,2-dithiol (0.17 g, 1.2 mmol) in 5 ml acetonitrile was added to a solution of (Et$_4$N)$_2$[WO$_2$S$_2$] (0.62 g, 1.1 mmol) in 20 ml acetonitrile with stirring at room temperature. The color of the solution changed from yellow to red-brown immediately. After 2 h, the solution was filtered. Slow addition of 4 ml diethyl ether by vapor diffusion to this filtrate afforded the red-brown crystals **20** after 10 days. Yield: 0.35 g (30 %). IR (KBr) (cm^{-1}): 1550(m), 1478(s), 1457(w), 1441(s), 1420(m), 1391(s), 1284(w), 1240(s), 1171(s), 1102(s), 1052(w), 998(s), 944(vs), 932(s), 904(w), 782(m), 747(s), 664(s), 437(s), 362(s), 335(m); ESI-MS: *m/z* (%) 746 (30) (M_a+H)$^+$, 604 (33) (M_a-bdt+H)$^+$; *Anal. Calc.* for C$_{28}$H$_{48}$N$_2$O$_2$S$_6$W$_2$ (1004.76 g/mol): C, 33.47; H, 4.82; N, 2.79; found: C, 33.56; H, 4.83; N, 2.65.

5.4.21. Synthesis of (Et$_4$N)$_2$[WO(bdt)$_2$] (21)

A solution of benzene-1,2-dithiol (0.33 g, 2.3 mmol) in 5 ml acetonitrile was added to a solution of (Et$_4$N)$_2$[WO$_2$S$_2$] (0.62 g, 1.1 mmol) in 20 ml acetonitrile with stirring at room temperature. The color of the solution changed from yellow to red-brown immediately. After 2 h, the solution was filtered. Slow addition of 4 ml diethyl ether by vapor diffusion to this filtrate afforded red-brown crystals. Yield: 0.56 g (67 %). IR (KBr) (cm^{-1}): 1546(m), 1480(vs), 1457(vs), 1438(vs), 1393(s), 1307(m), 1262(m), 1233(m), 1182(s), 1102(m), 1077(w), 1033(m), 1022(s), 1004(m), 948(m), 902(m), 885(vs), 848(s), 796(s), 752(s), 663(m), 660(m), 614(w), 544(w), 447(vs), 350(w), 319(m); ESI-MS: m/z (%) 479 (5) (M_a+H)$^+$, 338 (30) (M_a-bdt+H)$^+$; *Anal. Calc.* for C$_{28}$H$_{48}$N$_2$OS$_4$W (740.79 g/mol): C, 45.40; H, 6.53; N, 3.78; found: C, 43.89; H, 6.43; N, 4.04.

5.4.22. Synthesis of (Et$_4$N)[MoO(bdt)$_2$] (22)

A solution of benzene-1,2-dithiol (0.20 g, 1.4 mmol) in 5 ml DMF was added to a solution of (Et$_4$N)$_2$[MoO$_2$S$_2$] (0.65 g, 1.4 mmol) in 20 ml DMF with stirring at room temperature. The color of the solution changed from orange to wine red immediately. After 1 h, the solution was filtered. Slow addition of 4 ml diethyl ether by vapor diffusion to this filtrate afforded needle-like red-brown crystals. Yield: 0.45 g (60 %). IR (KBr) (cm^{-1}): 1480(s), 1430(m), 1417(m), 1393(m), 1262(vs), 1232(m), 1172(m), 1095(vs), 1019(vs), 900(s), 878(s), 799(vs), 753(s), 705(w), 660(m), 608(w), 552(w), 393(m), 356(s); ESI-MS: *m/z* (%) 394 (100) (M_a+H)$^+$, 254 (31) (M_a-bdt+H)$^+$; *Anal. Calc.* for C$_{20}$H$_{28}$MoONS$_4$ (522.63 g/mol): C, 45.96; H, 5.40; N, 2.68; found: C, 44.16; H, 5.09; N, 3.04.

5.4.23. Synthesis of W$_2$Cl$_2$(chd)$_2$ (23)

A solution of sodium *trans*-1,2-cyclohexanediolate (0.39 g, 2.4 mmol) in 20 ml dimethoxyethane was added to a solution of WCl$_4$(dme) (0.84 g, 2.0 mmol) in 10 ml dimethoxyethane at -50 ºC. After stirred at -50 ºC for 0.5 h and then another 1 h at room temperature, the solution was filtered and the filtrate was stand over one week at room temperature to afforded dark red crystals. Yield: 0.47 g (26 %). EI-MS: *m/z* (%) 895 (5) M^+, 821 (4) (M-2Cl)$^+$; *Anal. Calc.* for C$_{24}$H$_{40}$W$_2$O$_8$Cl$_2$ (895.18 g/mol): C, 32.20; H, 4.50; found: C, 32.01; H, 4.46.

5.4.24. Synthesis of Mo$_2$Cl$_2$(chd)$_2$ (24)

A solution of sodium *trans*-1,2-cyclohexanediolate (0.21 g, 1.3 mmol) in 20 ml dimethoxyethane was added to a solution of MoCl$_4$(dme) (0.33 g, 1.0 mmol) in 10 ml

dimethoxyethane at -50 ºC with stirring. After stirred at -50 ºC for 0.5 h and then another 1 h at room temperature, the solution was filtered and the filtrate was dried under vacuum to afford dark-green solid. Yield: 0.31 g (63 %). IR (KBr) (cm^{-1}): 2953(vs), 2859(vs), 1655(w), 1636(w), 1450(s), 1353(s), 1339(m), 1302(w), 1262(s), 1241(m), 1201(m), 1088(vs), 1024(vs), 975(vs), 925(m), 884(m), 854(s), 795(s), 658(vs), 589(m), 548(m), 407(m); EI-MS: *m/z* (%) 645 (4) (*M*-2Cl)$^{+}$, 535 (3) (*M*-2Cl-chd)$^{+}$; *Anal. Calc.* for C$_{12}$H$_{20}$Mo$_2$O$_4$Cl$_2$ (491.07 g/mol): C, 29.35; H, 4.11; Cl, 14.44; found: C, 30.06; H, 5.16; Cl, 13.81.

5.4.25. Synthesis of WCl$_2$(dme)(*cis*-1,2-cyclohexanedicarboxylate) (25)

A solution of sodium *cis*-1,2-cyclohexanedicarboxylate (0.516 g, 2.4 mmol) in 20 ml dimethoxyethane was added to a solution of WCl$_4$(dme) (0.79 g, 2.4 mmol) in 10 ml dimethoxyethane at -50 ºC with stirring. After stirred at -50 ºC for 0.5 h and then another 1 h at room temperature, the solution was filtered and the filtrate was dried under vacuum to afford brown solid. Yield: 0.57 g (58 %). IR (KBr) (cm^{-1}): 2936(s), 2860(s), 1942(w), 1853(w), 1713(vs), 1636(w), 1540(m), 1452(s), 1434(s), 1308(m), 1244(vs), 1192(m), 1127(s), 1088(s), 1031(s), 984(s), 904(w), 852(m), 802(s), 745(w), 662(m), 539(m), 435(m); EI-MS: *m/z* (%) 429 (4) (*M*-dme)$^{+}$; *Anal. Calc.* for C$_{12}$H$_{20}$WO$_6$Cl$_2$ (515.04 g/mol): C, 27.98; H, 3.91; found: C, 27.57; H, 3.92.

5.4.26. Synthesis of MoCl$_2$(dme)(*cis*-1,2-cyclohexanedicarboxylate) (26)

A solution of sodium *cis*-1,2-cyclohexanedicarboxylate (0.46 g, 2.1 mmol) in 30 ml dimethoxyethane was added to a solution of MoCl$_4$(dme) (0.57 g, 1.7 mmol) in 10 ml

dimethoxyethane at -50 ºC with stirring. After stirred at -50 ºC for 0.5 h and then another 1 h at room temperature, the solution was filtered and the filtrate was dried under vacuum to afford brown-green solid. Yield: 0.42 g (56 %). IR (KBr) (cm^{-1}): 2964(m), 1701(w), 1637(s), 1617(s), 1507(w), 1420(w), 1260(s), 1245(s), 1155(w), 1100(m), 1025(w), 985(w), 802(s), 618(m), 472(m), 398(m), 336(vs), 323(vs); EI-MS: *m/z* (%) 429 (5) *M*$^+$, 335 (66) (*M*-dme)$^+$; *Anal. Calc.* for $C_{12}H_{20}MoO_6Cl_2$ (427.13 g/mol): C, 33.74; H, 4.72; found: C, 33.25; H, 4.88.

5.4.27. Synthesis of Mo(dme)(tdt)$_2$ (27)

A solution of sodium 3,4-toluenedithiolato (0.30 g, 1.5 mmol) in 20 ml dimethoxyethane was added to a solution of MoCl$_4$(dme) (0.25 g, 0.8 mmol) in 10 ml dimethoxyethane at -50 ºC with stirring. After stirred at -50 ºC for 0.5 h and then another 1 h at room temperature, the solution was filtered and the filtrate was dried under vacuum to afford dark green solid. Yield: 0.22 g (61 %). Melting point > 400 ºC. IR (KBr) (cm^{-1}): 2964(m), 2917(w), 1578(s), 1454(s), 1375(m), 1260(s), 1203(m), 1190(m), 1100(s), 1081(s), 1027(s), 937(w), 859(m), 803(vs), 702(w), 686(m), 633(w), 544(s), 469(m), 433(m), 390(m), 354(s), 336(s), 302(m); EI-MS: *m/z* (%) 403 (4) (*M*-dme)$^+$, 247 (10) (*M*-dme-tdt-3H)$^+$; *Anal. Calc.* for $C_{18}H_{22}MoO_2S_4$ (494.55 g/mol): C, 43.71; H, 4.48; found: C, 43.76; H, 4.88.

5.4.28. Synthesis of Mo(dme)(bdt)$_2$ (28)

A solution of sodium benzene-1,2-dithiolato (0.64 g, 3.4 mmol) in 20 ml dimethoxyethane was added to a solution of MoCl$_4$(dme) (0.56 g, 1.7 mmol) in 10 ml dimethoxyethane at -50 ºC with stirring. After stirred at -50 ºC for 0.5 h and then another 1 h at room temperature, the solution was filtered and the filtrate was dried under vacuum to afford dark green solid. Yield: 0.51 g (65 %). Melting point > 400 ºC.

IR (KBr) (cm^{-1}): 3044(m), 2920(w), 2824(w), 1555(m), 1470(w), 1440(vs), 1422(s), 1365(m), 1261(s), 1242(s), 1189(m), 1155(m), 1119(m), 1103(s), 1080(vs), 1019(s), 855(s), 801(s), 744(vs), 708(m), 663(s), 473(m), 432(m), 348(s), 327(m); EI-MS: *m/z* (%) 235 (5) (*M*-dme-bdt)$^{+}$; *Anal. Calc.* for $C_{16}H_{18}MoO_2S_4$ (466.50 g/mol): C, 41.20; H, 3.86; found: C, 40.83; H, 3.86.

5.4.29. Synthesis of W(dme)(tdt)$_2$ (29)

A solution of sodium 3,4-toluenedithiolato (0.28 g, 1.4 mmol) in 20 ml dimethoxyethane was added to a solution of WCl$_4$(dme) (0.28 g, 0.7 mmol) in 10 ml dimethoxyethane at -50 ºC with stirring. After stirred at -50 ºC for 0.5 h and then another 1 h at room temperature, the solution was filtered and the filtrate was dried under vacuum to afford dark green solid. Yield: 0.25 g (63 %). Melting point > 400 ºC. IR (KBr) (cm^{-1}): 2964(s), 2860(s), 1942(w), 1853(w), 1585(m), 1552(w), 1457(s), 1436(s), 1380(m), 1261(vs), 1203(w), 1080(vs), 1037(vs), 866(m), 801(vs), 688(s), 667(s), 545(m), 484(w), 441(w), 390(s), 334(w); EI-MS: *m/z* (%) 492 (10) (*M*-dme)$^{+}$, 338 (46) (*M*-dme-tdt)$^{+}$; *Anal. Calc.* for $C_{18}H_{22}WO_2S_4$ (582.46 g/mol): C, 37.12; H, 3.81; found: C, 37.20; H, 3.98.

5.4.30. Synthesis of W(dme)(bdt)$_2$ (30)

A solution of sodium benzene-1,2-dithiolato (0.28 g, 1.5 mmol) in 20 ml dimethoxyethane was added to a solution of WCl$_4$(dme) (0.35 g, 0.8 mmol) in 10 ml dimethoxyethane at -50 ºC. After stirred at -50 ºC for 0.5 h and then another 1 h at room temperature, the solution was filtered and the filtrate was dried under vacuum to afford dark green solid. Yield: 0.36 g (78 %). Melting point > 400 ºC. IR (KBr) (cm^{-1}): 3048(m), 2964(m), 2923(m), 2823(m), 1700(w), 1653(w), 1617(w), 1559(m), 1470(w), 1442(vs), 1365(m), 1309(m), 1261(vs), 1243(vs), 1190(m), 1155(m),

1103(s), 1081(vs), 1029(m), 1019(m), 982(s), 948(w), 856(m), 803(s), 745(vs), 708(w), 661(m), 565(m), 514(w), 434(m), 393(w), 364(m), 350(w), 324(w), 302(w); EI-MS: *m/z* (%) 501 (26) (*M*-2CH$_3$-2CH$_2$)$^+$; *Anal. Calc.* for C$_{16}$H$_{18}$WO$_2$S$_4$ (554.41 g/mol): C, 34.66; H, 3.27; found: C, 34.99; H, 2.74.

6. Handling and Disposal of Solvents and Residual Waste

1. The recovered solvents were distilled or condensed into cold-traps under vacuum and collected in halogen-free or halogen-containing solvent containers, and stored for disposal.

2. Used NMR solvents were classified into halogen-free and halogen-containing solvents and were disposed as heavy metal wastes and halogen-containing wastes, respectively.

3. The heavy metal residues were dissolved in nitric acid and after neutralization stored in the containers for heavy metal wastes.

4. Drying agents such as KOH, $CaCl_2$, and P_4O_{10} were hydrolyzed and disposed as acid or base wastes.

5. Whenever possible, sodium metal used for drying solvents was collected for recycling. The non-reusable sodium metal was carefully hydrolyzed in cold ethanol and poured into the base-bath used for cleaning glassware.

6. Ethanol and acetone used for cold-bath were subsequently used for cleaning glassware.

7. The acid-bath used for cleaning glassware was neutralized with Na_2CO_3 and the resulting NaCl solution was washed-off in the communal water drainage.

8. The residue of the base-bath used for glassware cleaning was poured into the container for base wastes.

Amounts of various types of disposable wastes generated during the work:

Metal containing wastes	10L
Halogen-containing solvent wastes	5L
Halogen-free solvent wastes	35L
Acid wastes	5L
Base wastes	20L

7. Crystal Data and Refinement Details

Table CD1. Crystal data and structure refinement for 9

Empirical formula	$C_{24}H_{22}N_2O_2S_2W$
Formula weight	618.41
Temperature	100(2) K
Wavelength	1.54178 Å
Crystal system	Orthorhombic
Space group	*Pbca*
Unit cell dimensions	a = 12.187(3) Å
	b = 13.854(3) Å
	c = 27.063(3) Å
Volume	4.5693(16) Å^3
Z	8
Density (calculated)	1.798 Mg/m^3
Absorption coefficient	11.269 mm^{-1}
F(000)	2416
Theta range for data collection	3.27 to 74.60 °
Index ranges	-15<=h<=15, -13<=k<=13, -29<=l<=28
Reflections collected	39001
Independent reflections	3260 [R (int) = 0.0520]
Completeness to theta = 74.60°	69.8 %
Refinement method	Full-matrix least-squares on F^2
Data / restraints / parameters	3260 / 0 / 273
Goodness-of-fit on F^2	1.083
Final R indices [I>2sigma(I)]	R1 = 0.0237, wR2 = 0.0561
R indices (all data)	R1 = 0.0276, wR2 = 0.0585
Largest diff. peak and hole	0.929 and - 1.028 e$^-$ Å^{-3}

Table CD2. Crystal data and structure refinement for 11

Empirical formula	$C_{36}H_{34}Mo_2N_4O_4S_2 \cdot CH_3CN$
Formula weight	883.73
Temperature	133(2) K
Wavelength	0.71073 Å
Crystal system	Triclinic
Space group	*P-1*
Unit cell dimensions	a = 10.5896(13) Å, α = 73.800(13) º
	b = 10.6128(14) Å, β = 80.384(13) º
	c = 17.498(4) Å, γ = 86.842(10) º
Volume	1861.8(5) Å^3
Z	2
Density (calculated)	1.576 Mg/m^3
Absorption coefficient	0.833 mm^{-1}
F(000)	896
Theta range for data collection	1.95 to 24.79 º
Index ranges	-11<=h<=12, -12<=k<=12, -20<=l<=20
Observed reflections [I>2sigma(I)]	5318
Independent reflections	17552 / 6350 [R(int) = 0.0315]
Completeness to theta = 24.79°	99.0 %
Refinement method	Full-matrix least-squares on F^2
Data / restraints / parameters	6350 / 0 / 476
Goodness-of-fit on F^2	1.029
Final R indices [I>2sigma(I)]	R1 = 0.0225, wR2 = 0.0493
R indices (all data)	R1 = 0.0320, wR2 = 0.0511
Largest diff. peak and hole	0.331 and -0.416 e Å^{-3}

Table CD3. Crystal data and structure refinement for 14

Empirical formula	$C_4H_8MoNO_4$
Formula weight	230.05
Temperature	103(2) K
Wavelength	0.71073 Å
Crystal system	Monoclinic
Space group	*C2/c*
Unit cell dimensions	a = 6.6514(13) Å, α = 90 º
	b = 12.862(3) Å, β = 95.82(3) º
	c = 25.968(5) Å, γ = 90 º
Volume	2210.1(8) Å^3
Z	12
Density (calculated)	2.074 Mg/m^3
Absorption coefficient	1.738 mm^{-1}
F(000)	1356
Theta range for data collection	3.15 to 26.38 º
Index ranges	-8<=h<=8, -16<=k<=16, -32<=l<=32
Observed reflections [I>2sigma(I)]	22638
Independent reflections	2259 [R(int) = 0.0312]
Completeness to theta = 24.79°	100.0 %
Refinement method	Full-matrix least-squares on F^2
Data / restraints / parameters	2259 / 0 / 142
Goodness-of-fit on F^2	1.226
Final R indices [I>2sigma(I)]	R1 = 0.0237, wR2 = 0.0505
R indices (all data)	R1 = 0.0248, wR2 = 0.0510
Largest diff. peak and hole	0.409 and -0.723 e$\cdot$Å^{-3}

Table CD4. Crystal data and structure refinement for 20

Empirical formula	$C_{12}H_8O_2S_6W_2$ + 2x NEt_4
Formula weight	1004.74
Temperature	133(2) K
Wavelength	0.71073 Å
Crystal system	Orthorhombic
Space group	*Pbca*
Unit cell dimensions	a = 12.4588(4) Å, α = 90 º
	b = 17.3277(7) Å, β = 90 º
	c = 32.6412(15) Å, γ = 90 º
Volume	7046.7(5) $Å^3$
Z	8
Density (calculated)	1.894 Mg/m^3
Absorption coefficient	6.908 mm^{-1}
F(000)	3920
Theta range for data collection	2.06 to 24.90 º
Index ranges	-14<=h<=14, -20<=k<=20, -38<=l<=38
Observed reflections [I>2sigma(I)]	4337
Independent reflections	72404 / 6122 [R(int) = 0.1253]
Completeness to theta = 24.59°	99.7 %
Refinement method	Full-matrix least-squares on F^2
Data / restraints / parameters	6122 / 0 / 369
Goodness-of-fit on F^2	0.967
Final R indices [I>2sigma(I)]	R1 = 0.0287, wR2 = 0.0476
R indices (all data)	R1 = 0.0518, wR2 = 0.0503
Largest diff. peak and hole	0.698 and -1.405 e $Å^{-3}$

Table CD5. Crystal data and structure refinement for 21

Empirical formula	$C_{12}H_{19}OS_4W$
Formula weight	491.36
Temperature	133(2) K
Wavelength	0.71073 Å
Crystal system	triclinic
Space group	*C2/c*
Unit cell dimensions	a = 18.861(4) Å, α = 90 º
	b = 9.1989(18) Å, β = 93.61(3) º
	c = 18.141(4) Å, γ = 90 º
Volume	3141.2(11) Å^3
Z	4
Density (calculated)	1.039 Mg/m^3
Absorption coefficient	3.936 mm^{-1}
F(000)	948
Theta range for data collection	2.16 to 24.80 º
Index ranges	-22<=h<=22, -9<=k<=10, -21<=l<=21
Observed reflections [I>2sigma(I)]	2598
Independent reflections	16770 / 2695 [R(int) = 0.0591]
Completeness to theta = 24.59°	99.6 %
Refinement method	Full-matrix least-squares on F^2
Data / restraints / parameters	2695 / 0 / 160
Goodness-of-fit on F^2	2.201
Final R indices [I>2sigma(I)]	R1 = 0.0788, wR2 = 0.2338
R indices (all data)	R1 = 0.0804, wR2 = 0.2348
Largest diff. peak and hole	4.133 and -1.200 e Å^{-3}

Table CD6. Crystal data and structure refinement for 22

Empirical formula	$C_{28}H_{55}MoN_2OS_4$
Formula weight	659.92
Temperature	133(2) K
Wavelength	0.71073 Å
Crystal system	Monoclinic
Space group	*P2/n*
Unit cell dimensions	a = 18.144(4) Å, α = 90 º
	b = 9.1862(18) Å, β = 90.68(3) º
	c = 18.919(4) Å, γ = 90 º
Volume	3146.9(11) Å^3
Z	4
Density (calculated)	1.393 Mg/m^3
Absorption coefficient	0.706 mm^{-1}
F(000)	1404
Theta range for data collection	1.61 to 24.81 º
Index ranges	-21<=h<=21, -10<=k<=10, -22<=l<=22
Observed reflections [I>2sigma(I)]	4752
Independent reflections	43396 / 5409 [R(int) = 0.0758]
Completeness to theta = 24.59°	99.8 %
Refinement method	Full-matrix least-squares on F^2
Data / restraints / parameters	5409 / 0 / 286
Goodness-of-fit on F^2	1.083
Final R indices [I>2sigma(I)]	R1 = 0.0993, wR2 = 0.2459
R indices (all data)	R1 = 0.1099, wR2 = 0.2538
Largest diff. peak and hole	2.150 and −1.042 e. Å^{-3}

Table CD7. Crystal data and structure refinement for 23

Empirical formula	$C_{28}H_{50}Cl_2O_{10}W_2$
Formula weight	985.28
Temperature	133(2) K
Wavelength	0.71073 Å
Crystal system	triclinic
Space group	*P -1*
Unit cell dimensions	a = 9.3687(14) Å, α = 90.939(11) º
	b = 9.5601(14) Å, β = 77.028(11) º
	c = 10.1711(15) Å, γ = 70.212(12) º
Volume	831.1(2) Å^3
Z	1
Density (calculated)	1.969 Mg/m^3
Absorption coefficient	7.128 mm^{-1}
F(000)	480
Theta range for data collection	2.07 to 24.59 °
Index ranges	-10<=h<=10, -11<=k<=11, -11<=l<=11
Observed reflections [I>2sigma(I)]	2479
Independent reflections	7483 / 2778 [R(int) = 0.0647]
Completeness to theta = 24.59°	99.5 %
Refinement method	Full-matrix least-squares on F^2
Data / restraints / parameters	2778 / 0 / 200
Goodness-of-fit on F^2	1.062
Final R indices [I>2sigma(I)]	R1 = 0.0359, wR2 = 0.0845
R indices (all data)	R1 = 0.0437, wR2 = 0.0883
Largest diff. peak and hole	1.487 and -2.248 e Å^{-3}

References

1. F. A. Cotton, F. A. Cotton, G. Wilkinson, P. L. Gaus, Basic Inorganic Chemistry, New York [u.a.]: Wiley **1995**, 592-595.

2. R. Hille, *Chem. Rev.* **1996**, 96 (7), 2757-2816.

3. M. K. Johnson, D. C. Rees, M. W. W. Adams, *Chem. Rev.* **1996**, 96 (7), 2817-2840.

4. T. Hoff, K. M. Schnorr, C. Meyer, The Journal of Biological Chemistry **1995**, 270 (11), 6100-6107.

5. J. L. Johnson, B. E. Hainline, K. V. Rajagopalan, B. H. Arison, The Journal of Biological Chemistry **1984**, 259 (9), 5414-5422.

6. D. Collison, D. D. Garner, J. A. Joule, *Chem. Soc. Rev.* **1996**, 25, 25-32.

7. S. P. Kramer, J. L. Johnson, A. A. Ribeiro, D. S. Millington, K. V. Rajagopalan, The journal of Biological Chemistry **1987**, 262 (34), 16357-16363.

8. E. S. Davies, R. L. Beddoes, D. Collison, A. Dinmore, A. Docrat, J. A. Joule, C. R. Wilson, C. D. Garner, *J. Chem. Soc. Daloton Trans.* **1997**, 1985-1995.

9. N. Ueyama, H. Oku, M. Kondo, T. Okamura, N. Yoshinaga, A. Nakamura, Inorganic Chemistry **1996**, 35, 643-650.

10. L. M.Thomson, M. B. Hall, *J. Am. Chem. Soc.* **2001**, 123, 2995-4002.

11. H. Schindelin, C. Kisker, J. Hilton, K. V. Rajagopalan, D. C. Rees, Science. **1996**, 272, 1615-1621.

12. A. Thapper, C. Lorber, J. Fryxelius, A. Behrens, E. Nordlander, Inorganic Biochemistry **2000**, 79, 67-74.

13. Holleman-Wiberg, Inorganic Chemistry, San Diego, Calif. [u.a.]: Acad. Press [u.a.], c **2001**, p 1382-1402.

14. H. White, G. Strobl, R. Feicht, H. Simon, European Journal of Biochemistry **1989**, 184 (1), 89-96.

15. S. Mukund, M. W. W. Adams, Joural of Biological Chemisty **1990**, 265 (20), 11508-11516.

16. M. K. Chan, S. Mukund, A. Kletzin, M. W. W. Adams, D. C. Rees, Science **1995**,

267, 1463-1469.

17. H. Dobbek, R. Huber, *Met. Ions Biol. Syst.* **2002**, 39, 227-263.

18. A Kletzin, S. Mukund, Kelley-Crouse, L. Terry, M. K. Chan, D. C. Rees, M. W. W. Adams, Journal of Bacteriology **1995**, 177 (16), 4817-4819.

19. S. Mukund, M. W. W. Adams, Journal of Biological Chemistry **1991**, 266 (22), 14208-14216.

20. S. Mukund M. W. W. Adams, Journal of Biological Chemistry **1993**, 268 (18), 13952-13600.

21. S Mukund, M. W. W. Adams, Journal of Biological Chemistry **1995**, 270 (15), 8389-8392.

22. H. White, R. Feicht, C. Huber, F. Lottspeich, H. Simon, Biological Chmistry Hoppe-Seyler **1991**, 372 (11), 999-1005.

23. K. Ma, H. Loessner, J. Heider, M. K. Johnson, M. W. W. Adams, Journal of Bacteriology **1995**, 177 (16), 4748-4756.

24. C. M. H. Hensgens, W. R. Hagen, T. A. Hansen, Journal of Bacteriology **1995**, 177 (21), 6195-6200.

25. I. Yamamoto, T. Saiki, S. M. Liu, L. G. Ljungdahl, Journal of Biological Chemistry **1983**, 258 (3), 1826-1832.

26. J. B. Jones, T. C. Stadtman, Journal of Biological Chemistry **1981**, 256 (2), 656-663.

27. P. A. Bertram, R. K. Thauer, European Journal of Biochemistry **1994**, 226 (3), 811-818.

28. R. A. Schimitz, M. Richter, D. Linder, R. K. Thauer, European Journal of Biochemistry **1992**, 207 (2), 559-565.

29. B. M. Rosner, B. Schink, Journal of Bacteriology **1995**, 177 (20), 5767-5772.

30. J. H. Enemark, J. J. Cooney, J-J. Wang, R. H. Holm, *Chem. Rev.* **200**4, 104, 1175-1200.

31. J. A. McCleverty, Progress in Inorganic Chemistry **1968**, 10, 49-221.

32. S. J. N. Burgmayer, E. I. Stiefel, *J. Am. Chem. Soc.* **198**6, 108 (26), 8310-8311.

33. B. Fischer, H. Schmalle, E. Dubler, A Schaefer, M. Viscontini, Inorganic

Chemistry **1995**, 34 (23), 5726-5734.

34. E. S. Davies, R. L. Beddoes, D. Collison, A. Dismore, A. Docrat, H. A. Joule, C. R. Wilson, C. D. Garner, *J. Chem. Soc. Daloton Trans.***1997**, 21, 3985-3996.

35. B. S. Lim, J. P. Donahue, R. H. Holm, Inorganic Chemistry **2000**, 39 (2), 263-273.

36. J. P. Donahue, C. R. Goldsmith, U Nadiminti, R. H. Holm, *J. Am. Chem. Soc.* **1998**, 120 (49), 12869-12881.

37. S. K. Das, P. K. Chaudhury, D. Biswas, S. Sarkar, *J. Am. Chem. Soc.* **1994**, 116 (20), 9061-9070.

38. C. Lorber, M. R. Plutino, L. I. Elding, E. Nordlander, *J. Chem. Soc. Daloton Trans.* **1997**, 21, 3997-4004.

39. H. Oku, N. Ueyama, M. Kondo, A. Nakamura, Inorganic Chemistry **1994**, 33 (2), 209-216.

40. H. Oku, N. Ueyama, A. Nakamura, Inorganic Chemistry **1997**, 36 (7), 1504-1516.

41. M. A. Ansari, J. Chandrasekaran, S. Sarkar, Inorganica Chimica Acta **1987**, 133 (1), 133-136.

42. D. Coucouvanis, A. Hadjikyriacou, A. Toupadakis, S. M. Koo, O. Ileperuma, M. Draganjac, A. Salifoglou, Inorganic Chemistry **1991**, 30 (4), 754-767.

43. G-E. Matsubayashi, T. Nojo, T. Tanaka, Inorganica Chimica Acta **1988**, 154 (2), 133-135.

44. J. A. McCleverty, J. Locke, B. Ratcliff, E. J. Wharton, Inorganica Chimica Acta **1969**, 3 (2), 283-286.

45. N. Ueyama, H. Oku, M. Kondo, T. Okamura, N. Yoshinaga, A. Nakamura, Inorganic Chemistry **1996**, 35 (3), 643-650.

46. H. Oku, N. Ueyama, K. Nakamura, Inorganic Chemistry **1995**, 34 (14), 3667-3676.

47. B. S. Lim, R. H. Holm, *J. Am. Chem. Soc.* **2001**, 123 (9), 1920-1930.

48. S. Boyde, S. R. Ellis, C. D. Garner, W. Clegg, Journal of the Chemical Society, Chemical Communications **1986**, 20, 1541-1543.

49. S. K. Das, S. Biswas, R. Maiti, S. Sarkar, *J. Am. Chem. Soc.* **1996**, 118 (6), 1387-1397.

50. N. Ueyama, H. Oku, A. Nakamura, *J. Am. Chem. Soc.* **1992**, 114 (18), 7310-7311.

51. J. Wang, O. P. Kryatova, E. V. Rybak-Akimova, R. H. Holm, Inorganic Chemistry **2004**, 43, 8092-8101.

52. K. Most, J. Hoßbach, D. Vidovic, J. Magull, N. C. Mösch-Zanetti, *Adv. Synth. Catal.* **2005**, 347, 463-372.

53. J. M. Berg, R. H. Holm, *J. Am. Chem. Soc.* **1984**, 106, 3035-3036.

54. M. Abrantes, A. M. Santos, J. Mink, F. E. Kühn, C. C. Romão, Organomettallics **2003**, 22, 2112-2118.

55. R. R. Schrock, *J. Mol. Catal. A: Chem.* **2004**, 213, 21-30.

56. A. Lehtonen, R. Sillanpää, Polyhedron **2005**, 24, 257-265.

57. R. H. Holm, *J. Am. Chem. Soc.* **2004**, 126 (31), 9874-9874.

58. C. Lorber, J. P. Donahue, C. A. Goddard, E. Nordlander, R. H. Holm, *J. Am. Chem. Soc.* **1998**, 120, 8102-8112.

59. C. A. Goddard, R. H. Holm, Inorganic Chemistry **1999**, 38, 5389-5398.

60. K. Sung, R. H. Holm, *J. Am. Chem. Soc.* **2001**, 123, 1931-1943.

61. K. Sung, R. H. Holm, *J. Am. Chem. Soc.* **2002**, 124, 4312-4320.

62. H. Sugimoto, M. Tarumizu, K. Tanaka, H. Miyake, H. Tsukube, *Dalton Trans.* **2005**, 3558-3565.

63. V. C. Gibson, T. P. Kee, A. Shaw, Polyhedron **1990**, 9 (18), 2293-2298.

64. A. J. Millar, J. M. White, C. J. Doonan, C. G. Young, Inorganic Chemistry **2000**, 39, 5151-5155.

65. C. A. McConnachie, E. I. Stiefel, Inorganic Chemistry **1999**, 38, 964-972.

66. A. Lehtonen, R. Sillanpää, Inorganic Chemistry **2004**, 43, 6501-6506.

67. A. A. Eagle, E. R. T. Ttiekink, C. G. Young, Inorganic Chemistry **1997**, 36, 6315-6322.

68. I. W. Boyd, I. G. Dnace, K. S. Murray, A. G. Webb, *Aust. J. Chem.* **1978**, 31, 279-284.

69. I. W. Boyd, I. G. Dnace, K. S. Murray, A. G. Webb, *Aust. J. Chem.* **1978**, 31, 2423-2430.

70. G. R. Hanson, A. A. Brunette, A. C. McDonell, K. S. Murray, A. G. Webb, *J. Am.*

Chem. Soc. **1981**, 103, 1953-1959.

71. K. Dreisch, D. Andersson, C. Stalhandske, Polyhedron **1991**, 10, 52417-52421.

72. T. Robin, F. Montilla, A. Galindo, C. Ruiz, J. Hartmann, Polyhedron **1999**, 18, 1485-1490.

73. C. G. Hull, M. H. Stiddard, *J. Chem. Soc. A* **1966**, 1633-1635.

74. B. J. Brisdon, Inorganic Chemistry **1967**, 6, 1791-1795.

75. B. Soptrajanov, M. Tripkovska, L. Pejov, *Croat. Chem. Acta* **1999**, 72, 663-672.

76. A. Al-Ajlouni, A. A. Valente, C. D. Nunes, M. Pillinger, A. M. Santos, J. Zhao, C. C. Romao, I. S. Goncalves, F. E. Kühn, *Eur. J. Inorg. Chem.* **2005**, 1716-1723.

77. F. E. Kühn, M. Groarke, E. Bencze, E. Herdtweck, A. Prazeres, A. M. Santos, M. J. Calhorda, C. C. Romao, I. S. Goncalves, A. D. Lopes, M. Pillinger, *Chem. Eur. J.* **2002**, 8, 2370-2383.

78. A. W. Herrmann, W. R. Thiel, E. Herdtweck, *Chem. Ber.* **1990**, 123, 271-276.

79. H. Arzoumanian, G. Agrigoglio, M. V. Capparelli, R. Atencio, A. Briceño, A. Alvarez-Larena, Inorganica Chimica Acta **2006**, 359, 81-89.

80. A. Müller, S. K. Das, E. Krichemeyer, C. Kahlmann, *Inorg. Synth.* **2004**, 34, 191-200.

81. A. Müller, S. Roy, *Eur. J. Inorg. Chem.* **2005**, 18, 3561-3570.

82. A. Müller, L. Toma, H. Bögge, M. Henry, E. T. K. Haupt, A. Mix, F. L. Sousa, *Chem. Commun.* **2006**, 3396-3398.

83. G. J. J. Chen, J. W. McDonald, W. E. Newton, Inorganic Chemistry **1976**, 15 (11), 2612-2615.

84. S. D. Garton, J. Hilton, H. Oku, B. R. Crouse, K. V. Rajagopalan, M. K. Johnson, *J. Am. Chem. Soc.* **1997**, 119, 12906-12916.

85. R. F. Lang, T. D. Ju, C. D. Hoff, J. C. Bryan, G. J. Kubas, *J. Am. Chem. Soc.* **1994**, 116, 9747-9748.

86. J. F. De Wet, M. R. Caira, B. J. Gellatly, *Acta Crystallogr., Sect. B* **1978**, 34, 762-766.

87. S. Oh, S. Mo, *J. Kor. Chem. Soc.* **1995**, 39, 318-322.

88. M. Miao, M. W. Willer, R. H. Holm, Inorganic Chemistry **2000**, 39, 2843-2849.

89. M. B. Hursthouse, W. Levason, R. Ratnani, G. Reid, Polyhedron **2004**, 23, 1915-1921.

90. R. J. Butcher, B. R. Penfold, E. Sinn, *J. Chem. Soc. Daloton Trans.* **197**9, 668-675.

91. G. Wang, G. Chen, R. L. Luck, Z. Wang, Z. Mu, D. G. Evans, X. Duan, Inorganica Chimica Acta **2004**, 357, 3223-3229.

92. A. Thapper, J. P. Donahue, K. B. Musgrave, M. W. Willer, E. Nordlander, K. B. Hedman, K. O. Hodgson, R. H. Holm, Inorganic Chemistry **1999**, 38, 4104-4114.

93. I. G. Dance, A. G. Wedd, I. W. Boyd, *Aust. J. Chem.* **1978**, 31, 519-526.

94. M. G. B. Drew, A. Kay, *J. Chem. Soc. A* **1971**, 1846-1850.

95. J. R. Knox, C. K. Prout, *Acta Cryst.* **1969**, B 25, 1857-1866.

96. X. Ma, K. Starke, C. Schulzke, H. –G. Schmidt, M. Noltemeyer, *Eur. J. Inorg. Chem.* **2006**, 628-637.

97. D. V. Partyka, R. H. Holm, Inorganic Chemistry **2004**, 43 (26), 8609-8616.

98. N. Ueyama, M. Nakata, T. Araki, A. Nakamura, S. Yamashita, T. Yamashita, Inorganic Chemistry **1981**, 20, 1934-1937.

99. H. Hou, Y. Wei, Y. Song, Y. Zhu, Y. Fan, Inorganica Chimica Acta **200**4, 357, 421-428.

100. A. Müller, W-O Nolte, B: Krebs, *Angew. Chem. Int. Ed. Engl.* **1978**, 17 (4), 279-279.

101. W. E. Newton, J. L. Corbin, D. C. Bravard, J. E. Searles, J. W. McDonald, Inorganic Chemistry **1974**, 13 (5), 1100-1104.

102. B. B. Kaul, J. H. Enemark, S. L. Merbs, J. T. Spence, *J. Am. Chem. Soc.* **1985**, 107 (10), 2885-2891.

103. D. Dowerah, J. T. Spence, R. Singh, A. G. Wedd, G. L. Wilson, F. Farchione, J. H. Enemark, J. Kristofzski, M. Bruck, *J. Am. Chem. Soc.* **1987**, 109 (19), 5655-5665.

104. N. Yoshinaga, N. Ueyama, T. Okamura, A. Nakamuran, *Chem. Lett.* **1990**, 1655-1656.

105. H. Oku, N. Ueyama, A. Nakamura, Y. Kai, N. Kanehisa, *Chem. Lett.* **1994**, 607-610.

106. J. M. Berg, K. O. Hodgson, S. P. Cramer, J. L. Corbin, A. Elseberry, N.

Pariyadath, E. I. Stiefel, *J. Am. Chem. Soc.* **1979**, 101, 2774-2776.

107. S. V. Mozgin, M. G. Felin, N. A. Subbotina, V. I. Spitsyn, *Zh. Neorg. Khim.* **1982**, 27, 1193-1198.

108. J. Liimatainen, A. Lehtonen, R. Sillanpää, Polyhedron **2000**, 19, 1133-1138.

109. J. Fridgen, W. A. Herrmann, G. Eickerling, A. M. Sntos, F. E. Kühn, Journal of Organometallic Chemistry **2004**, 689, 2752-2761.

110. a. S. A. Roberts, C. G. Young, C. A. Kipke, W. E. Cleland, Jr., K. Yamanouchi, M. D. Carducci, J. H. Enemark, Inorganic Chemistry **1990**, 29 (19), 3650-3656. b. Y. Wong, Y. Yan, E. S. H. Chan, Q. Yang, T. C. W. Mak, D. K. P. Ng, *J. Chem. Soc. Daloton Trans.* **1998**, 3075-3064.

111. J.J. A. Cooney, M. D. Carducci, A. E. McElhaney, H.D.Selby, J. H. Enemark, Inorganic Chemistry **2002**, 41, 7086-7093.

112. R. S. Pilato, K. A. Eriksen, M. A. Greaney, E. I. Stiefel, S. Goswami, L. Kilpatrick, T. G. Spiro, E. C. Taylor, A. L. Rheingold, *J. Am. Chem. Soc.* **1991**, 113 (24), 9372-9374.

113. K. Baba, T. Okamura, H. Yamamoto, T. Yamamoto, M. Ohama, N. Ueyama, Inoganic Chemistry **2006**, 45, 8365-8371.

114. S. Liu, L. Ma, D. McGowty, J. Zubieta, Polyhedron **1990**, 9, 1541-1553.

115. P. Barbaro, C. Bianchini, G. Scapacci, D. Masi, P. Zanello, *Inorg. Chem.* **1994**, 33, 3180-3186.

116. P. Barbaro, T. R. Belderrain, C. Bianchini, G. Scapacci, D. Masi, Inorganic Chemistry **1996**, 35, 3362-3368.

117. S. Bhattacharjee, R. Bhattacharyya, *J. Chem. Soc. Dalton Trans.* **1993**, 7, 1151-1158.

118. Glowiak, L. Jerzykiewicz, J. M. Sobczak, J.J. Ziolkowski, *Inorg. Chim. Acta* **2003**, 356-387.

119. C. P. Rao, A. Sreedhara, P. V. Roa, M. B. Verghese, K. Rissanen, E. Kolehmainen, N. K. Lokanath, M. A. Sridhar, J. S. Prasad, *Dalton Trans.* **1998**, 14, 2383-2393.

120. C. M. Bolinger, T. B. Rauchfuss, Inorganic Chemistry **1982**, 21 (11), 3947-3954.

121. C. M. Bolinger, T. B. Rauchfuss, A. L. Rheingold, Organometallics **1982**, 1 (11),

1551-1553.

122. J. T. Goodman, T. B. Rauchfuss, Inorganic Chemistry **1998**, 37 (20), 5040-5041.

123. T. R. Halbert, W. H. Pan, E. I. Stiefel, *J. Am. Chem. Soc.* **1983**, 105 (16), 5476-5477.

124. D. Coucouvanis, A. Toupadakis, J. D. Lane, S. M. Koo, C. G. Kim, A. Hadjikyriacou, *J. Am. Chem. Soc.* **1991**, 113 (14), 5271-5282.

125. R. Dessapt, C. Simonnet-Jégat, J. Marrot, F. Sécheresse, Inorganic Chemistry **2001**, 40, 4072-4074.

126. A. A. Eagle, S. M. Harben, E. R. T. Tiekink, C. G. Young, *J. Am. Chem. Soc.* **1994**, 116 (21), 9749-9750.

127. H. Kawaguchi, K. Tatsumi, *J. Am. Chem. Soc.* **1995**, 117 (13), 3885-3886.

128. G. Bunzey, J. H. Enemark, J. K. Howie, D. T. Sawyer, *J. Am. Chem. Soc.* **1977**, 99, 4168-4170.

129. J. I. Gelder, J. H. Enemark, Inorganic Chemistry **1976**, 15 (8), 1839-1843.

130. L. G. Marzilli, B. E. Hanson, T. J. Kistenmacher, L. A. Epps, R. C. Stewart, Inorganic Chemistry **1976**, 15 (7), 1661-1665.

131. W. Pan, T. Chandler, J. H. Enemark, E. I. Stiefel, Inorganic Chemistry **1984**, 23, 4265-4269.

132. S. A. Cohen, E. I. Stiefel, Inorganic Chemistry **1985**, 24, 4657-4662.

133. R. Dessapt, C. S- Jégat, A. Amallard, H. Lavanant, J. Marrot, F. Sécheresse, Inorganic Chemistry **2003**, 42, 6425-6431.

134. B. R. Davis, I. Bernal, *J. Cryst. Mol. Struct.* **1972**, 2, 135-142.

135. D. Coucouvanis, M. E. Draganjac, S. M. Koo, A. Toupadakis, A. I. Hadjikyriacou, Inorganic Chemistry **1992**, 31 (7), 1186-1196.

136. J. T. Huneke, K. Yamanouchi, J. H. Enemark, Inorganic Chemistry **1978**, 17 (12), 3695-3697.

137. H. Oku, N. Ueyama, A. Nakamura, *Bull, Chem. Soc. Jpn.* **1996**, 69, 3139-3150.

138. P. Subramanian, S. Burgmayer, S. Richards, V. Szalai, T. G. Spiro, Inorganic Chemistry **1990**, 29, 3849-3853.

139. F. E. Inscore, R. McNaughton, B. L. Westcott, M. E. Helton, R. Jones, I. K.

Dhawan, J. H. Enemark, M. L. Kirk, Inorganic Chemistry **1999**, 38 (7), 1401-1410.

140. S. R. Ellis, D. Collison, C. D. Garner, W. Clegg, *J. Chem. Soc., Chem. Commun.* **1986**, 483-1485.

141. G. N. George, J. Hilton, K. V. Rajagopalan, *J. Am. Chem. Soc.* **1996**, 118, 1113-1117.

142. J. P. Donahue, C. Lorber, E. Nordlander, R. H. Holm, *J. Am. Chem. Soc.* **1998**, 120, 3259-3260.

143. G. N. George, J. Hilton, C. Temple, R. C. Prince, K. V. Pajagopalan, *J. Am. Chem. Soc.* **1999**, 121, 1256-1266.

144. F. A. Cotton, D. DeMarco, B. W. S. Kolthammer, R. A. Walton, Inorganic Chemistry **1981**, 20 (9), 3048-3051.

145. F. A. Cotton, D. DeMarco, L. R. Falvello, R. A. Walton, *J. Am. Chem. Soc.* **1982**, 104, 7375-7376.

146. L. B. Anderson, F. A. Cotton, D. DeMarco, L. R. Falvello, S. M. Tetrick, R. A. Walton, *J. Am. Chem. Soc.* **1984**, 106, 4743-4749.

147. A. Bino, F. A. Cotton, Z. Dori, S. Koch, H. Kueppers, M. Millar, J. C. Sekutowski, Inorganic Chemistry **1978**, 17 (11), 3245-3253.

148. F. A. Cotton, D. A. Ucko, Inorganica Chimica Acta **1972**, 6, 161-172.

149. J. Buc, C. Santini, R. Giordani, M. Czjzek, L. Wu, G. Gaiordano, *Mol. Microbiol.* **1999**, 32, 159-168.

150. L. J. Stewart, S. Bailey, B. Bennett, J. M. Charnock, C. D. Garner, A. S. McAlpine, *J. Mol. Biol.* **2000**, 299, 593-600.

151. F. E. Inscore, R. McNaughton, B. L. Westcott, M. E. Helton, R. Jones, I. K. Dhawan, J. H. Enemark, M. L. Kirk, Inorganic Chemistry **1999**, 38, 1401-1410.

152. R. H. Holm, *Chem. Rev.* **1987**, 87, 1401-1449.

153. C. D. Garner, M. R. Hyde, F. E. Mabbs, V. I. Routledge, Nature **1974**, 252, 579-580.

154. B. E. Schultz, R. Hille, R. H. Holm, *J. Am. Chem. Soc.* **1995**, 117 (2), 827-828.

155. J. M. Berg, R. H. Holm, *J. Am. Chem. Soc.* **1985**, 107 (4), 917-925.

156. J. M. Berg, R. H. Holm, *J. Am. Chem. Soc.* **1985**, 107 (4), 925-932.

157. E. W. Harlan, J. M. Berg, R. H. Holm, *J. Am. Chem. Soc.* **1986**, 108 (22), 6992-7000.

158. J. P. Caradonna, E. W. Harlan, R. H. Holm, *J. Am. Chem. Soc.* **1986**, 108 (24), 7856-7858.

159. J. P. Caradonna, P. R. Reddy, R. H. Holm, *J. Am. Chem. Soc.* **1988**, 110 (7), 2139-2144.

160. J. A. Craig, R. H. Holm, *J. Am. Chem. Soc.* **1989**, 111 (6), 2111-2115.

161. S. D. Garton, J. Hilton, H. Oku, B. R Crouse, K. V. Rajagopalan, M. K. Johnson, *J. Am. Chem. Soc.* **1997**, 119, 12906-12916.

162. H. H. Szmant, O. Cox, *J. Org. Chem.* **1966**, 31, 1595-1598.

163. X. Ma, C. Shulzke, H. Schmidt, M. Noltemeyer, Dalton Trans. **2007**, 1773-1780.

164. C. Shulzke, *Dalton Trans.* **2005**, 713-720.

165. G. C. Tucci, J. P. Donahue, R. H. Holm, Inorganic Chemistry **1998**, 37, 1602-1608.

166. S. Lee, D. L. Staley, A. L. Rheigold, N. J. Cooper, Inorganic Chemistry **1990**, 29, 4391-4396.

167. D. F. Shriver, M. A. Drezdzon, *The Manipulation of Air-Sensitive Compounds*, 2nd ed., McGraw-Hill, New York, **1969**.

168. D. D. Perrin, W. L. F.Armarego, *Purification of Laboratory Chemicals*, 3rd ed., Pergamon, London, **1988**.

169. G. M. Sheldrick, " SHELXS-97, Program for Structure Solution", *Acat Crystallogr. Sect. A* **1990**, 46, 467-473.

170. G. M. Sheldrick, SHELXL-97, *Program for Crystal Structure Refinement*, Universität Göttingen, FRG, **1997**.

171. C. Persson, C. Andersson,   Inorganica Chimica Acta **1993**, 203, 235-238.

172. C. Persson, C. Andersson, Polyhedron **1991**, 10 (18), 2089-2093.

173. F. Stoffelbach, D. Saurenz, R. Poli, *Eur. J. Inorg. Chem.* **2001**, 2699-2703.

174. K. Dreisch, D. Andersson, C. Stalhandske, Polyhedron **1991**, 10 (20/21), 2417-2421.

175. J. W. McDonald, G. D. Friesen, L. D. Rosenhein, W. E. Newton, Inorganica Chimica Acta **1983**, 72, 205-210.

176. U. Herzog, U. Böhme, G. Rheinwald, Journal of Organometallic Chemistry **2000**, 612, 133-140.

Lebenslauf

Name:	Qingwei Zhang
Geboren:	Dalian, Liaoning, P. R. China, am 17. 04. 1979
Staatsangehörigkeit:	Chinesisch
Familienstand:	ledig

Schulausbildung

09/1985 – 07/1991:	Primary school in Dalian, Liaoning, China
09/1991 – 07/1997:	Middle school and high school in Dalian, Liaoning, China

Hochschulausbildung

09/1997 - 07/2001:	B. Sc. study in School of Material Science and Engineering, Tianjin University, Tianjin, China
07/2001:	*Bachelor of Engineering*
09/2001 – 03/2004:	M. Sc. study in School of Material Science and Engineering, Tianjin University, Tianjin, China
03/2004:	*Master of Engineering*
05/2004 – 06/2004:	Äquivalenzprüfung zum Diplomexamen – Fach Chemie
05/2004 – 05/2007:	Anfertigung der Dissertation unter Anleitung von Jun.-Prof. Dr. rer. nat. C. Schulzke am Institut für Anorganische Chemie der Georg-August-Universität zu Göttingen